

The Galactic Center Environment and Dark Matter Annihilation

Tim Linden

CCAPP Postdoctoral Fellow

Center for Cosmology and Astro-Particle Physics

The Ohio State University



Washington University

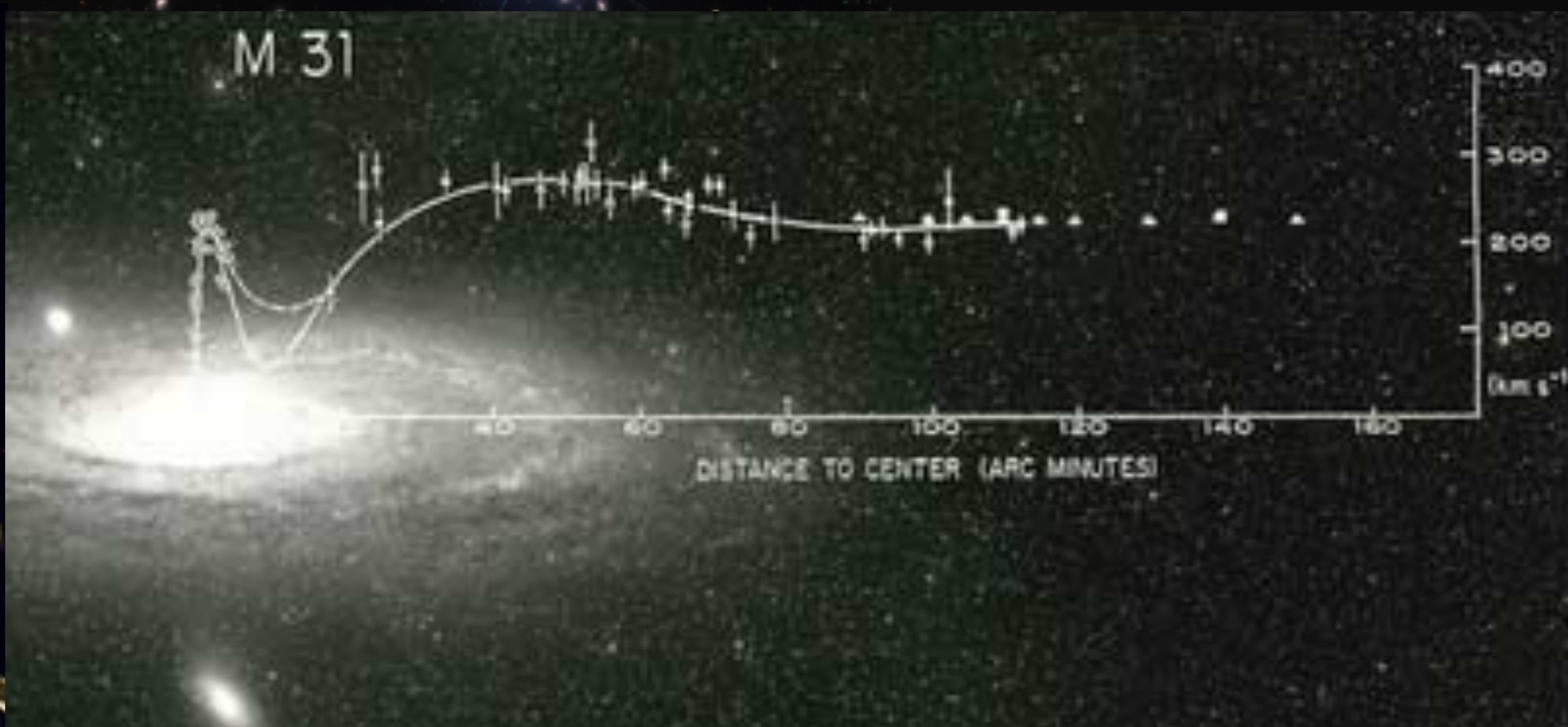
11/3/16

Gravitational Dark Matter



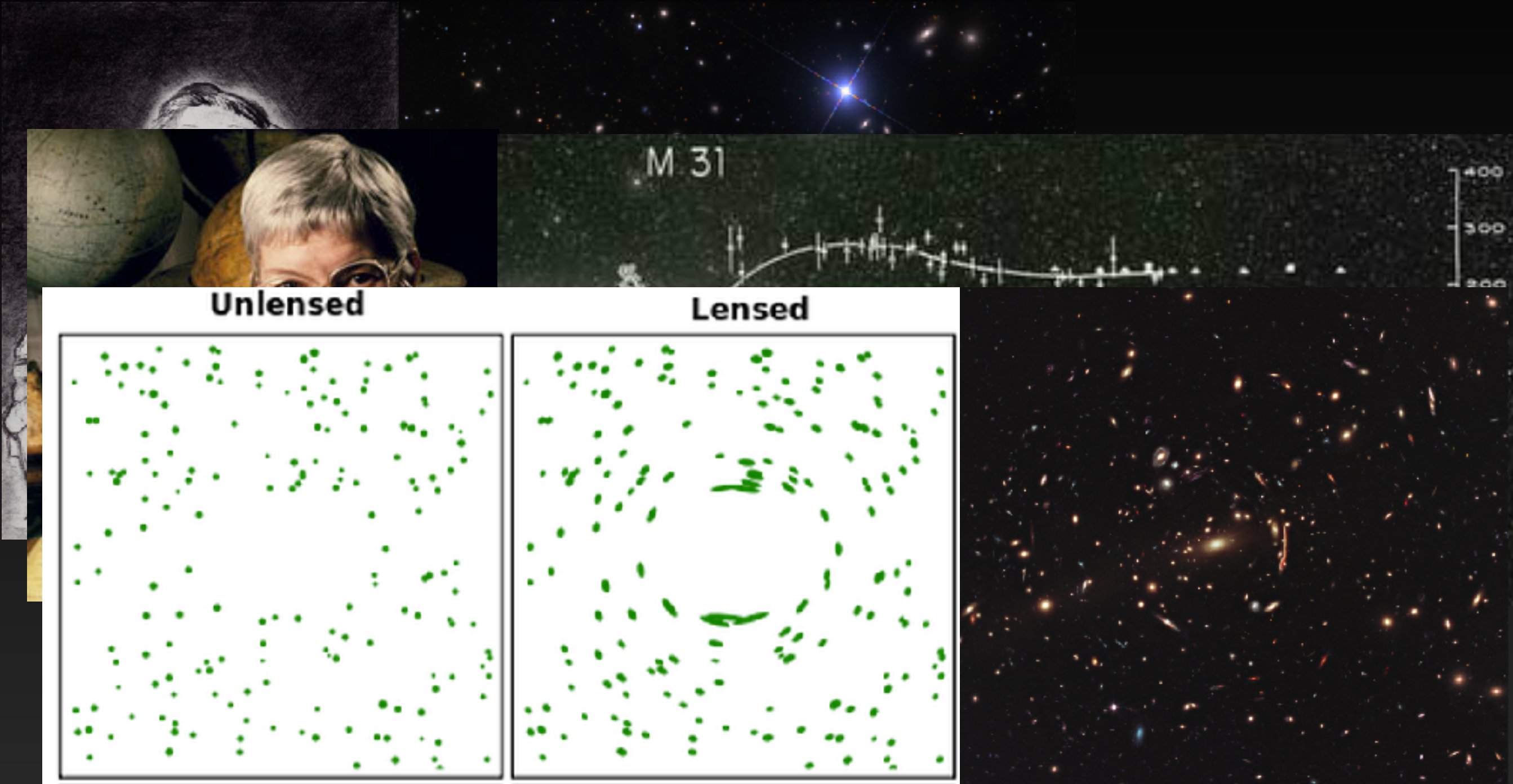
1933: Zwicky observes dark matter in Coma Cluster

Gravitational Dark Matter



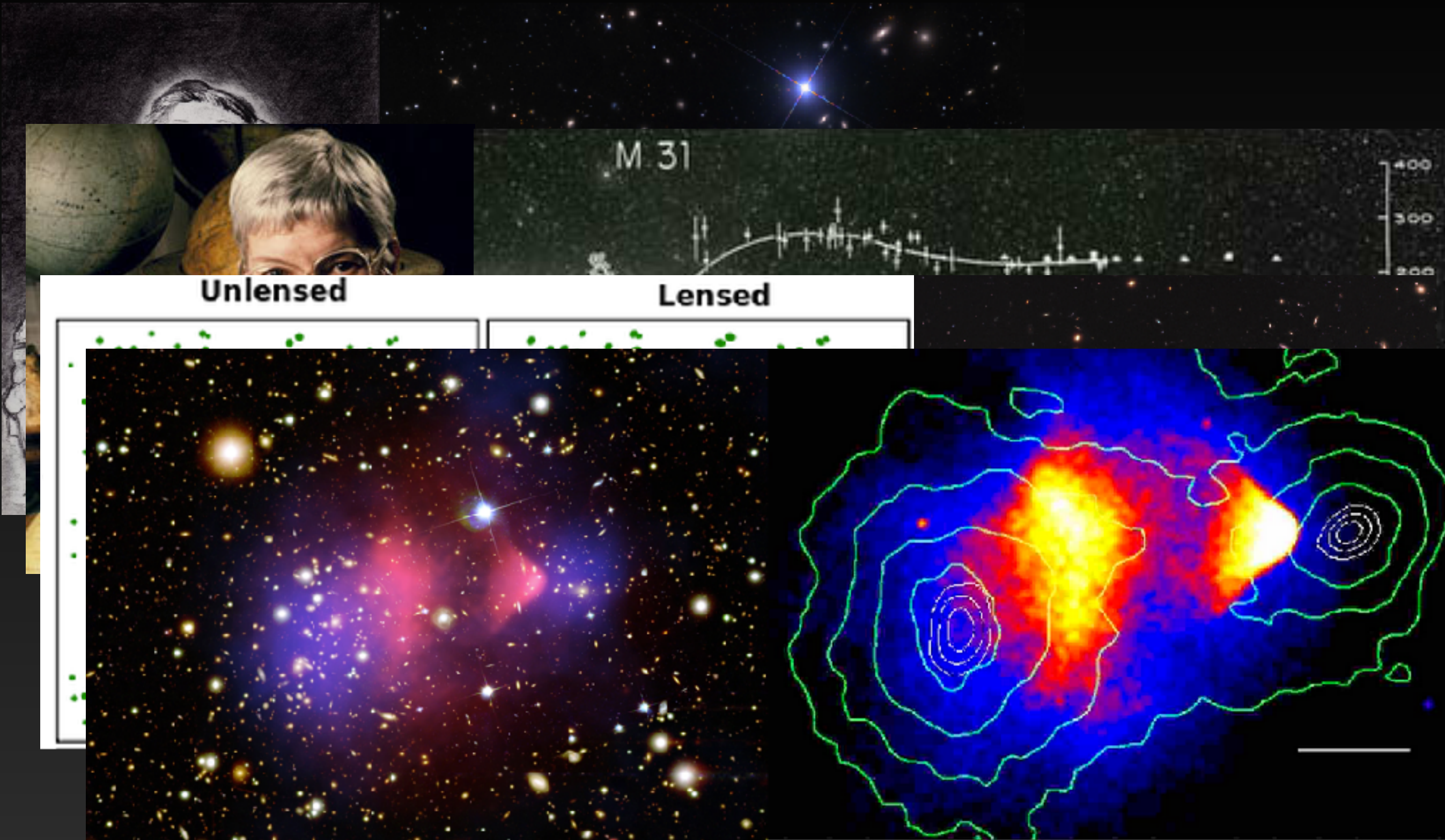
1970s: Vera Rubin observes anomalous rotation velocities in M31

Gravitational Dark Matter



1996: Weak Gravitational Lensing Observed from Dark Matter Halos

Gravitational Dark Matter



2006: Bullet Cluster Observations Show Offset Between Mass and Hot Gas

Gravitational Dark Matter

WMAP

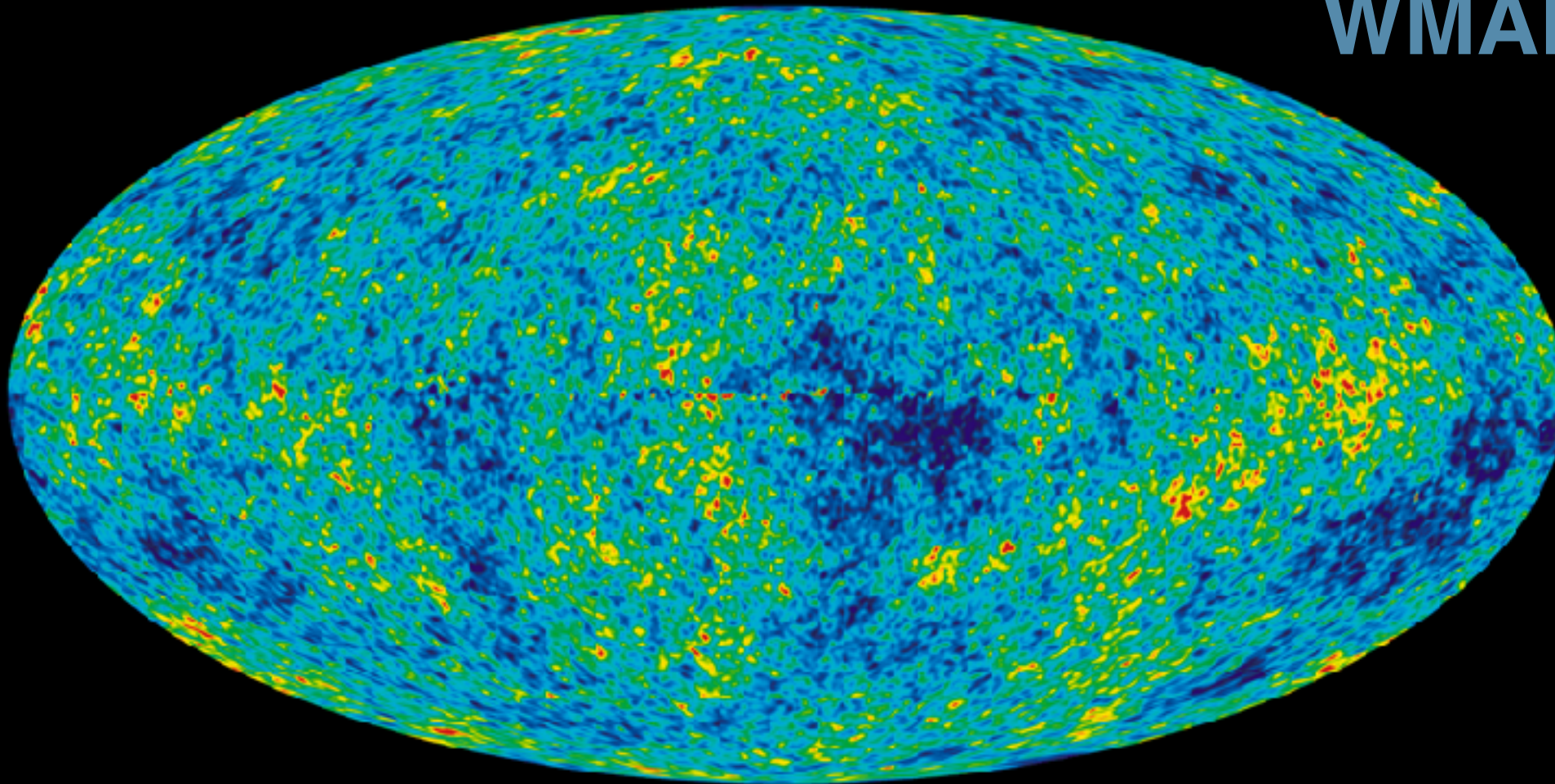
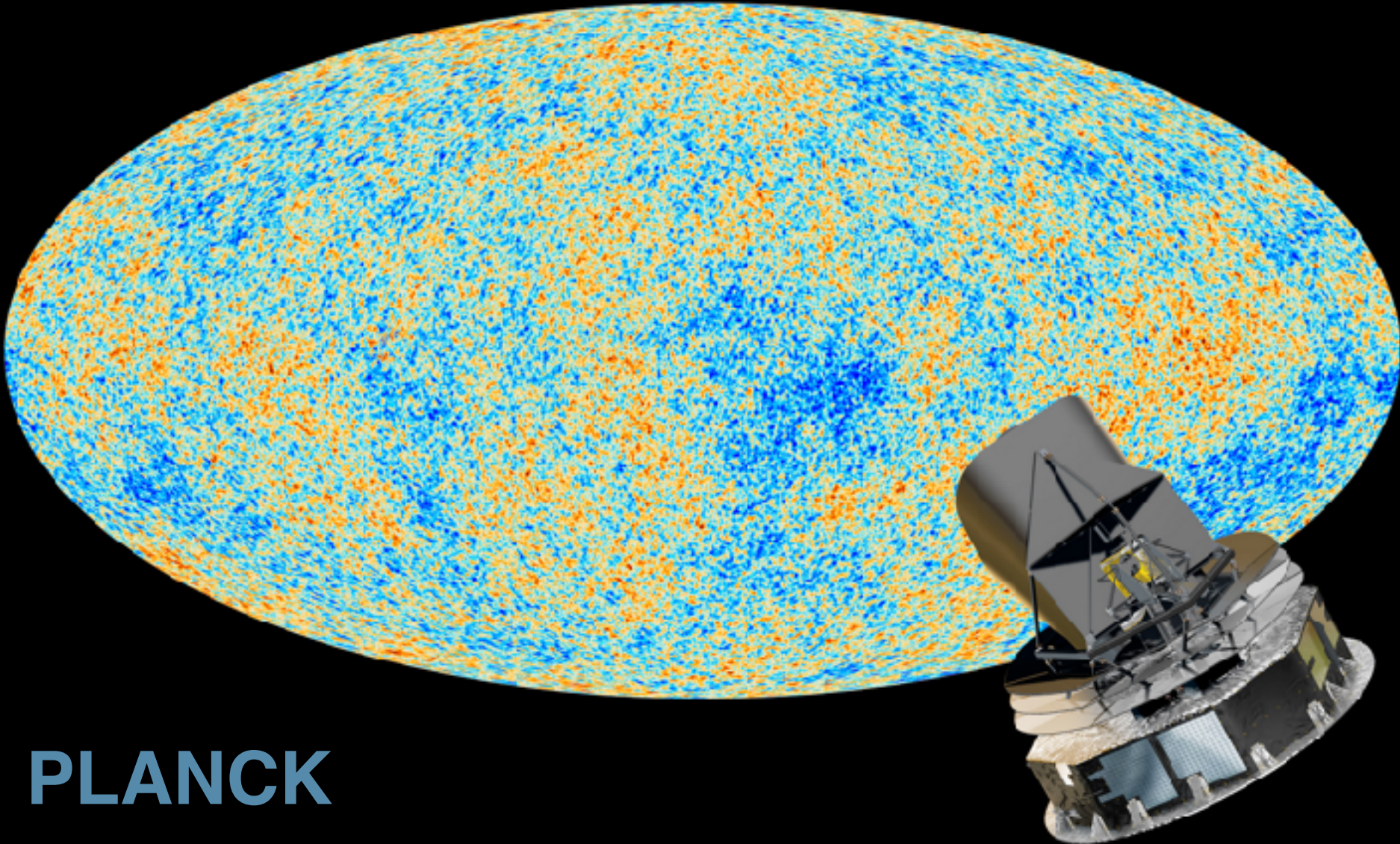


Table 6. Cosmological Parameter Summary

Description	Symbol	WMAP-only
Parameters for Standard Λ CDM Model ^a		
Age of universe	t_0	13.69 ± 0.13 Gyr
Hubble constant	H_0	$71.9^{+2.6}_{-2.7}$ km/s/Mpc
Baryon density	Ω_b	0.0441 ± 0.0030
Physical baryon density	$\Omega_b h^2$	0.02273 ± 0.00062
Dark matter density	Ω_c	0.214 ± 0.027

Gravitational Dark Matter

Parameter	Planck		Planck+lensing		Planck+WP	
	Best fit	68% limits	Best fit	68% limits	Best fit	68% limits
$\Omega_b h^2$	0.022068	0.02207 ± 0.00033	0.022242	0.02217 ± 0.00033	0.022032	0.02205 ± 0.00028
$\Omega_c h^2$	0.12029	0.1196 ± 0.0031	0.11805	0.1186 ± 0.0031	0.12038	0.1199 ± 0.0027
$100\theta_{MC}$	1.04122	1.04132 ± 0.00068	1.04150	1.04141 ± 0.00067	1.04119	1.04131 ± 0.00063
τ	0.0925	0.097 ± 0.038	0.0949	0.089 ± 0.032	0.0925	$0.089^{+0.012}_{-0.014}$
n_s	0.9624	0.9616 ± 0.0094	0.9675	0.9635 ± 0.0094	0.9619	0.9603 ± 0.0073
$\ln(10^{10} A_s)$	3.098	3.103 ± 0.072	3.098	3.085 ± 0.057	3.0980	$3.089^{+0.024}_{-0.027}$
Ω_Λ	0.6825	0.686 ± 0.020	0.6964	0.693 ± 0.019	0.6817	$0.685^{+0.018}_{-0.016}$
Ω_m	0.3175	0.314 ± 0.020	0.3036	0.307 ± 0.019	0.3183	$0.315^{+0.016}_{-0.018}$
σ_8	0.8344	0.834 ± 0.027	0.8285	0.823 ± 0.018	0.8347	0.829 ± 0.012



Age of u
Hubble c
Baryon c
Physical
Dark ma

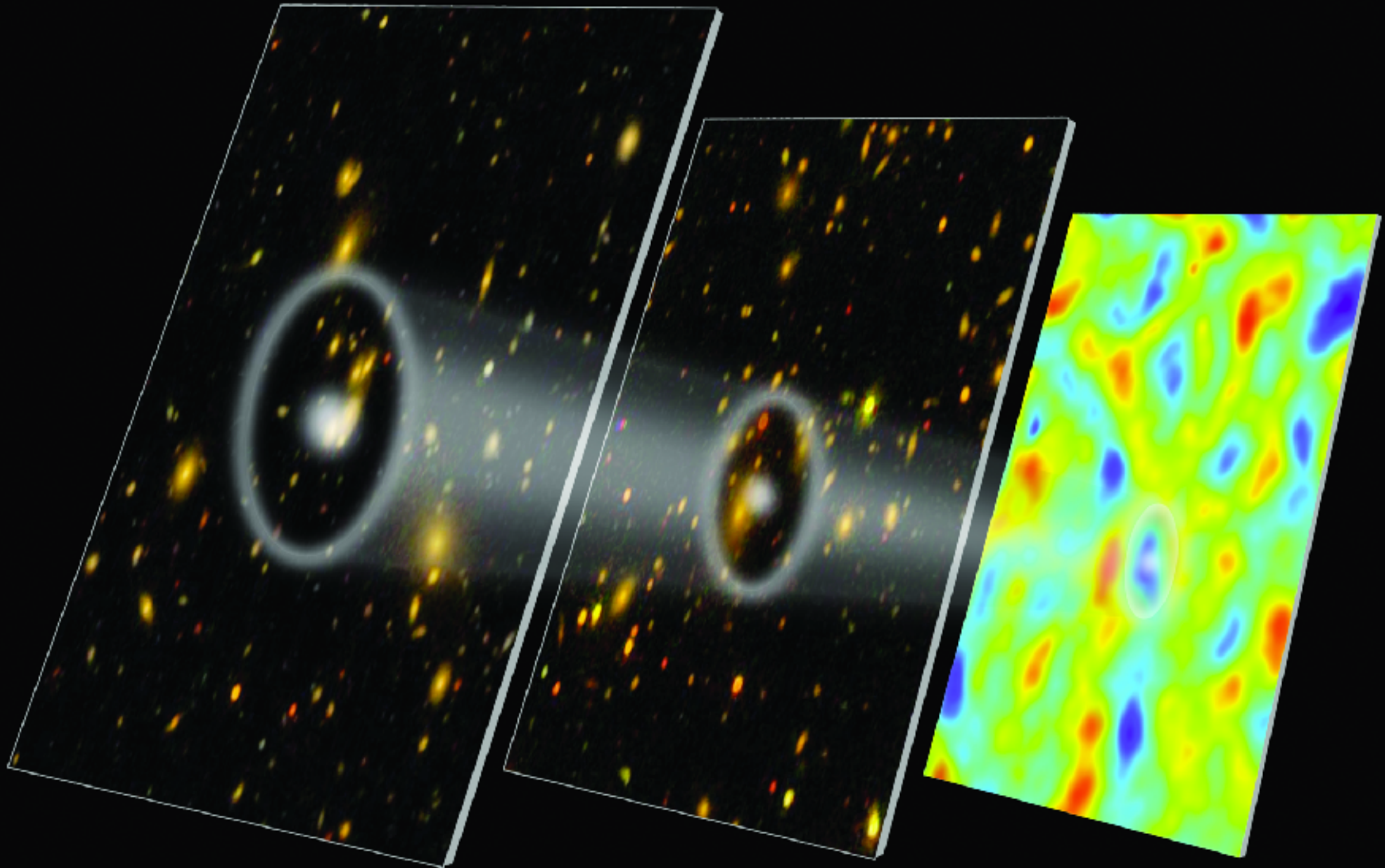
Gravitational Dark Matter

A visualization of the cosmic web, showing a vast network of dark matter filaments and galaxy clusters. The filaments are represented by thin, glowing yellow lines against a dark blue background, forming a complex, interconnected web. The clusters are represented by denser, brighter yellow regions. The overall structure is highly irregular and fractal-like, illustrating the large-scale structure of the universe.

Large Scale Structure

Gravitational Dark Matter

Baryonic Acoustic Oscillations



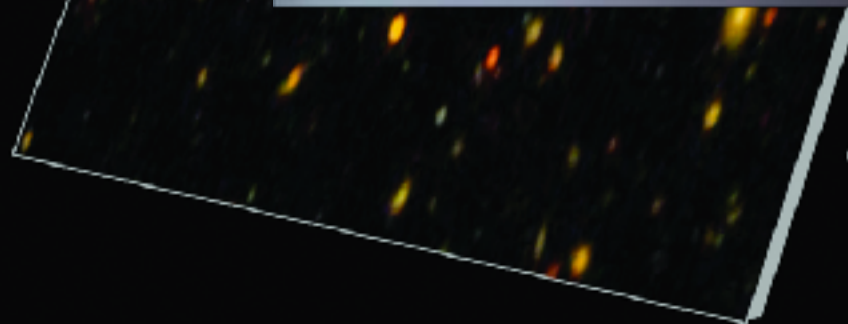
Galaxy map 3.8 billion years ago

Galaxy map 5.5 billion years ago

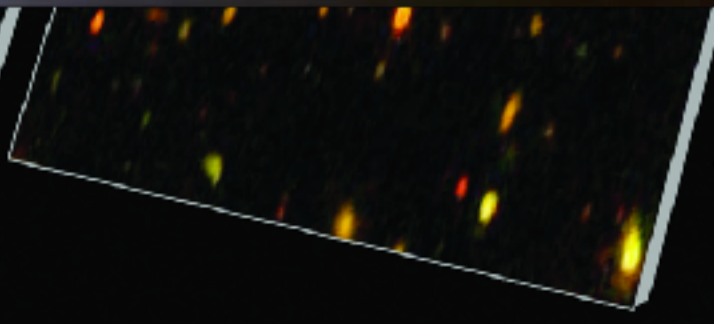
CMB 13.7 billion years ago

Gravitational Dark Matter

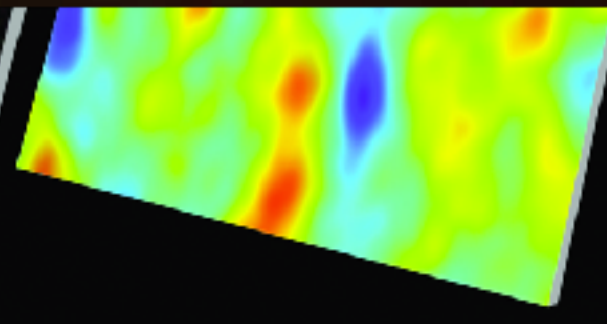
Type 1A Supernove



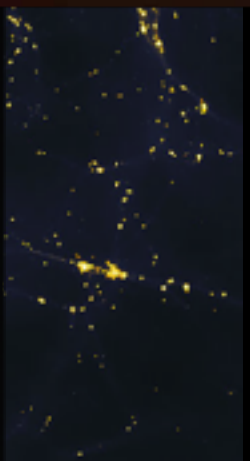
Galaxy map 3.8 billion years ago



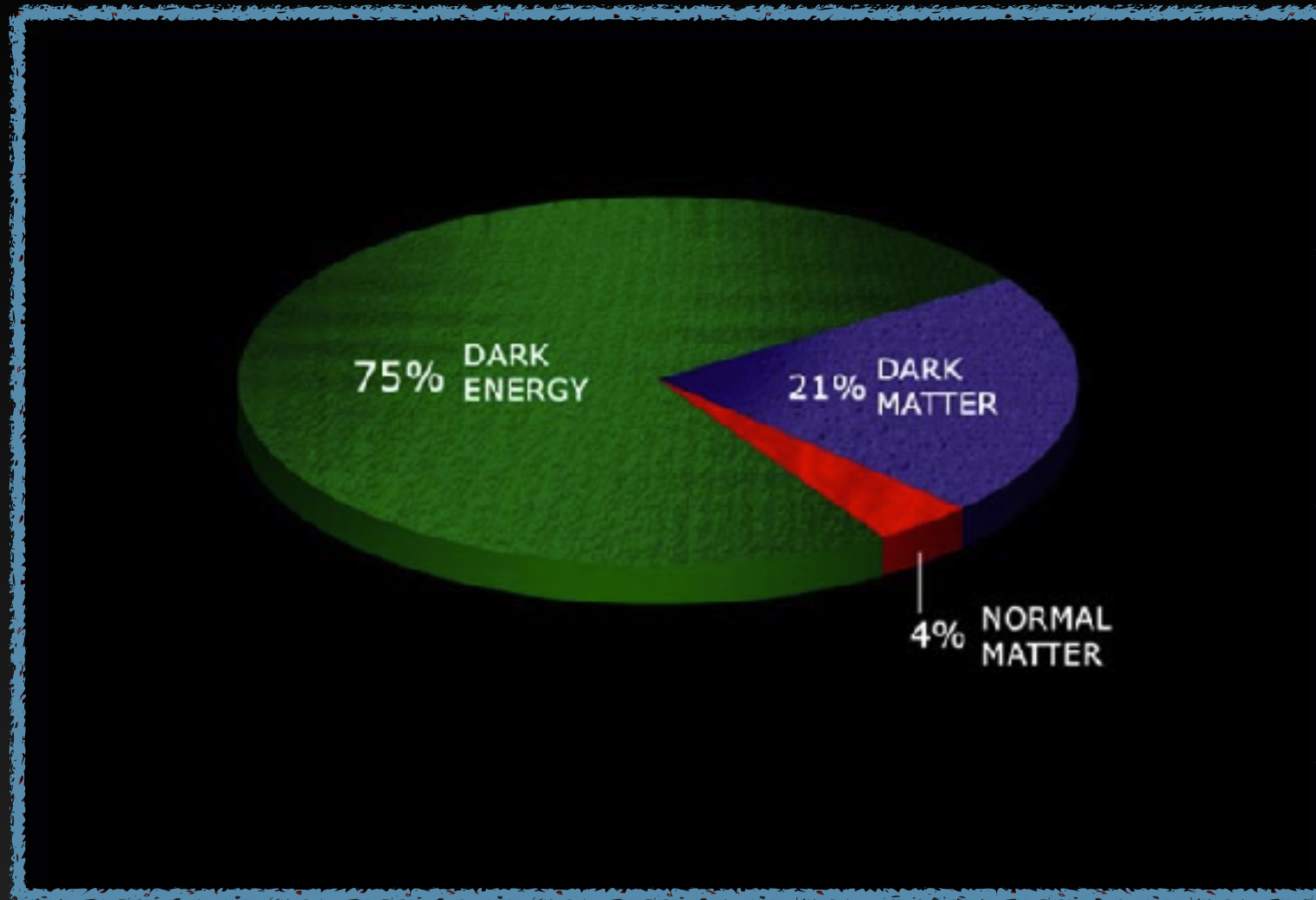
Galaxy map 5.5 billion years ago



CMB 13.7 billion years ago



Dark Matter Cosmology

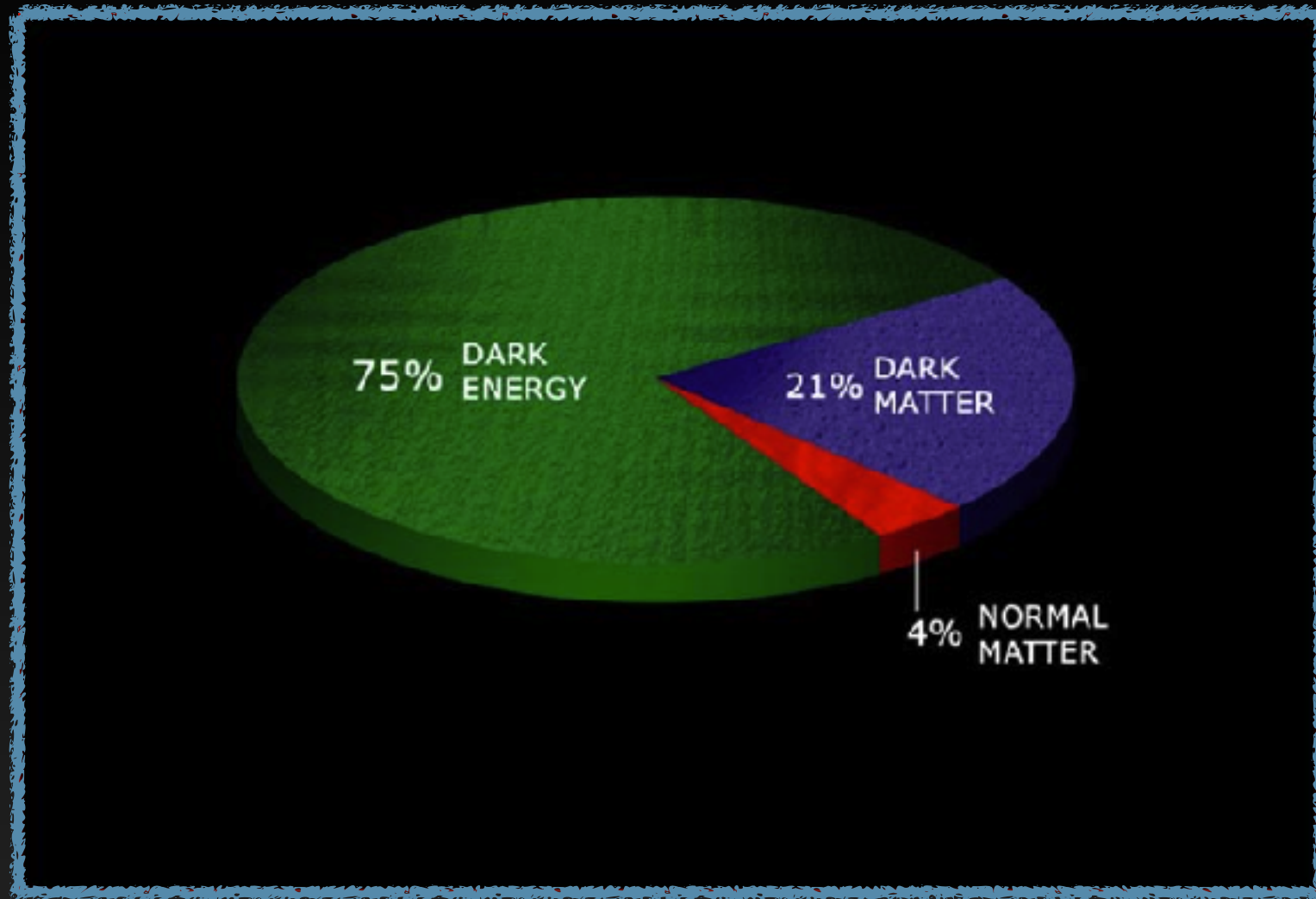


Dark Matter Is:

- 1.) Dark
- 2.) Stable
- 3.) Cold
- 4.) Collisionless

No known particle has these properties!

Particle Dark Matter



The Density of Dark Matter is similar to the density of protons in our universe.

This requires either significant fine tuning, or a dynamical interaction - which in QFT must correspond to some force.

Particle Dark Matter

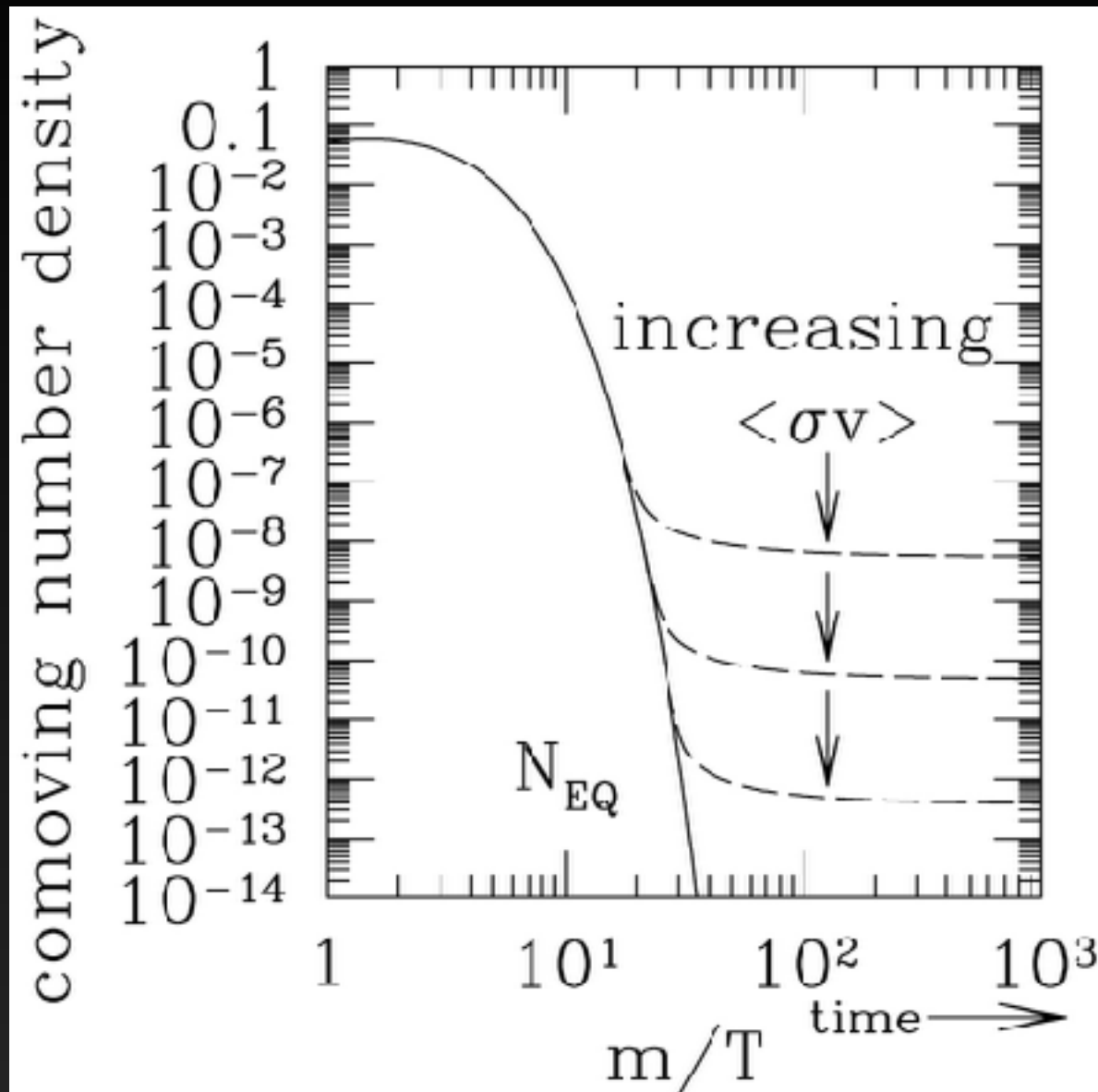
Gravity is Weak!

- The search for a dark matter particle must rely on another force.

Does the dark matter particle have any other interactions?

- Electromagnetic Interactions
- Strong Force Interactions
- Weak Force Interactions
- Planck Scale Interactions
- Something Else?

Dark Matter in Thermal Equilibrium



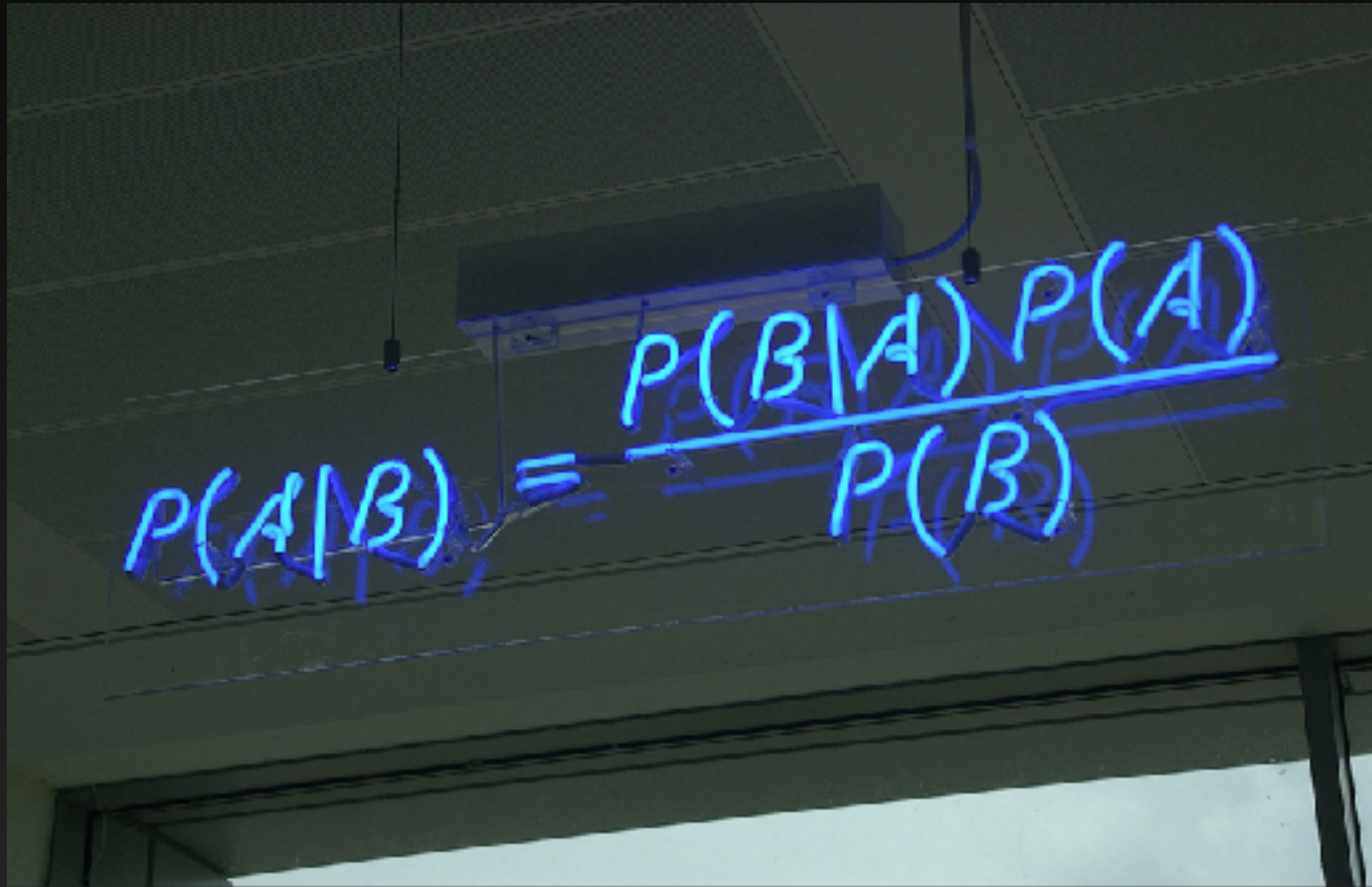
A particle with a weak interaction cross-section and a mass on the weak scale is expected to naturally obtain the correct relic abundance through thermal freeze-out in the Early Universe.

$$\left(\frac{\Omega_\chi}{0.2}\right) \simeq \frac{x_{\text{f.o.}}}{20} \left(\frac{10^{-8} \text{ GeV}^{-2}}{\sigma}\right)$$

$$\langle\sigma v\rangle \sim 10^{-8} \text{ GeV}^{-2} \left(3 \times 10^{-28} \text{ GeV}^2 \text{ cm}^2\right) 10^{10} \frac{\text{cm}}{\text{s}} = 3 \times 10^{-26} \frac{\text{cm}^3}{\text{s}}$$

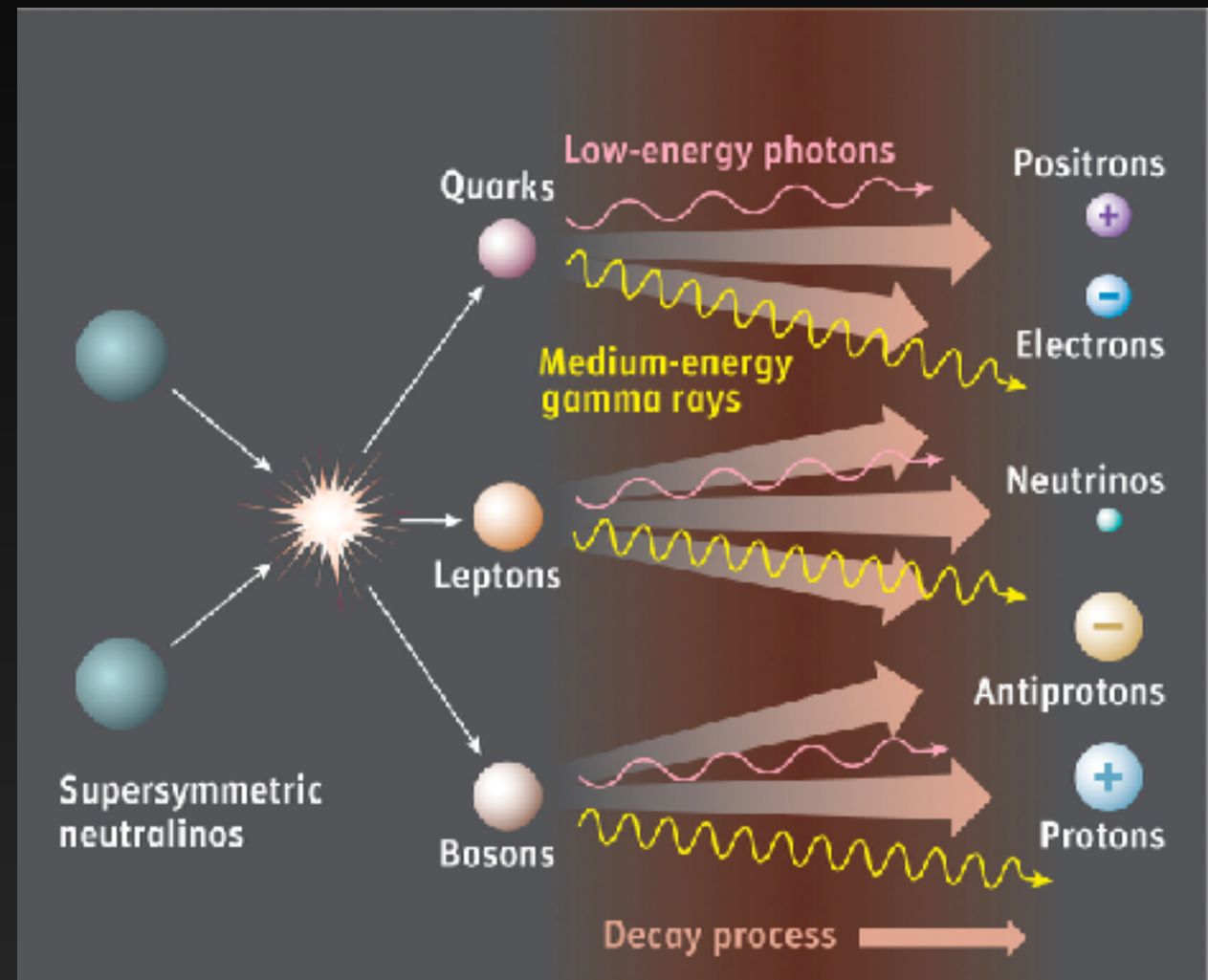
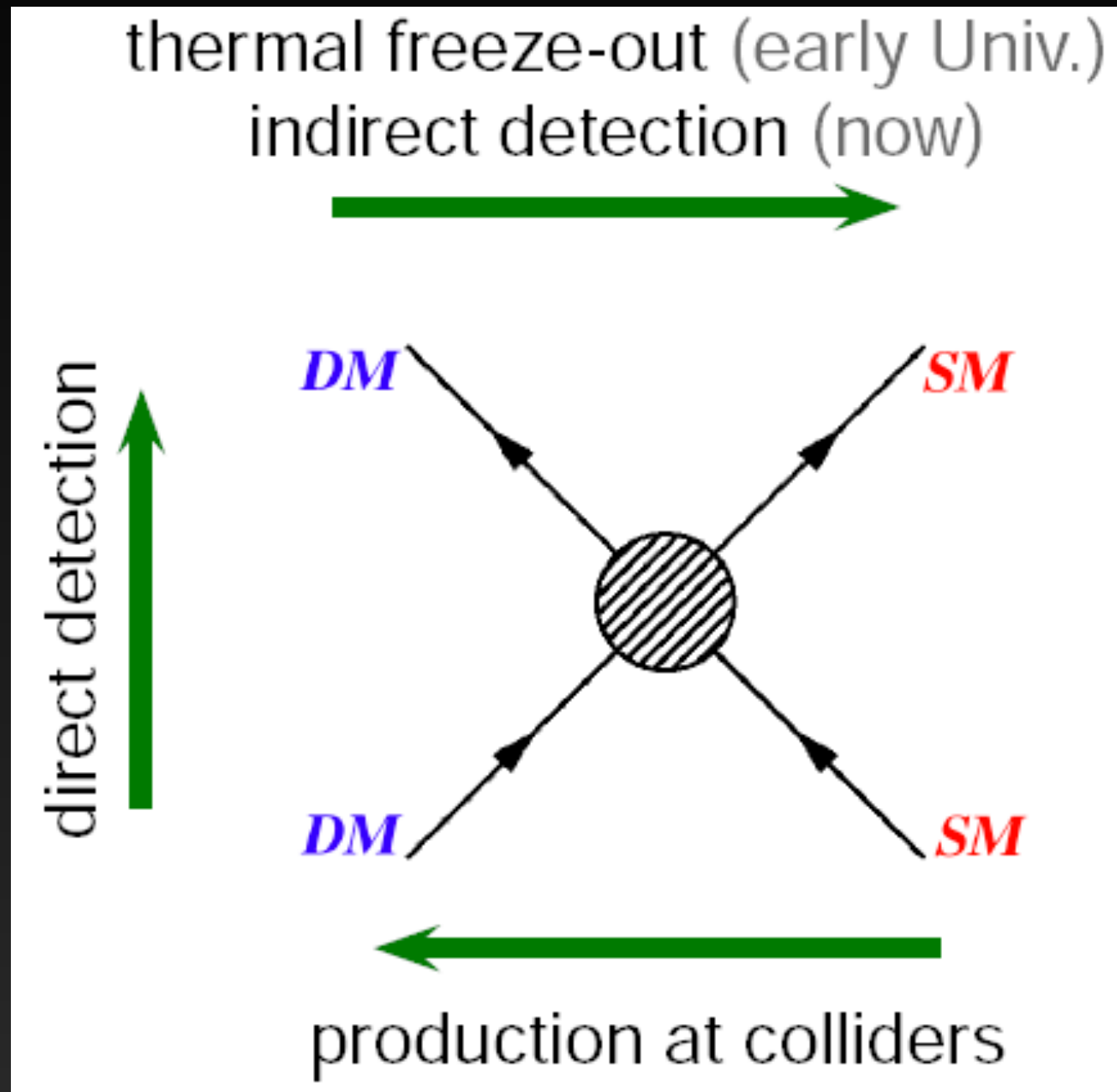
Observing a Dark Matter Particle

Myriad Evidence Suggests Dark Matter exists, and should have non-gravitational interactions:

A photograph of a blue neon sign mounted on a wall. The sign displays the formula for conditional probability: $P(A|B) = \frac{P(B|A)P(A)}{P(B)}$. The sign is made of several pieces of neon tubing, with some parts appearing slightly blurred or overlapping.
$$P(A|B) = \frac{P(B|A)P(A)}{P(B)}$$

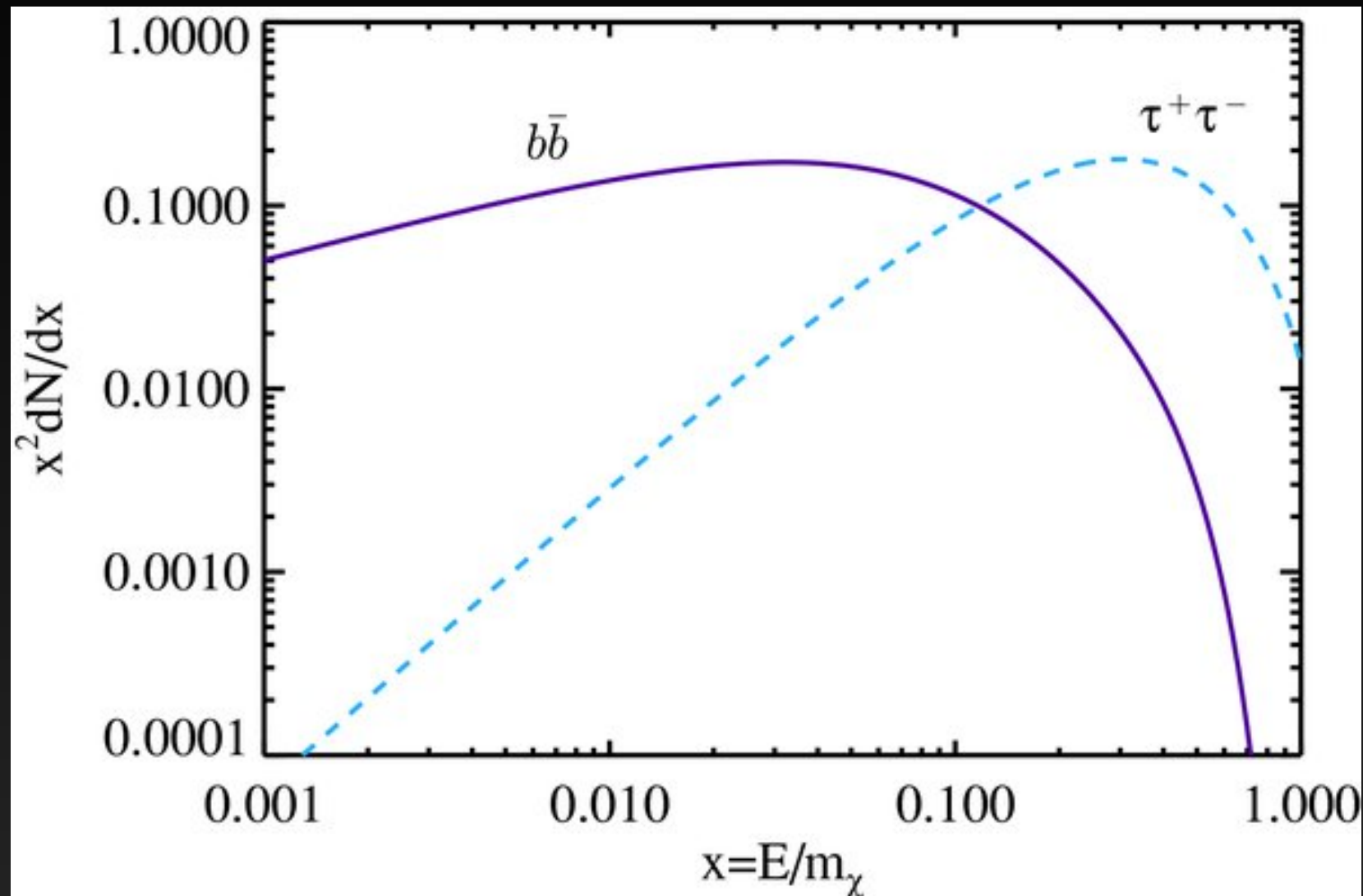
We shouldn't think of dark matter searches as a "needle in a haystack". Our theoretical priors should lead us to bet that particle dark matter can be feasibly observed.

Gamma-Rays from WIMPs



If dark matter had a thermal cross-section in the early universe, it should still have an observable cross-section today.

Gamma-Rays from WIMPs



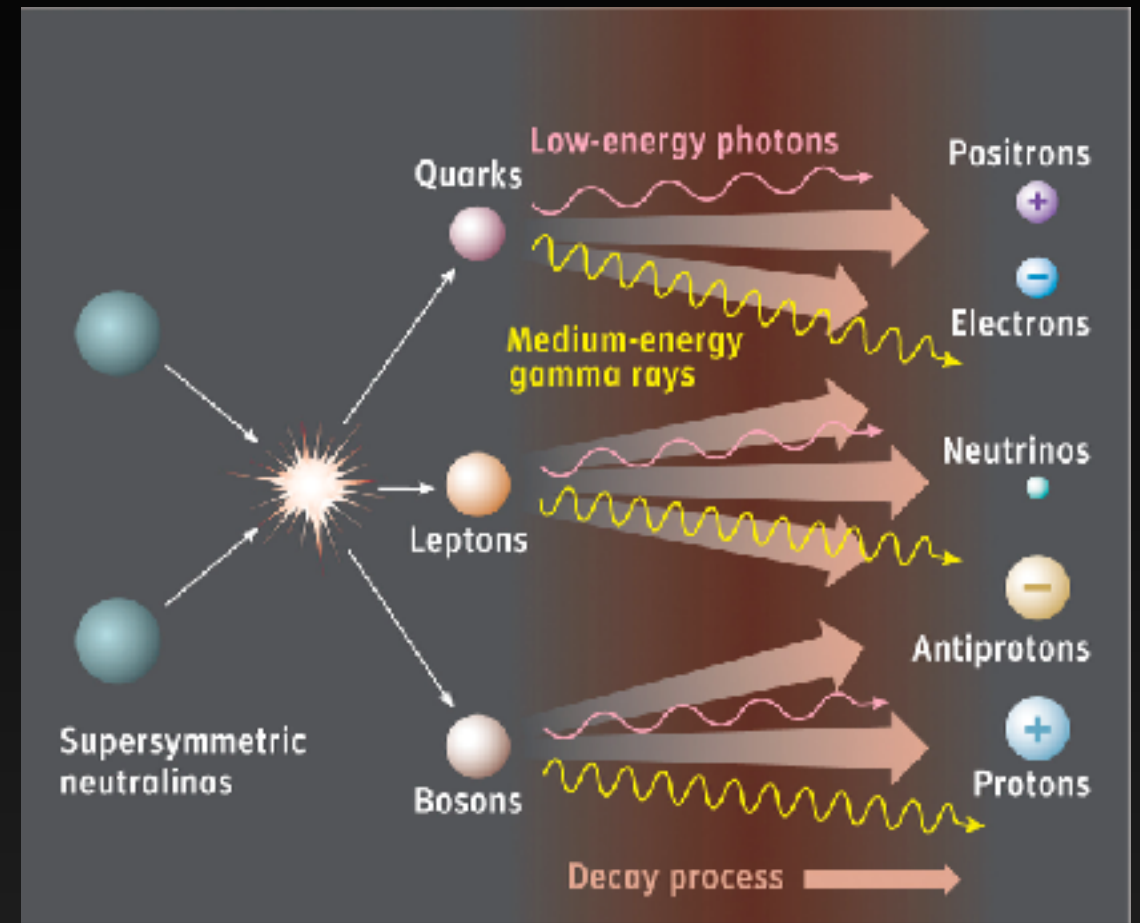
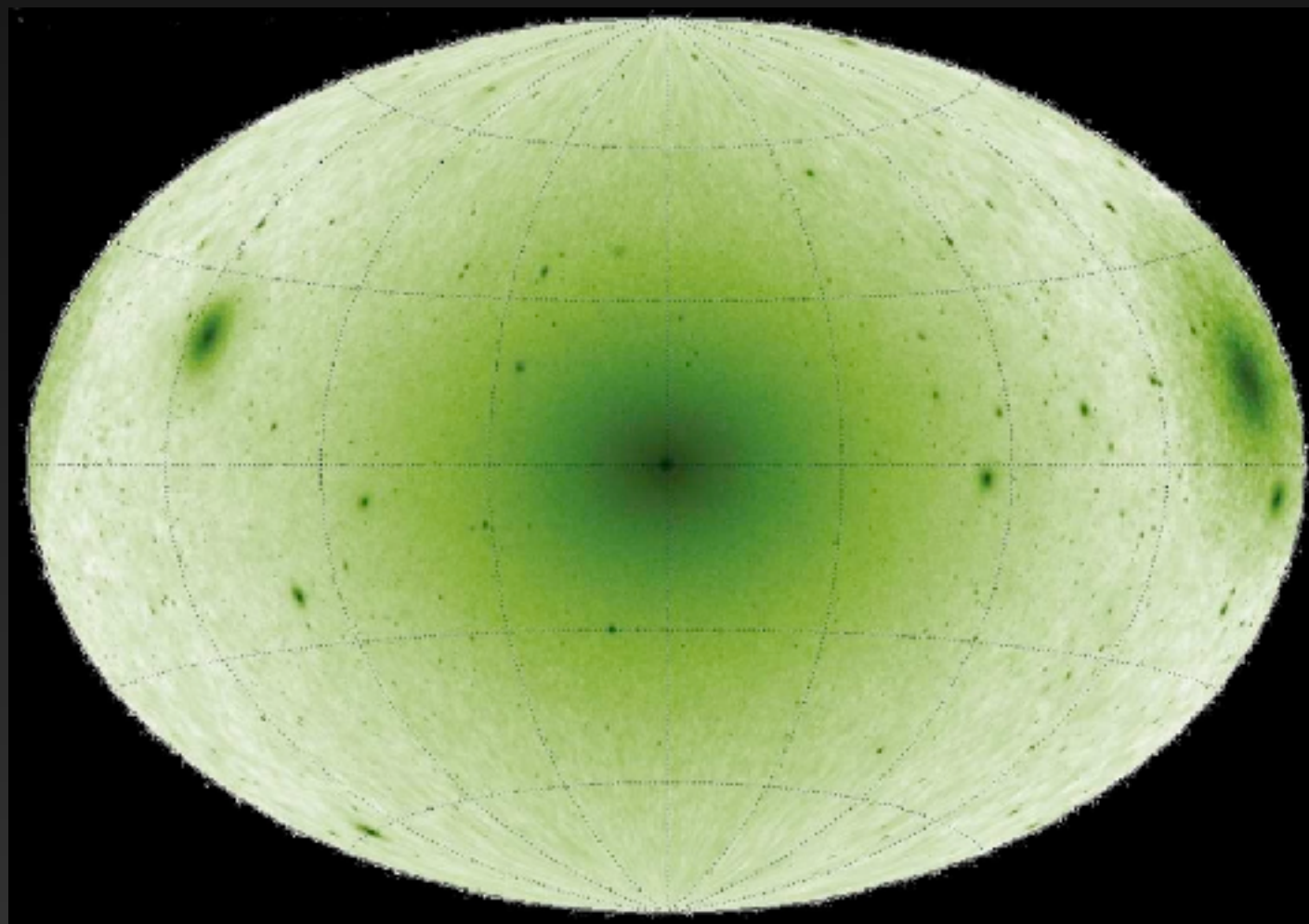
Once a standard model final state is selected, the resulting photon spectrum can be calculated from known physics.

For WIMP scale dark matter, photon energy peaks in the GeV range.

Dark Matter Annihilation in the Galactic Center

WIMPs are currently among the most well-motivated dark matter models.

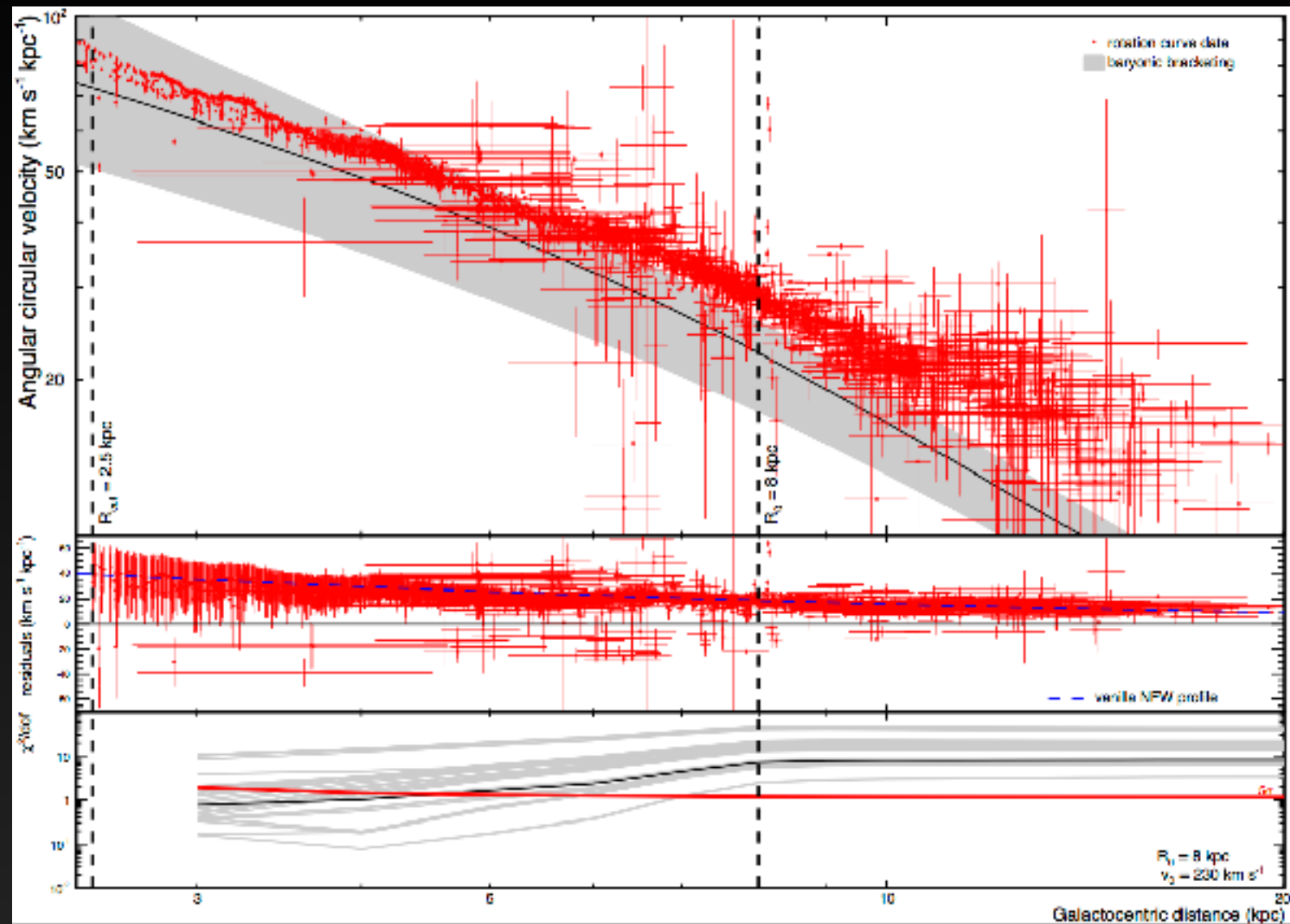
WIMP annihilation naturally produces a significant cosmic-ray (and gamma-ray) flux.



Dark Matter structure simulations uniformly predict that the GC is the brightest source of WIMP annihilations.

Standard scenarios predict the flux from the GC exceeds dSphs by a factor of $\sim 100 - 1000$.

Dark Matter Annihilation in the Galactic Center



Recently, observations by Iocco, Pato & Bertone (2015) have used stellar velocity measurements to directly measure the dark matter density in the Milky Way (to within 3 kpc of the GC).

Future measurements (employing Gaia data) will have the ability to significantly improve these measurements.

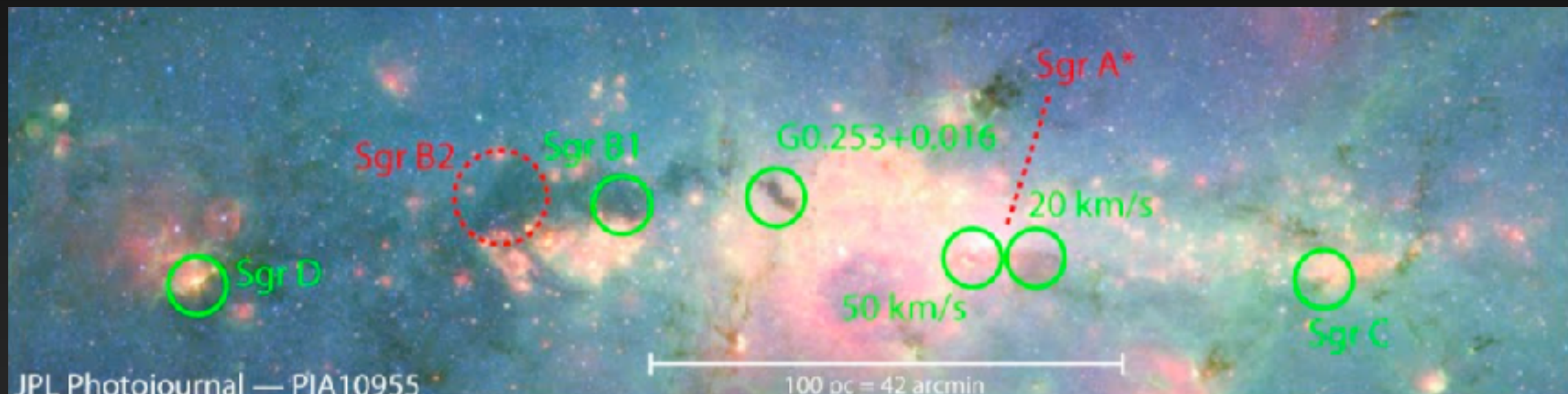
Iocco, Pato & Bertone (2015)

Dark Matter Annihilation in the Galactic Center

**But What About
Astrophysics?**

The Central Molecular Zone

- 400 pc x 80 pc
- $10^7 M_{\odot}$ of gas in Molecular Clouds
- Conditions similar to nearby starburst galaxies

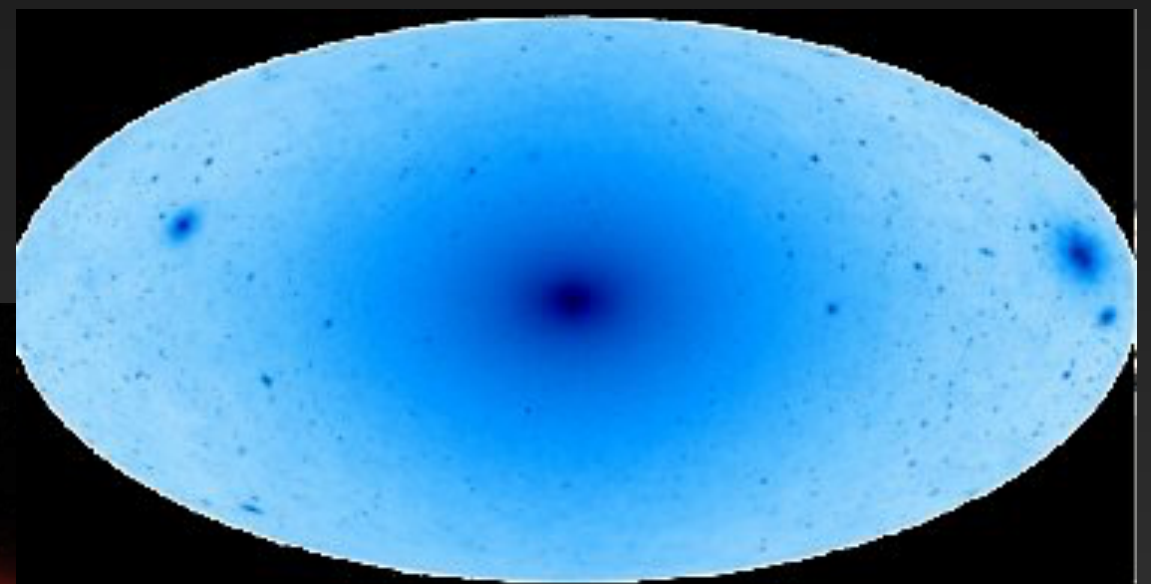
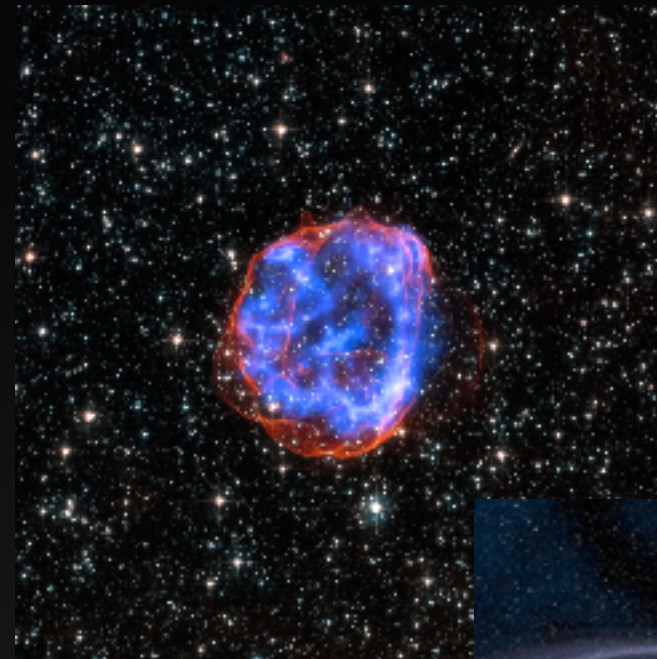


- Molecular Gas clouds in the Central Molecular Zone are hot (~ 50 - 100 K)
- Indicative of heating by a significant cosmic-ray population confined in the central molecular zone. (Yusef-Zadeh et al. 2013)

What Generates these Cosmic-Rays?

The Galactic center region is known to contain nearly every known cosmic-ray acceleration mechanism.

- 1.) Supernovae
- 2.) Pulsars
- 3.) Sgr A*
- 4.) Reacceleration
- 5.) Dark Matter Annihilation?



The Galactic Center Supernovae

Multiwavelength observations indicate that the Galactic Center is a dense star-forming environment.

3-20% of the total Galactic Star Formation Rate is contained within the Central Molecular Zone.

2-4% - ISOGAL Survey Immer et al. (2012)

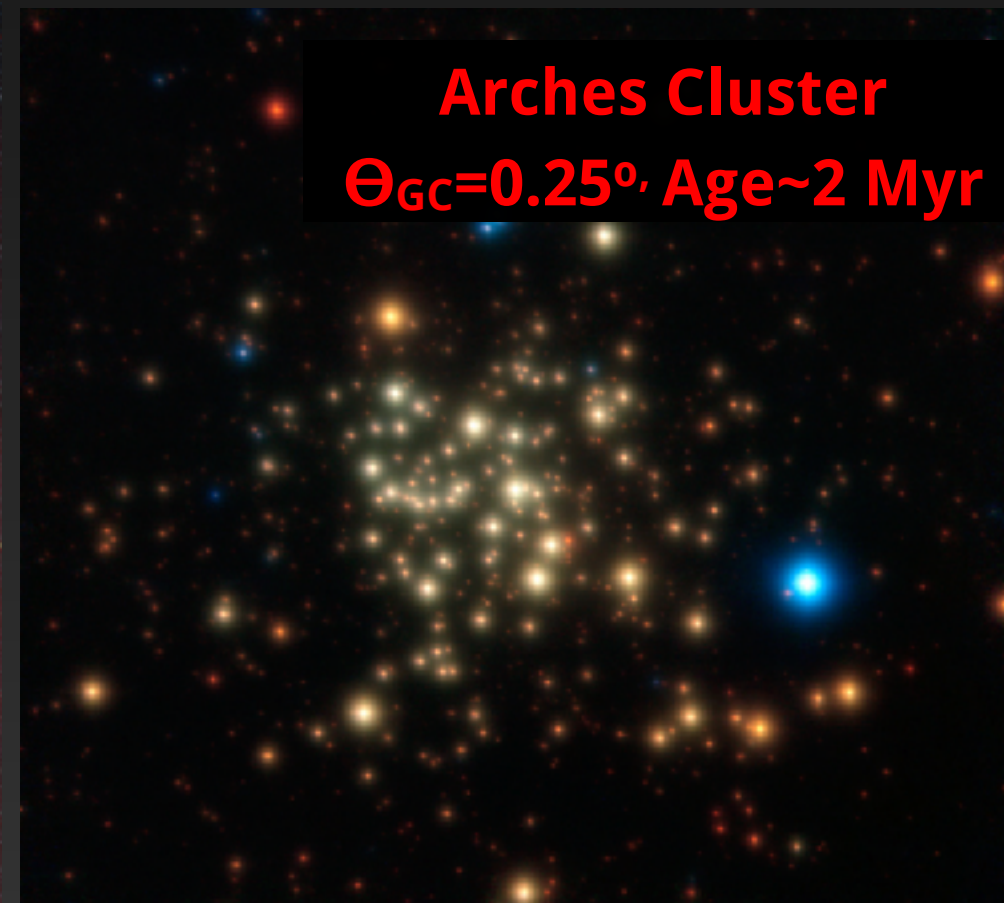
2.5-5% - Young Stellar Objects Yusef-Zadeh et al. (2009)

5-10% - Infrared Flux Longmore et al. (2013)

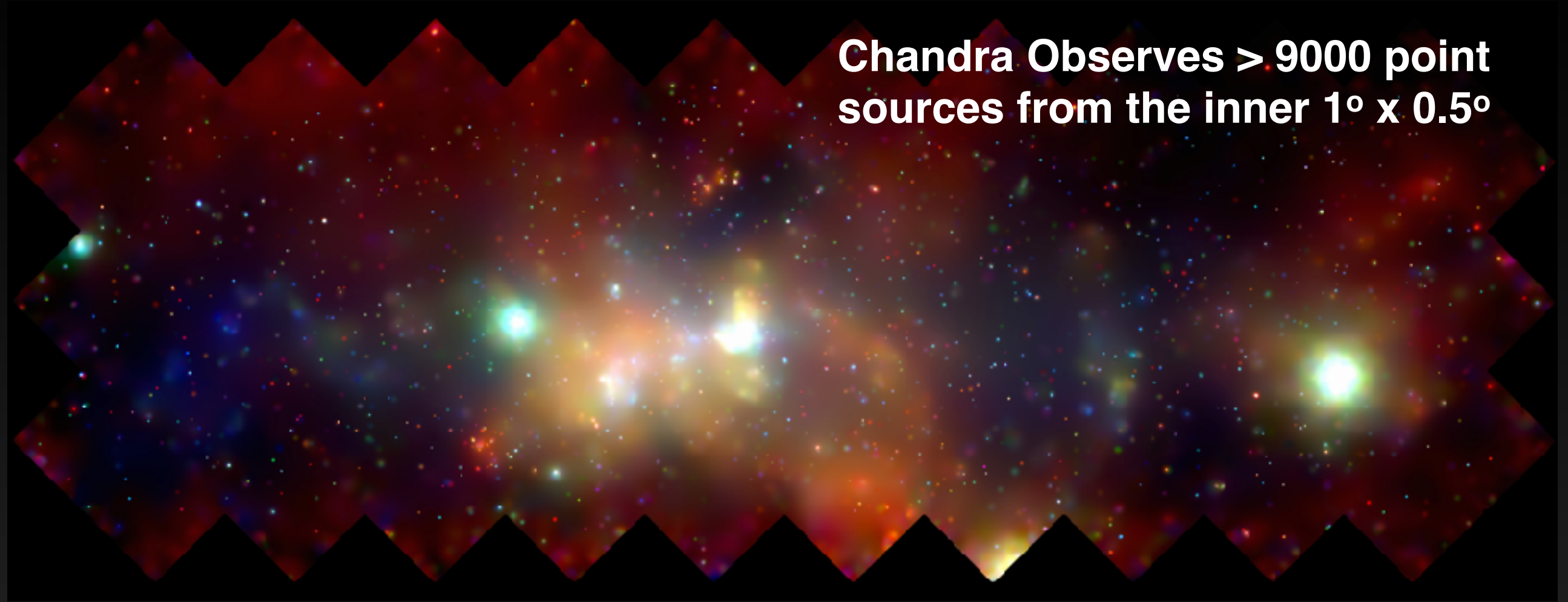
10-20% - Wolf-Rayet Stars Rosslowe & Crowther (2014)

2% - Far-IR Flux Thompson et al. (2007)

2.5-6% - SN1a Schanne et al. (2007)



Galactic Center Pulsars

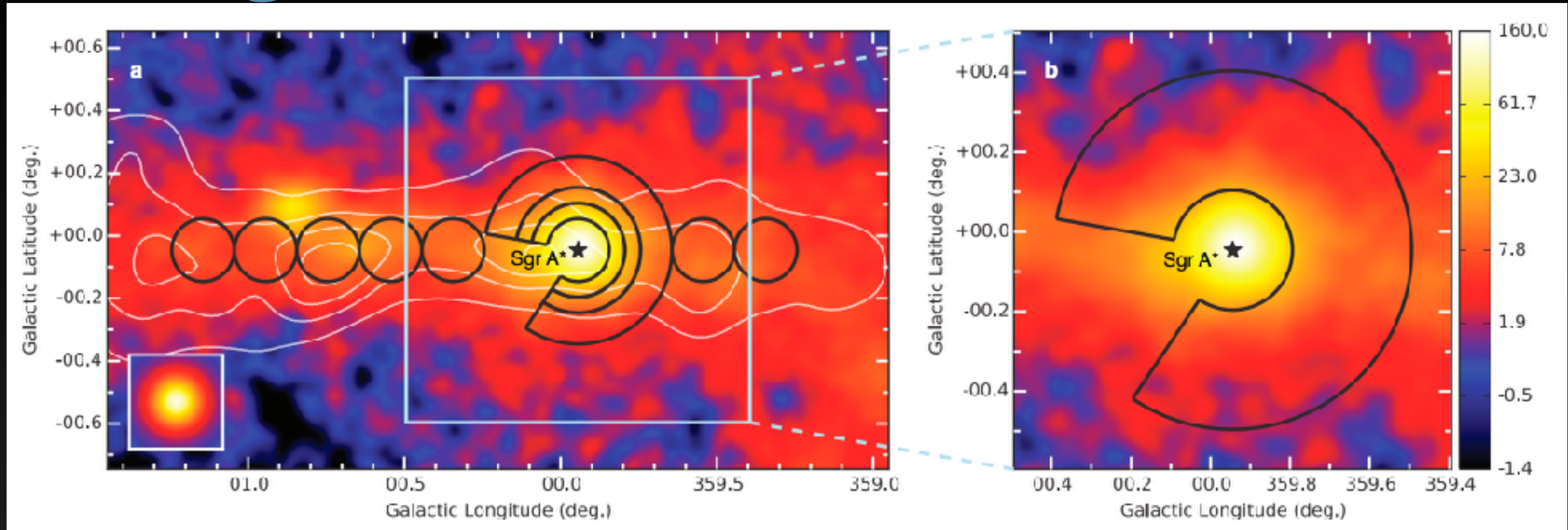


Chandra Observes > 9000 point sources from the inner 1° x 0.5°

The Galactic Center is expected to host a significant population of both young pulsars (due to its high SFR), and millisecond pulsars (in part from the disruption of Globular Clusters).

Over the lifetime of a young (recycled) pulsar, $\sim 10^{50}$ erg of energy is released, primarily in the form of relativistic e^+e^- pairs.

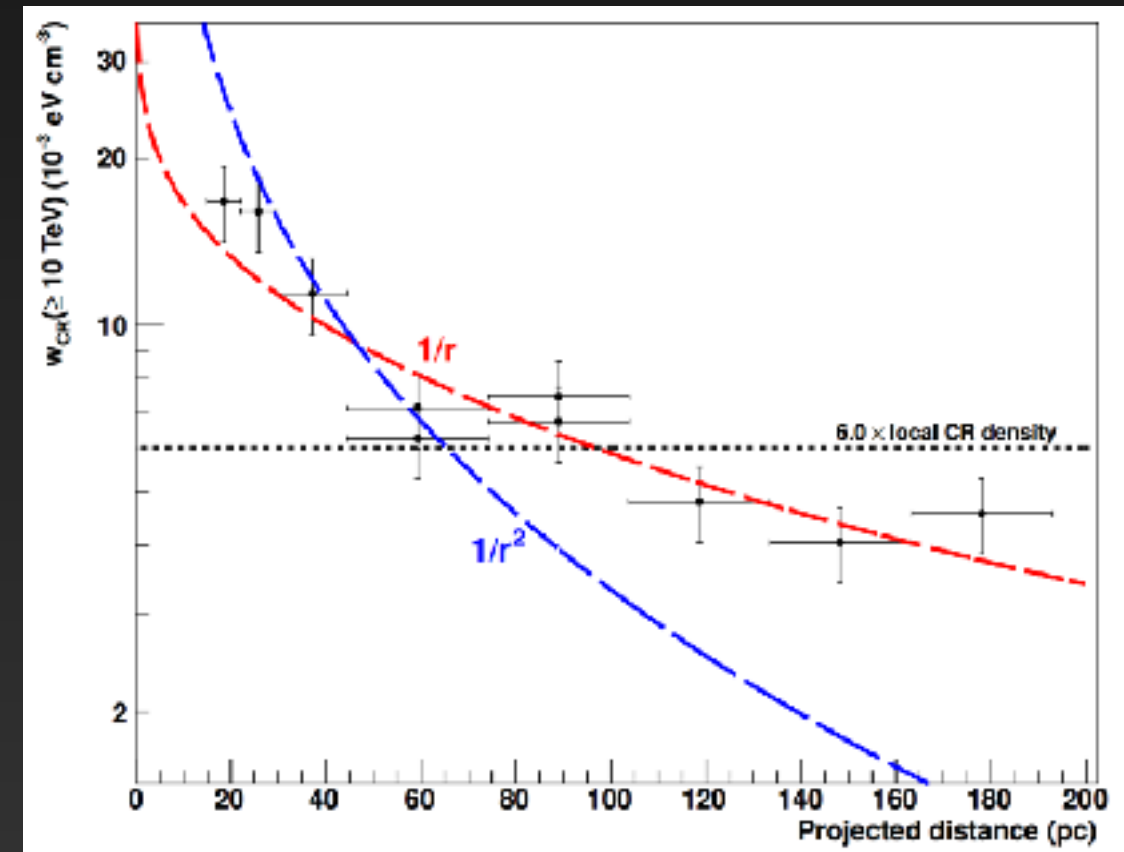
The Sgr A* Source



HESS has detected diffuse gamma-ray emission at energies ~ 100 TeV.

This is not observed in even the youngest supernova remnants.

The emission profile is indicative of diffusion from the central BH.

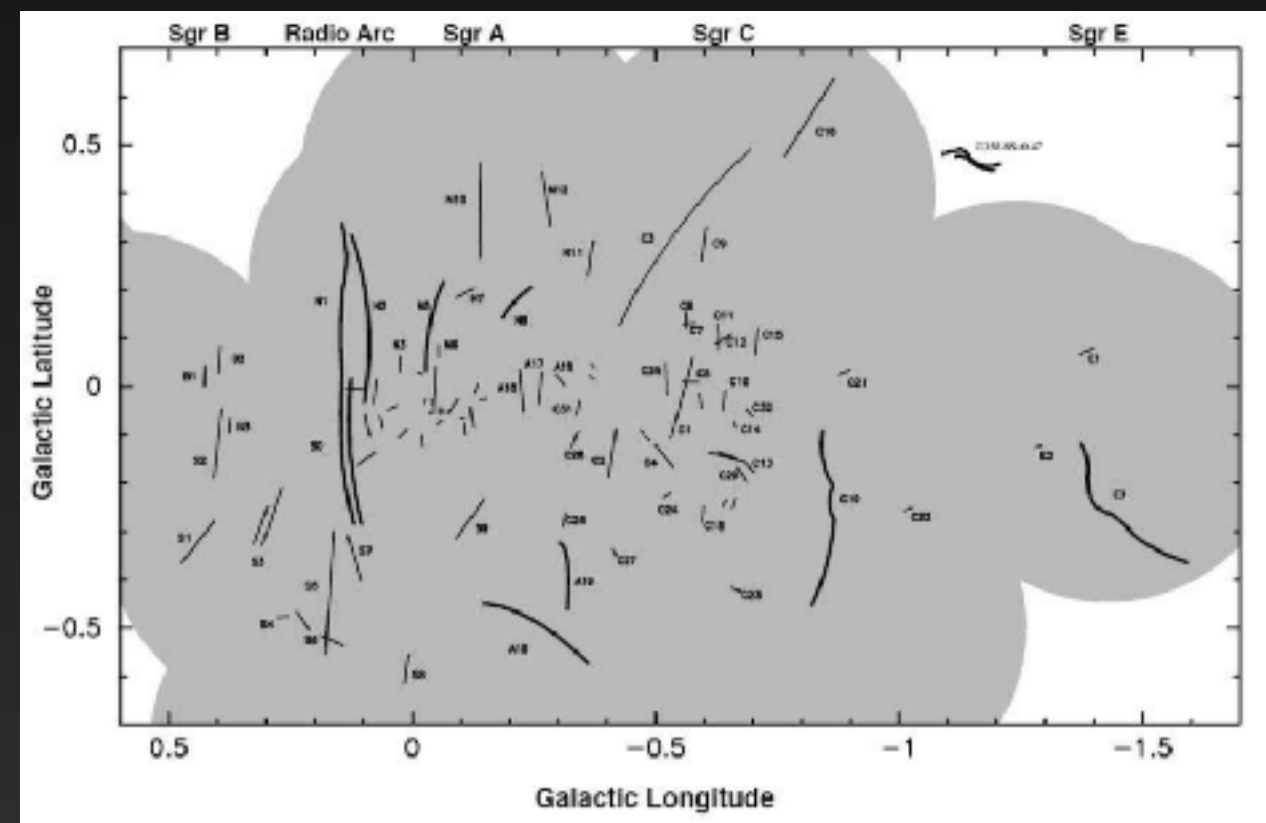


Reacceleration

More than 80 filamentary structures identified in the central $2^\circ \times 1^\circ$.

The filaments are observed as highly polarized, hard-spectrum synchrotron sources – indicative of strongly ordered magnetic fields and hard injected electron spectra.

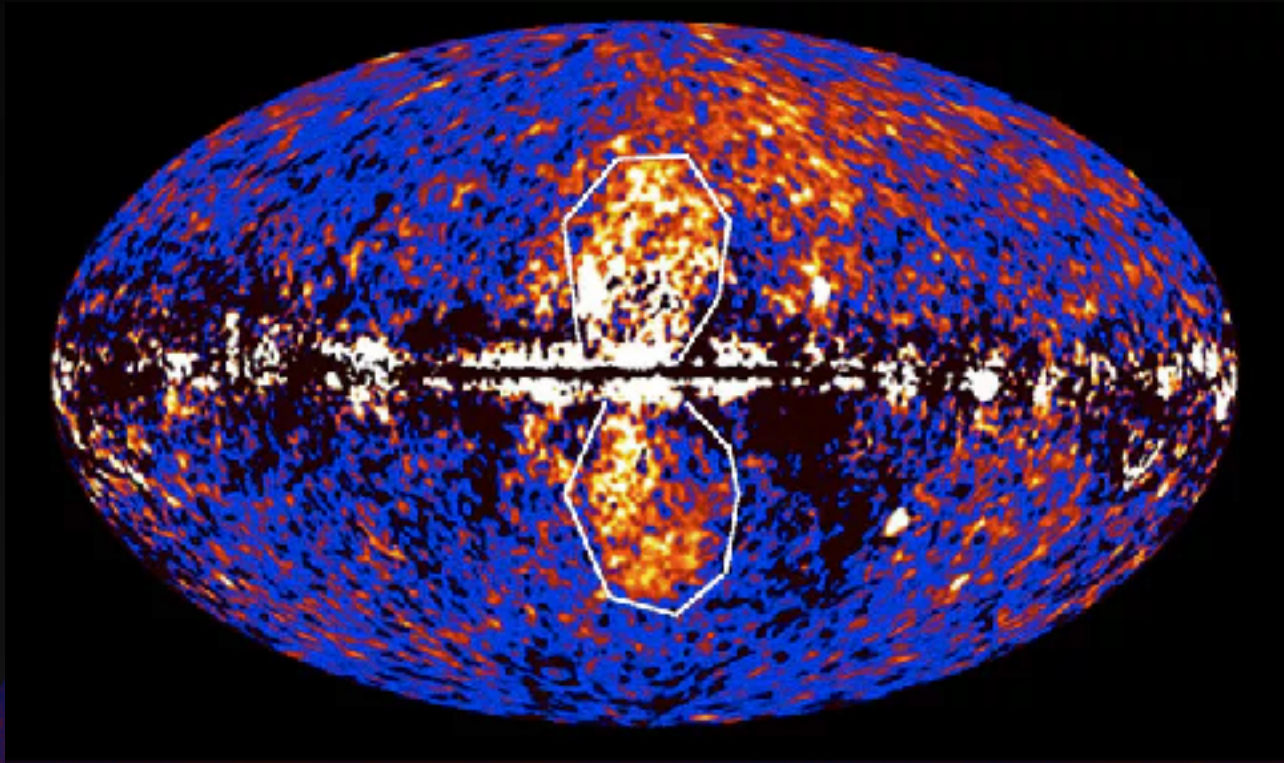
The best astrophysical explanation involves significant re-acceleration via magnetic reconnection (Lesch & Riech 1992, Lieb et al. (2004).



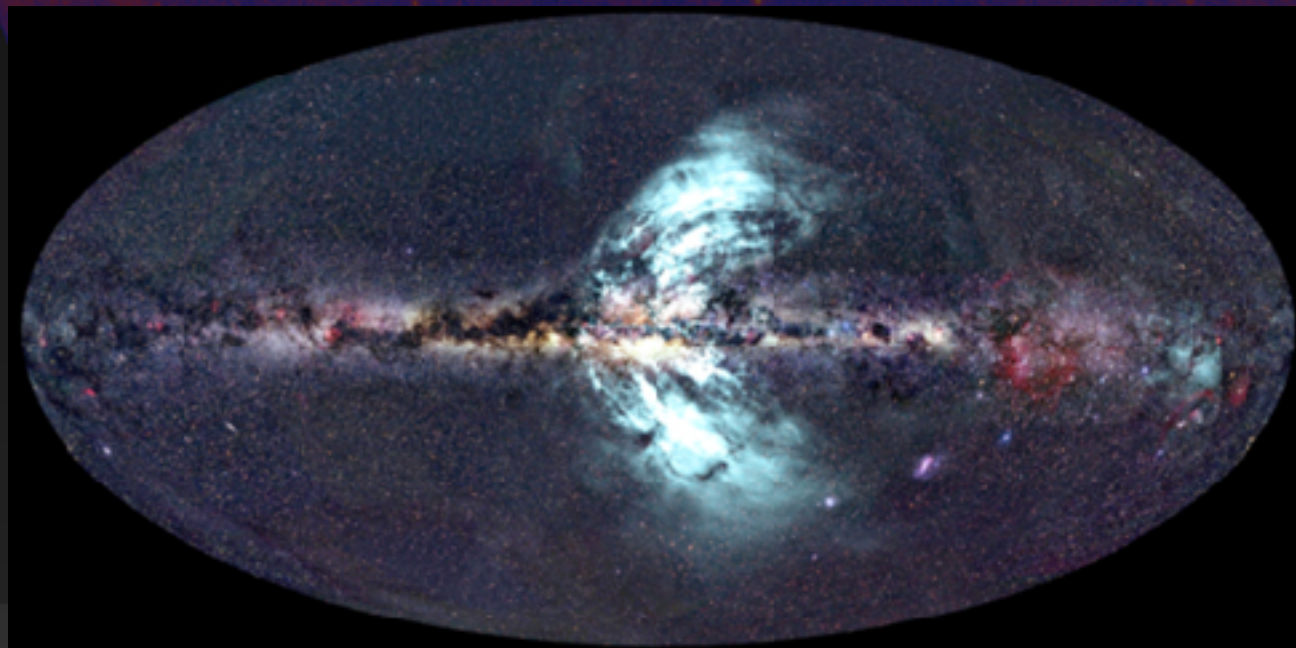
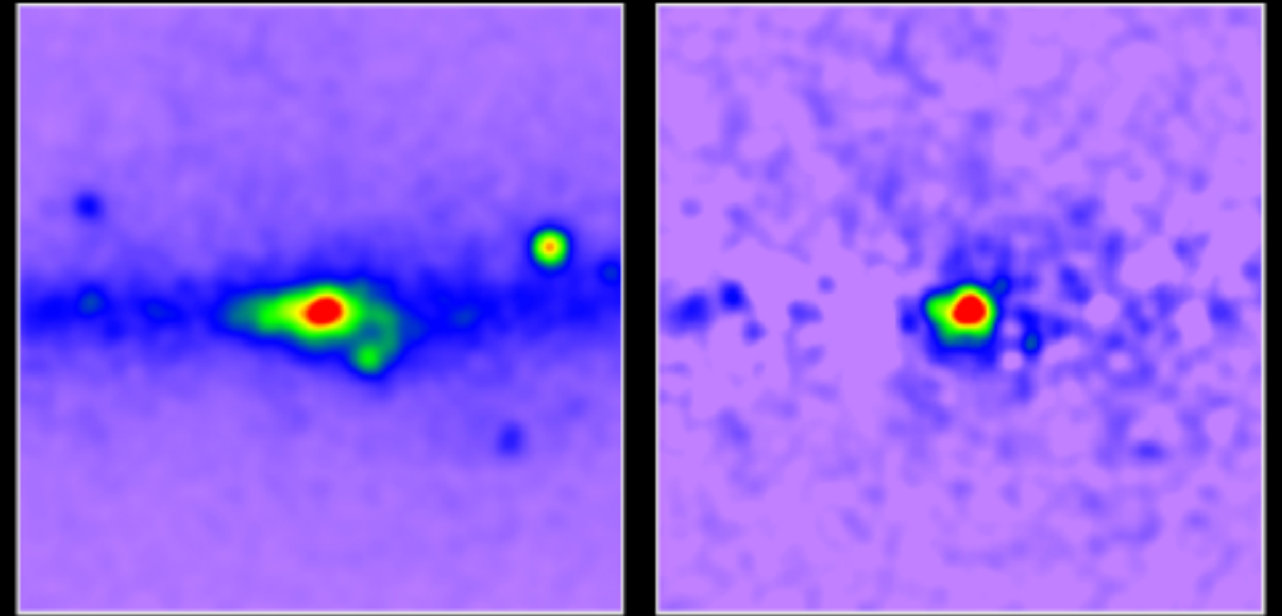
Yusef-Zadeh et al. (2004)

Non-Thermal Emission (Observables)

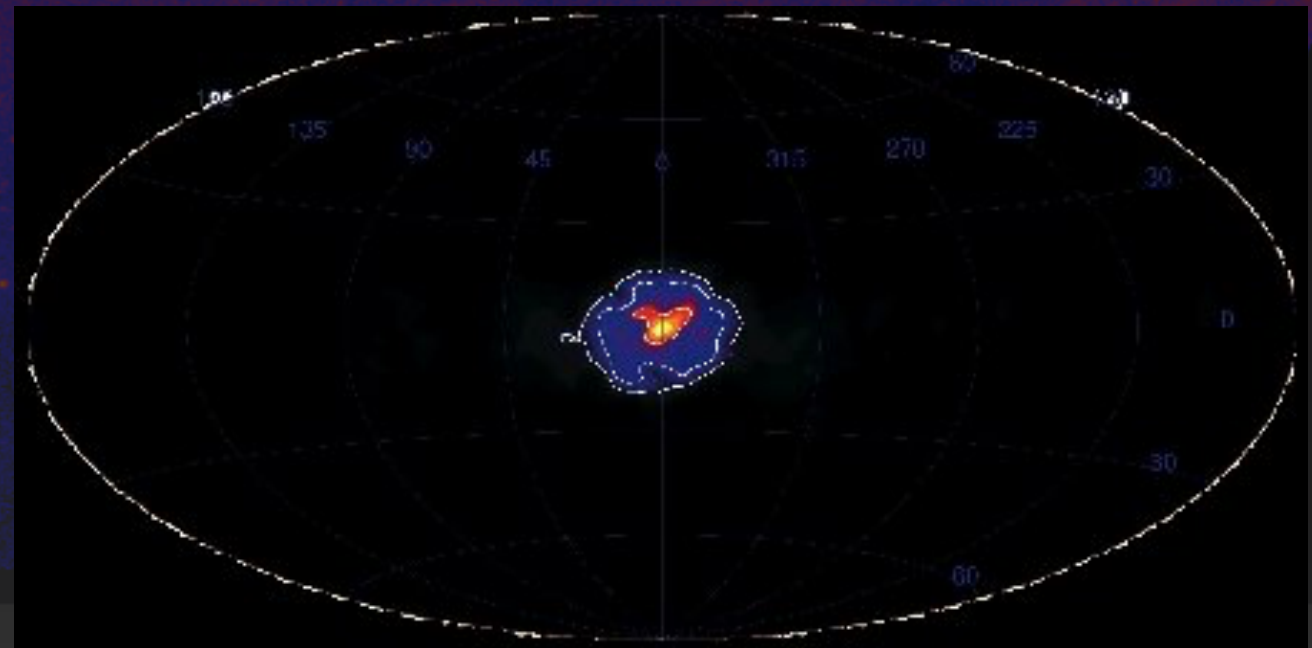
Fermi Bubbles



GeV Excess



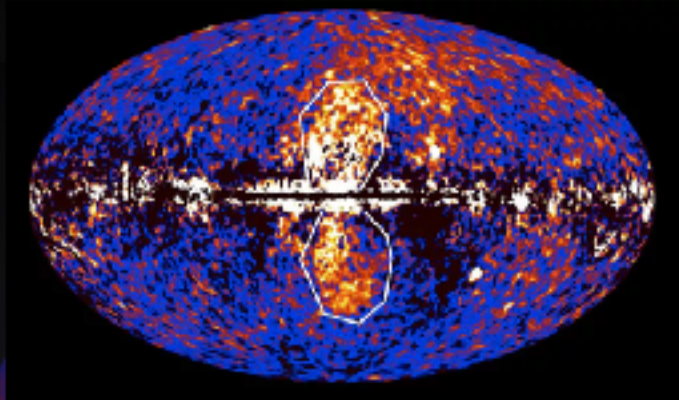
WMAP/PLANCK Haze



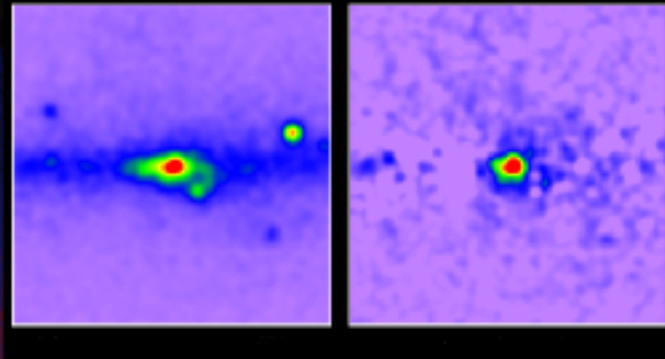
Integral 511 keV Excess

Non-Thermal Emission (Observables)

Fermi Bubbles

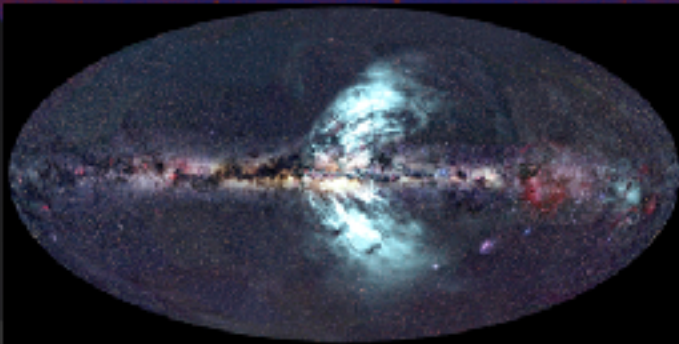


GeV Excess

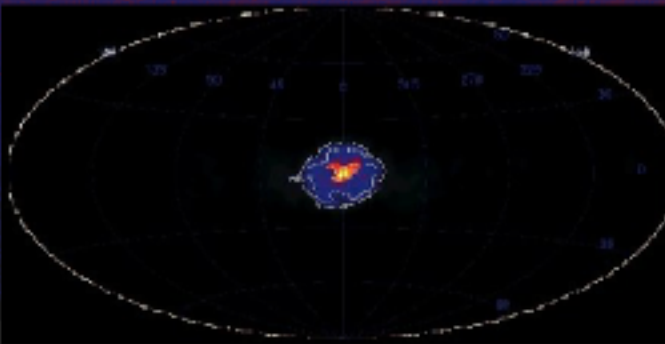


The photon excesses extend very far from the central molecular region!

WMAP/PLANCK Haze



Integral 511 keV Excess



This:

- (a) Indicates the relative power of Galactic center accelerators, compared to the Galactic plane.
- (b) Provides a large field of view for studies of GC emission.
- (c) Implies that propagation is important!

Cosmic-Ray Propagation



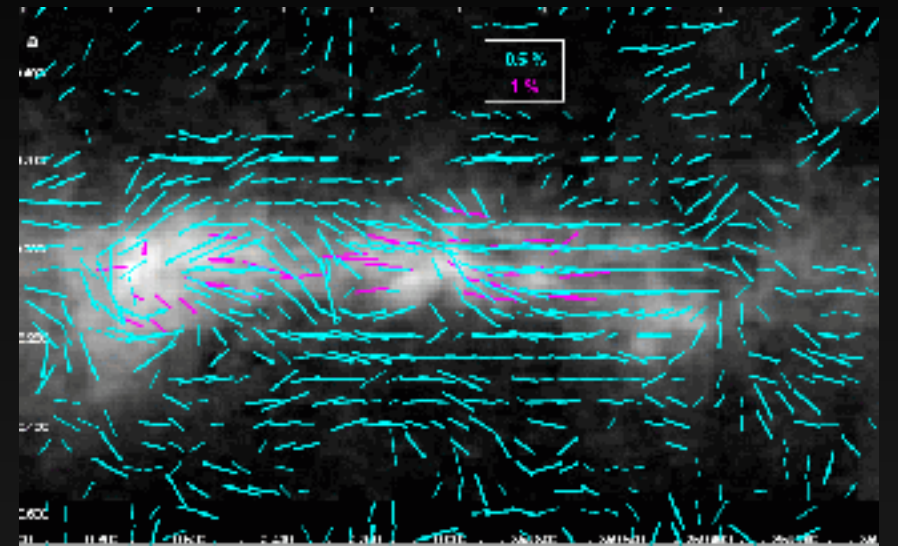
Start with a source of relativistic cosmic-rays

Cosmic-Ray Propagation



Start with a source of relativistic cosmic-rays

cosmic rays propagate



$$\frac{\partial \psi}{\partial t} = q(\vec{r}, p) + \vec{\nabla} \cdot (D_{xx} \vec{\nabla} \psi - \vec{V} \psi) + \frac{\partial}{\partial p} p^2 D_{pp} \frac{\partial}{\partial p} \frac{1}{p^2} \psi - \frac{\partial}{\partial p} \left[\dot{p} \psi - \frac{p}{3} (\vec{\nabla} \cdot \vec{V}) \psi \right] - \frac{1}{\tau_f} \psi - \frac{1}{\tau_r} \psi$$

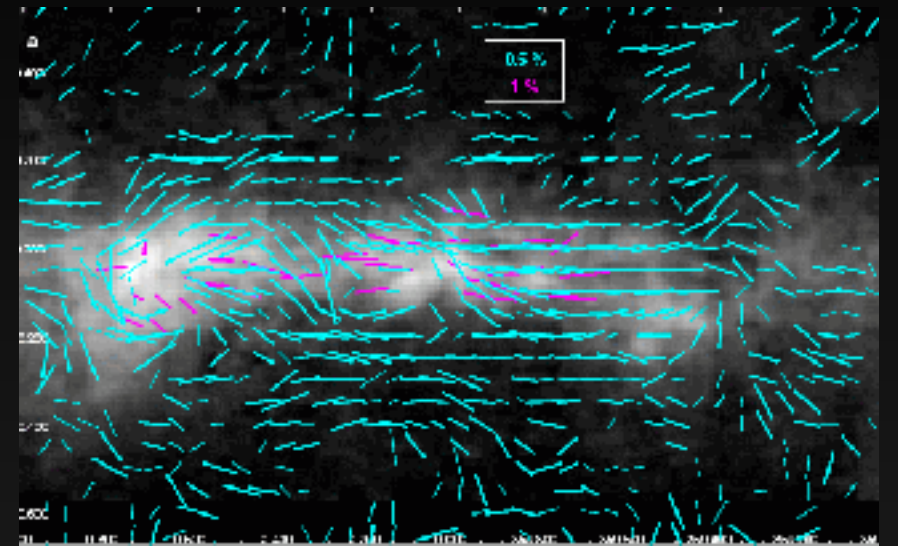
Solved Numerically:
e.g. Galprop

Cosmic-Ray Propagation



Start with a source of relativistic cosmic-rays

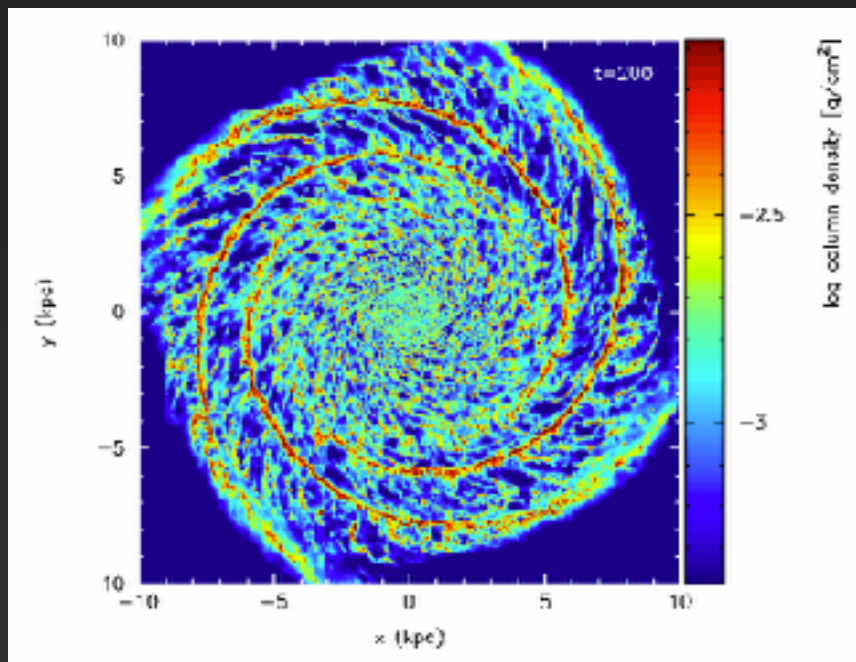
cosmic rays propagate



$$\frac{\partial \psi}{\partial t} = q(\vec{r}, p) + \vec{\nabla} \cdot (D_{xx} \vec{\nabla} \psi - \vec{V} \psi) + \frac{\partial}{\partial p} p^2 D_{pp} \frac{\partial}{\partial p} \frac{1}{p^2} \psi - \frac{\partial}{\partial p} \left[\dot{p} \psi - \frac{p}{3} (\vec{\nabla} \cdot \vec{V}) \psi \right] - \frac{1}{\tau_f} \psi - \frac{1}{\tau_r} \psi$$

Solved Numerically:
e.g. Galprop

Gas/ISRF

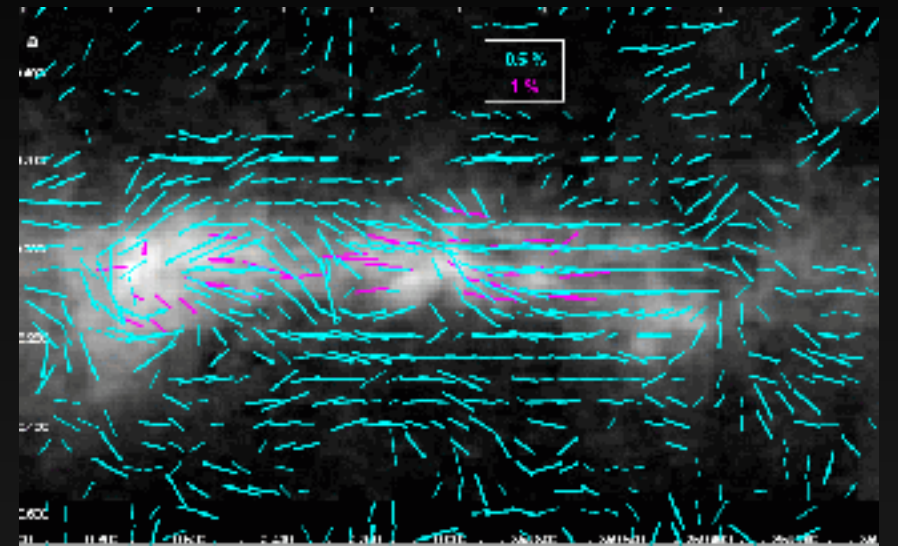


Cosmic-Ray Propagation



Start with a source of relativistic cosmic-rays

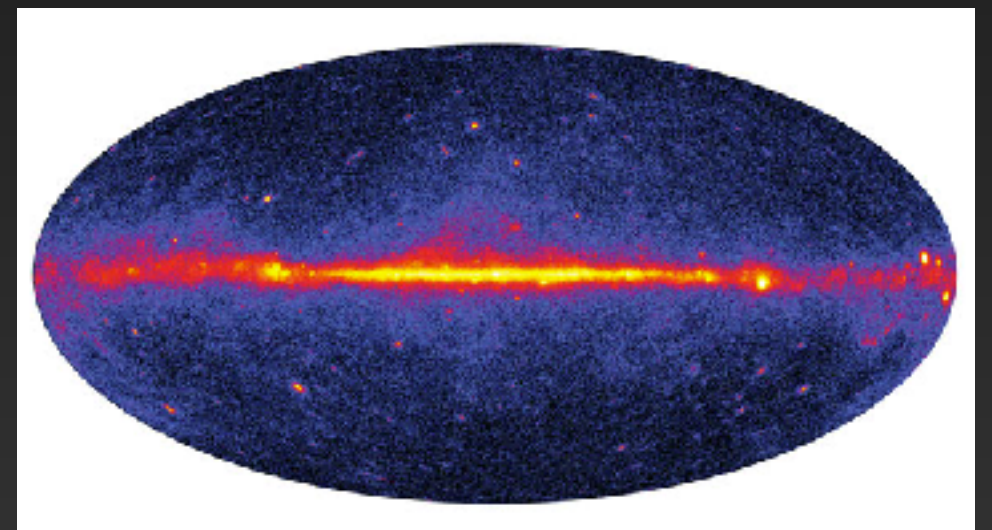
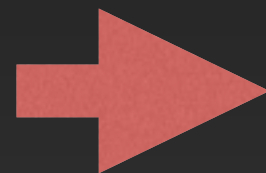
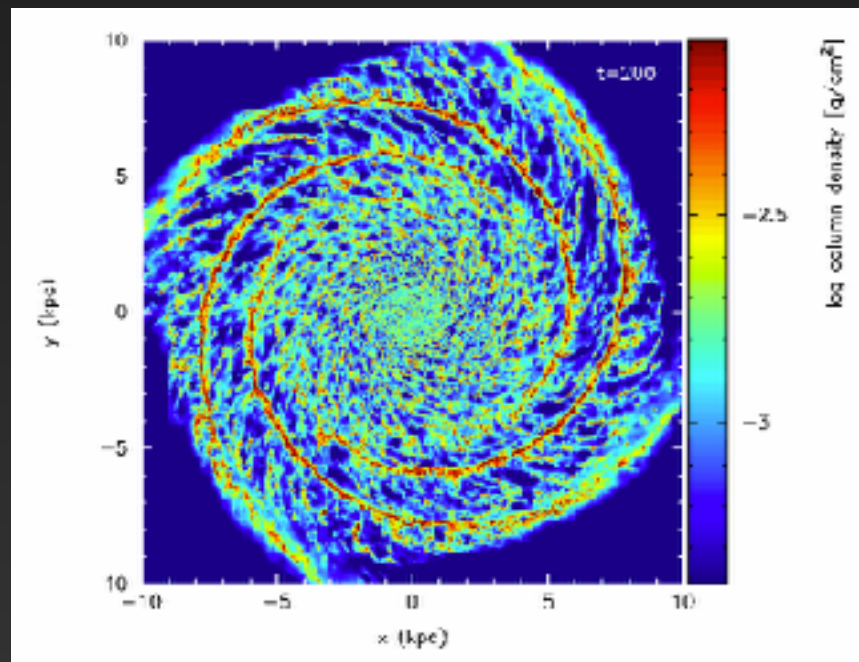
cosmic rays propagate



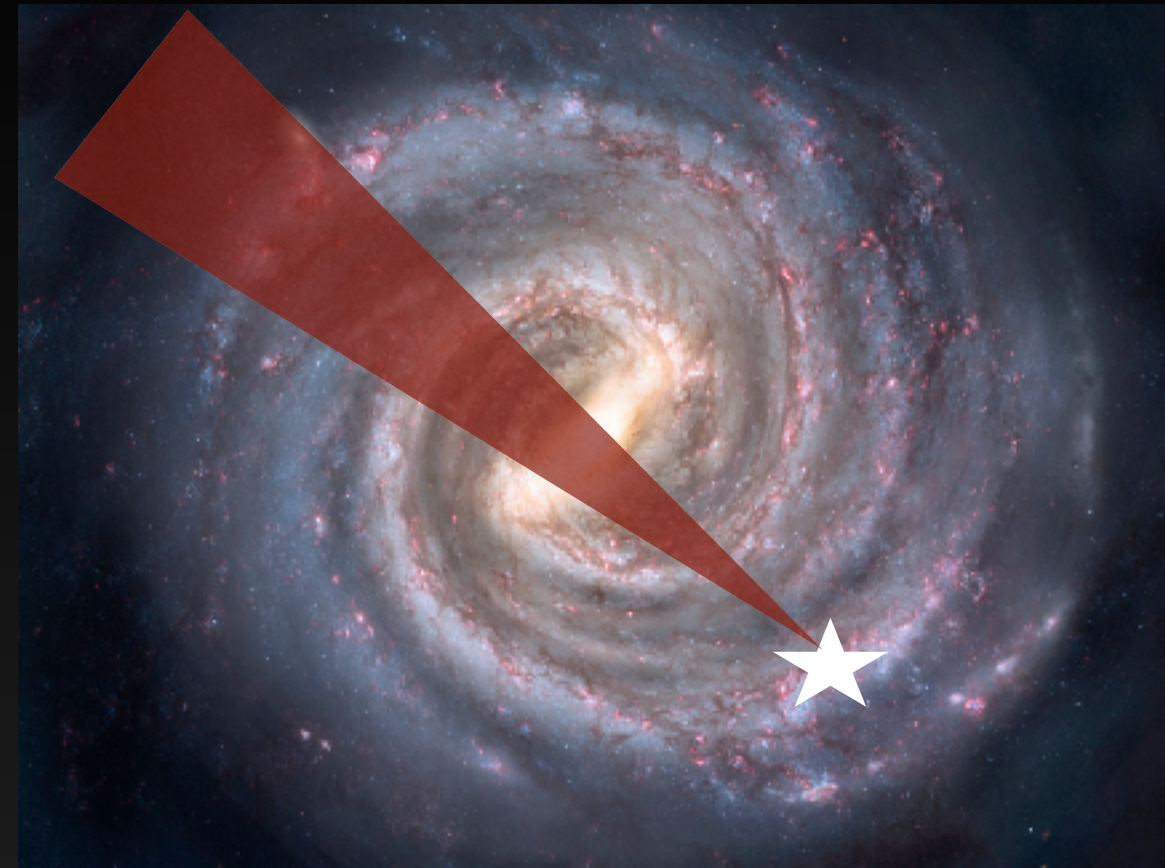
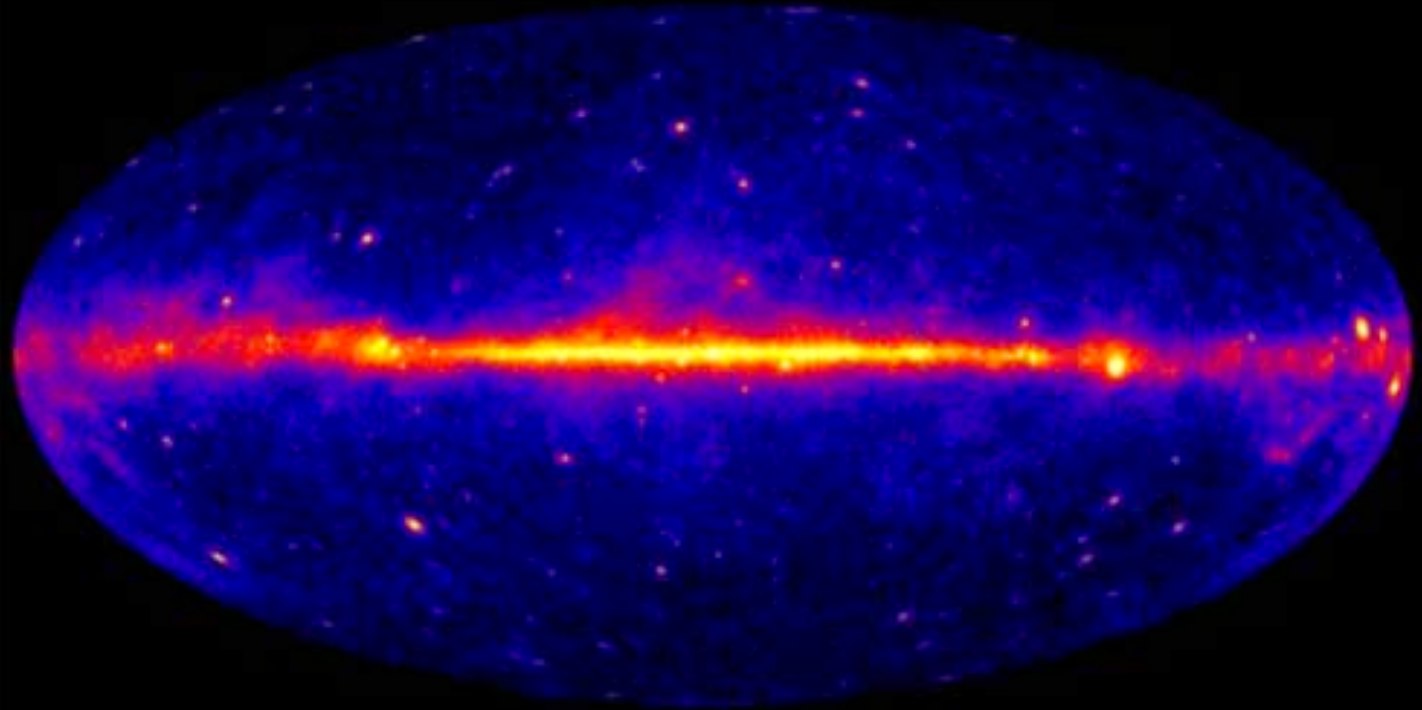
$$\frac{\partial \psi}{\partial t} = q(\vec{r}, p) + \vec{\nabla} \cdot (D_{xx} \vec{\nabla} \psi - \vec{V} \psi) + \frac{\partial}{\partial p} p^2 D_{pp} \frac{\partial}{\partial p} \frac{1}{p^2} \psi - \frac{\partial}{\partial p} \left[\dot{p} \psi - \frac{p}{3} (\vec{\nabla} \cdot \vec{V}) \psi \right] - \frac{1}{\tau_f} \psi - \frac{1}{\tau_r} \psi$$

Solved Numerically:
e.g. Galprop

Gas/ISRF



A Fermi-LAT Based Game

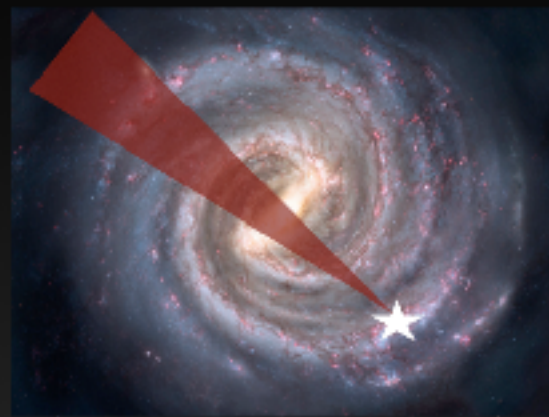


Total Gamma-Ray Flux (>1 GeV) in inner 1° is **$1.1 \times 10^{-9} \text{ erg cm}^2 \text{ s}^{-1}$**

Approximately half of this emission is produced along the line of sight towards the GC, and thus we approximate the total gamma-ray luminosity of the central one degree to be **$5 \times 10^{36} \text{ erg s}^{-1}$**

What models can power this emission?

A Fermi-LAT Based Game



Total Gamma-Ray Flux (>1 GeV) in inner 1° is $1.1 \times 10^{-9} \text{ erg cm}^2 \text{ s}^{-1}$

Approximately half of this emission is produced along the line of sight towards the GC, and thus we approximate the total gamma-ray luminosity of the central one degree to be $5 \times 10^{36} \text{ erg s}^{-1}$

Supernovae:

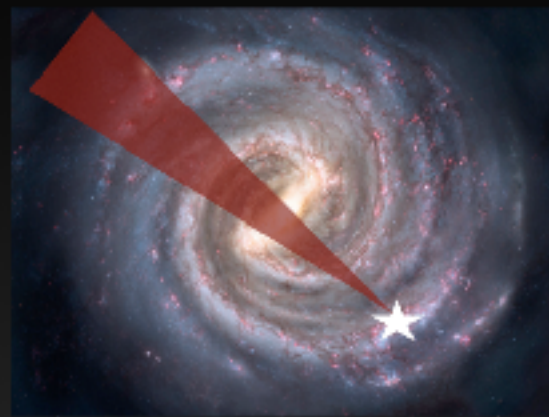
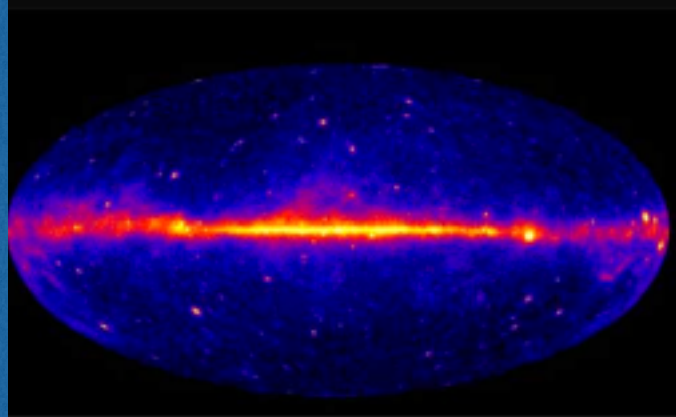
A Supernovae produces
 $\sim 10^{51}$ erg of energy.

$\sim 10\%$ to CR protons.

Assuming 1 Galactic center SN every 250 years (10% the Galactic Rate), this provides an energy flux of $1.3 \times 10^{40} \text{ erg s}^{-1}$.

If these cosmic-rays are trapped for 10 kyr in a 100 pc box ($D_0 = 5 \times 10^{28} \text{ cm}^2 \text{ s}^{-1}$), filled with Hydrogen gas at density 100 cm^{-3} , this will produce a total gamma-ray emission:

A Fermi-LAT Based Game



Total Gamma-Ray Flux (>1 GeV) in inner 1° is $1.1 \times 10^{-9} \text{ erg cm}^2 \text{ s}^{-1}$

Approximately half of this emission is produced along the line of sight towards the GC, and thus we approximate the total gamma-ray luminosity of the central one degree to be $5 \times 10^{36} \text{ erg s}^{-1}$

Supernovae:

A Supernovae produces
 $\sim 10^{51}$ erg of energy.

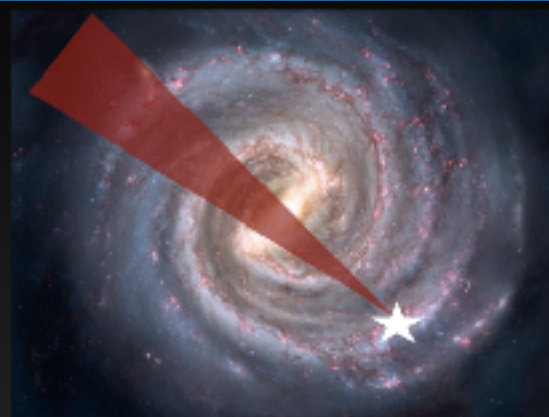
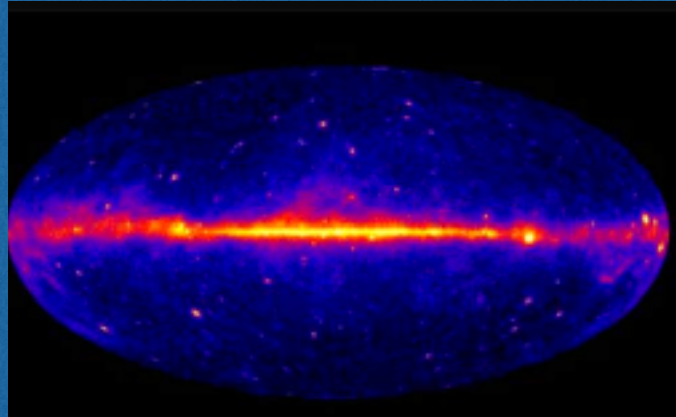
$\sim 10\%$ to CR protons.

Assuming 1 Galactic center SN every 250 years (10% the Galactic Rate), this provides an energy flux of $1.3 \times 10^{40} \text{ erg s}^{-1}$.

If these cosmic-rays are trapped for 10 kyr in a 100 pc box ($D_0 = 5 \times 10^{28} \text{ cm}^2 \text{ s}^{-1}$), filled with Hydrogen gas at density 100 cm^{-2} , this will produce a total gamma-ray emission:

$$6.7 \times 10^{37} \text{ erg s}^{-1} \quad \checkmark$$

A Fermi-LAT Based Game



Total Gamma-Ray Flux (>1 GeV) in inner 1° is $1.1 \times 10^{-9} \text{ erg cm}^2 \text{ s}^{-1}$

Approximately half of this emission is produced along the line of sight towards the GC, and thus we approximate the total gamma-ray luminosity of the central one degree to be $5 \times 10^{36} \text{ erg s}^{-1}$

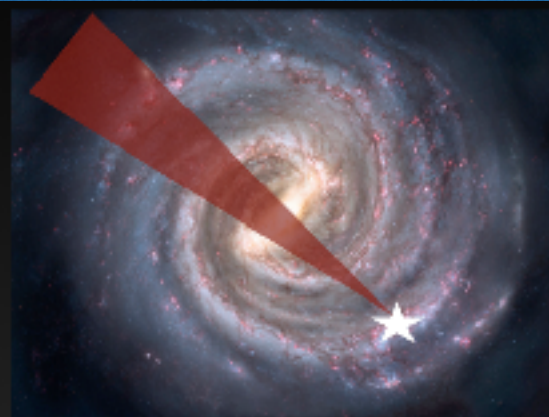
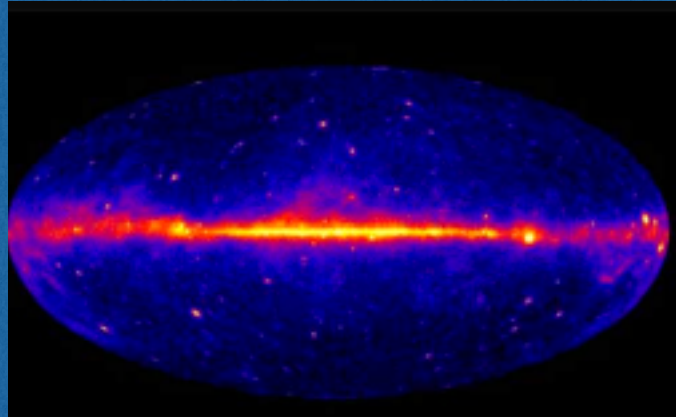
Sgr A*:

A tidal disruption event releases $\sim 10^{45} \text{ erg s}^{-1}$ for a period of $\sim 0.2 \text{ yr}$.

Sgr A* is expected to produce a tidal disruption event every $\sim 10^5 \text{ yr}$, producing a time-averaged energy output of $2 \times 10^{39} \text{ erg s}^{-1}$.

If these CRs are primarily leptonic, and the electrons remain trapped in a region with a 40 eV cm^{-3} ISRF and a $200 \mu\text{G}$ magnetic field the gamma-ray flux from inverse Compton scattering is:

A Fermi-LAT Based Game



Total Gamma-Ray Flux (>1 GeV) in inner 1° is $1.1 \times 10^{-9} \text{ erg cm}^2 \text{ s}^{-1}$

Approximately half of this emission is produced along the line of sight towards the GC, and thus we approximate the total gamma-ray luminosity of the central one degree to be $5 \times 10^{36} \text{ erg s}^{-1}$

Sgr A*:

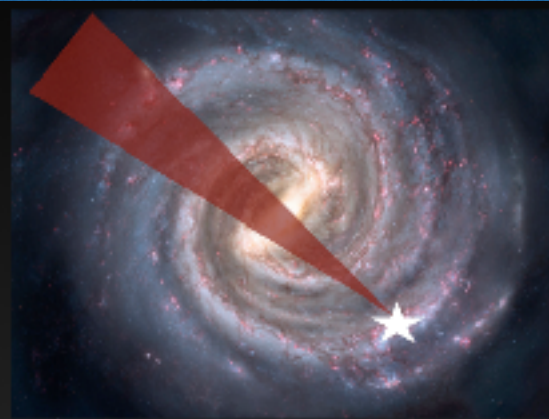
A tidal disruption event releases $\sim 10^{45} \text{ erg s}^{-1}$ for a period of $\sim 0.2 \text{ yr}$.

Sgr A* is expected to produce a tidal disruption event every $\sim 10^5 \text{ yr}$, producing a time-averaged energy output of $2 \times 10^{39} \text{ erg s}^{-1}$.

If these CRs are primarily leptonic, and the electrons remain trapped in a region with a 40 eV cm^{-3} ISRF and a $200 \mu\text{G}$ magnetic field the gamma-ray flux from inverse Compton scattering is:

$7.0 \times 10^{37} \text{ erg s}^{-1}$ ✓

A Fermi-LAT Based Game



Total Gamma-Ray Flux (>1 GeV) in inner 1° is $1.1 \times 10^{-9} \text{ erg cm}^2 \text{ s}^{-1}$

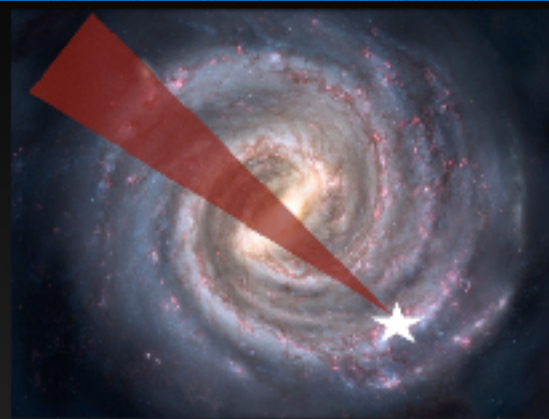
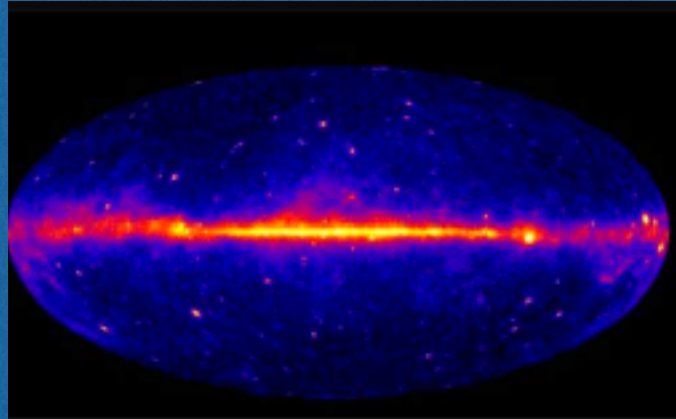
Approximately half of this emission is produced along the line of sight towards the GC, and thus we approximate the total gamma-ray luminosity of the central one degree to be $5 \times 10^{36} \text{ erg s}^{-1}$

Pulsars

MSPs observed in the galactic field are fit by a population with a mean gamma-ray flux of $3 \times 10^{34} \text{ erg s}^{-1}$. (Hooper & Mohlabeng 2015)

Given the population of 129 MSPs among 124 globular clusters (with a total stellar mass $\sim 5 \times 10^7 M_\odot$). For the $1 \times 10^9 M_\odot$ of stars formed in the inner degree of the Milky Way, we get:

A Fermi-LAT Based Game



Total Gamma-Ray Flux (>1 GeV) in inner 1° is $1.1 \times 10^{-9} \text{ erg cm}^2 \text{ s}^{-1}$

Approximately half of this emission is produced along the line of sight towards the GC, and thus we approximate the total gamma-ray luminosity of the central one degree to be $5 \times 10^{36} \text{ erg s}^{-1}$

Pulsars

MSPs observed in the galactic field are fit by a population with a mean gamma-ray flux of $3 \times 10^{34} \text{ erg s}^{-1}$. (Hooper & Mohlabeng 2015)

Given the population of 129 MSPs among 124 globular clusters (with a total stellar mass $\sim 5 \times 10^7 M_\odot$). For the $1 \times 10^9 M_\odot$ of stars formed in the inner degree of the Milky Way, we get:

$$7.7 \times 10^{37} \text{ erg s}^{-1} \quad \checkmark$$

A Fermi-LAT Based Game



Total Gamma-Ray Flux (>1 GeV) in inner 1° is $1.1 \times 10^{-9} \text{ erg cm}^2 \text{ s}^{-1}$

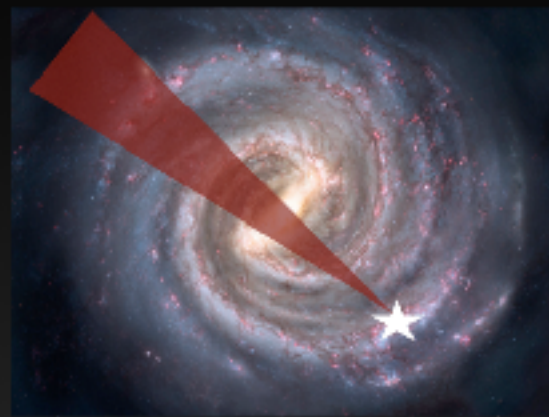
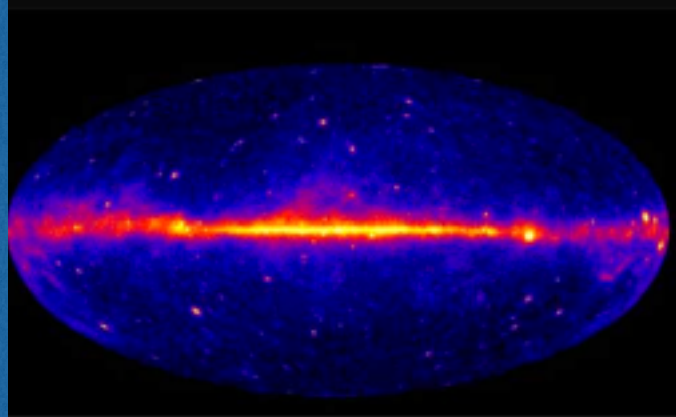
Approximately half of this emission is produced along the line of sight towards the GC, and thus we approximate the total gamma-ray luminosity of the central one degree to be $5 \times 10^{36} \text{ erg s}^{-1}$

Dark Matter

For a 35 GeV dark matter particle annihilating at the thermal cross-section to bb , and a slightly adiabatically contracted $r^{-1.35}$ density profile.

The dark matter annihilation rate is $8.6 \times 10^{38} \text{ ann s}^{-1}$, which produces a gamma-ray flux of:

A Fermi-LAT Based Game



Total Gamma-Ray Flux (>1 GeV) in inner 1° is $1.1 \times 10^{-9} \text{ erg cm}^2 \text{ s}^{-1}$

Approximately half of this emission is produced along the line of sight towards the GC, and thus we approximate the total gamma-ray luminosity of the central one degree to be $5 \times 10^{36} \text{ erg s}^{-1}$

Dark Matter

For a 35 GeV dark matter particle annihilating at the thermal cross-section to $b\bar{b}$, and a slightly adiabatically contracted $r^{-1.35}$ density profile.

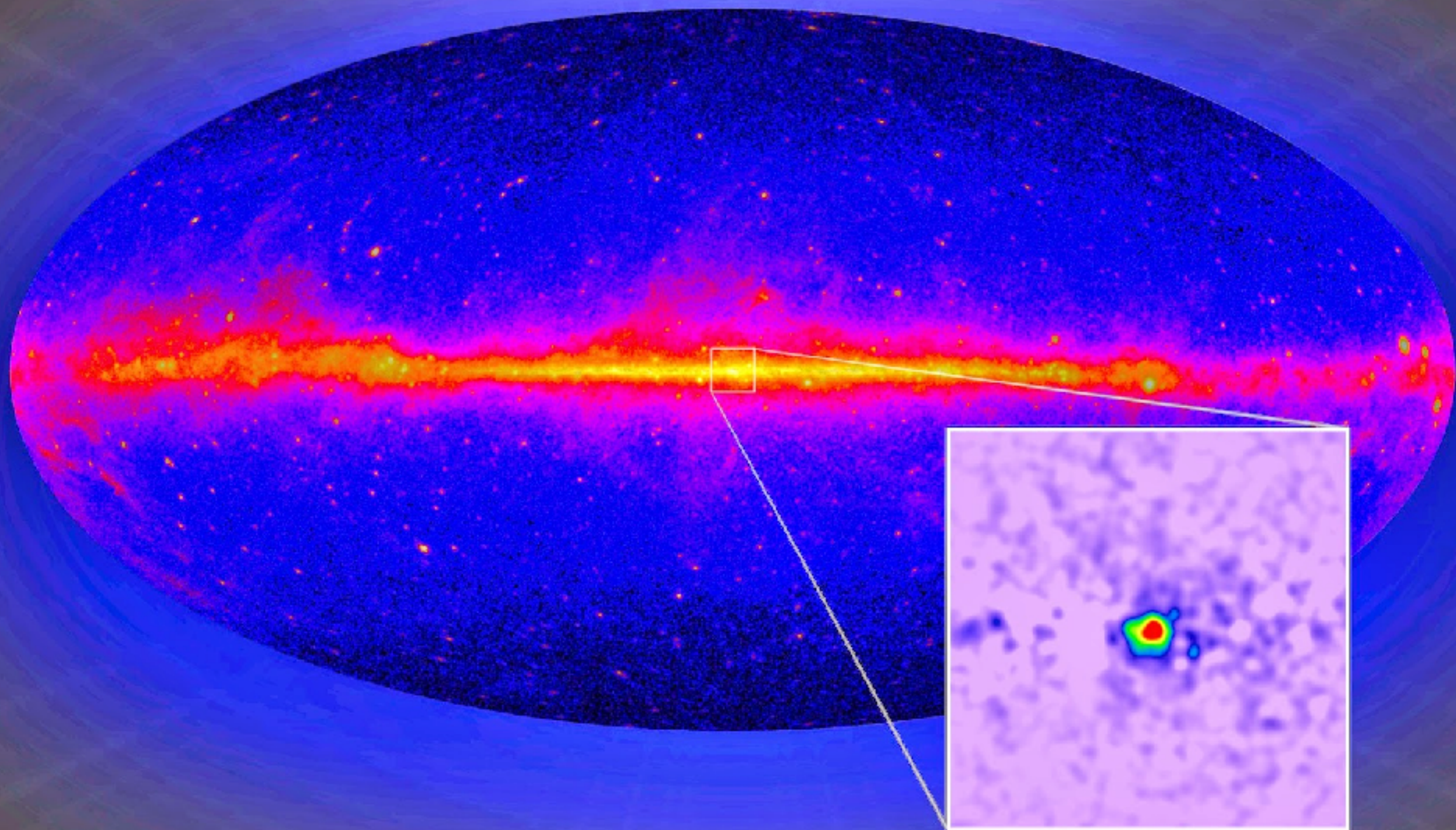
The dark matter annihilation rate is $8.6 \times 10^{38} \text{ ann s}^{-1}$, which produces a gamma-ray flux of:

$$6.9 \times 10^{36} \text{ erg s}^{-1} \quad \checkmark$$

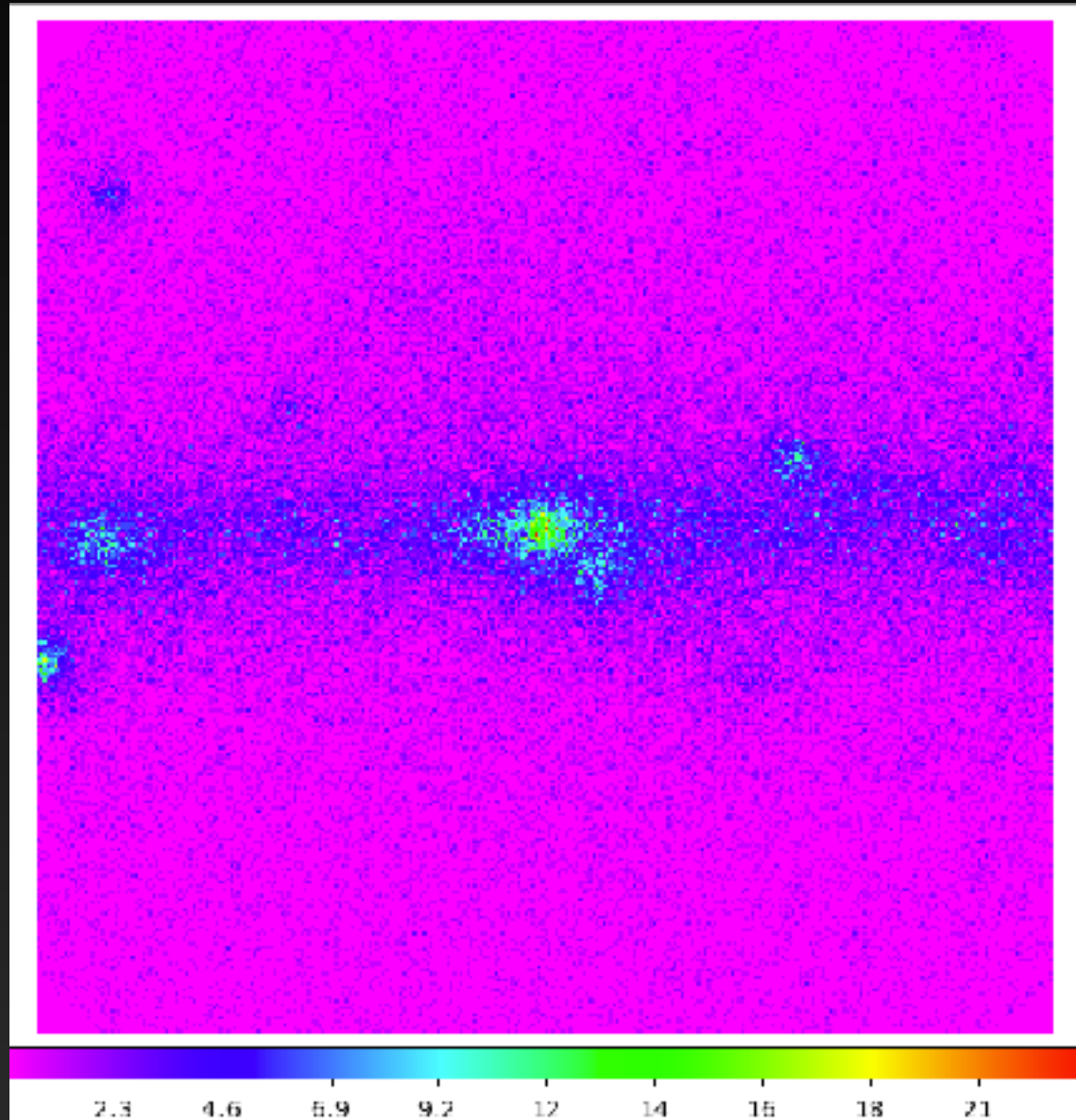
Conclusion:
Every Model is Correct

Conclusion:
Every Model is Correct

Is this (theorist) heaven?
or is this hell?



Modeling the Galactic Center

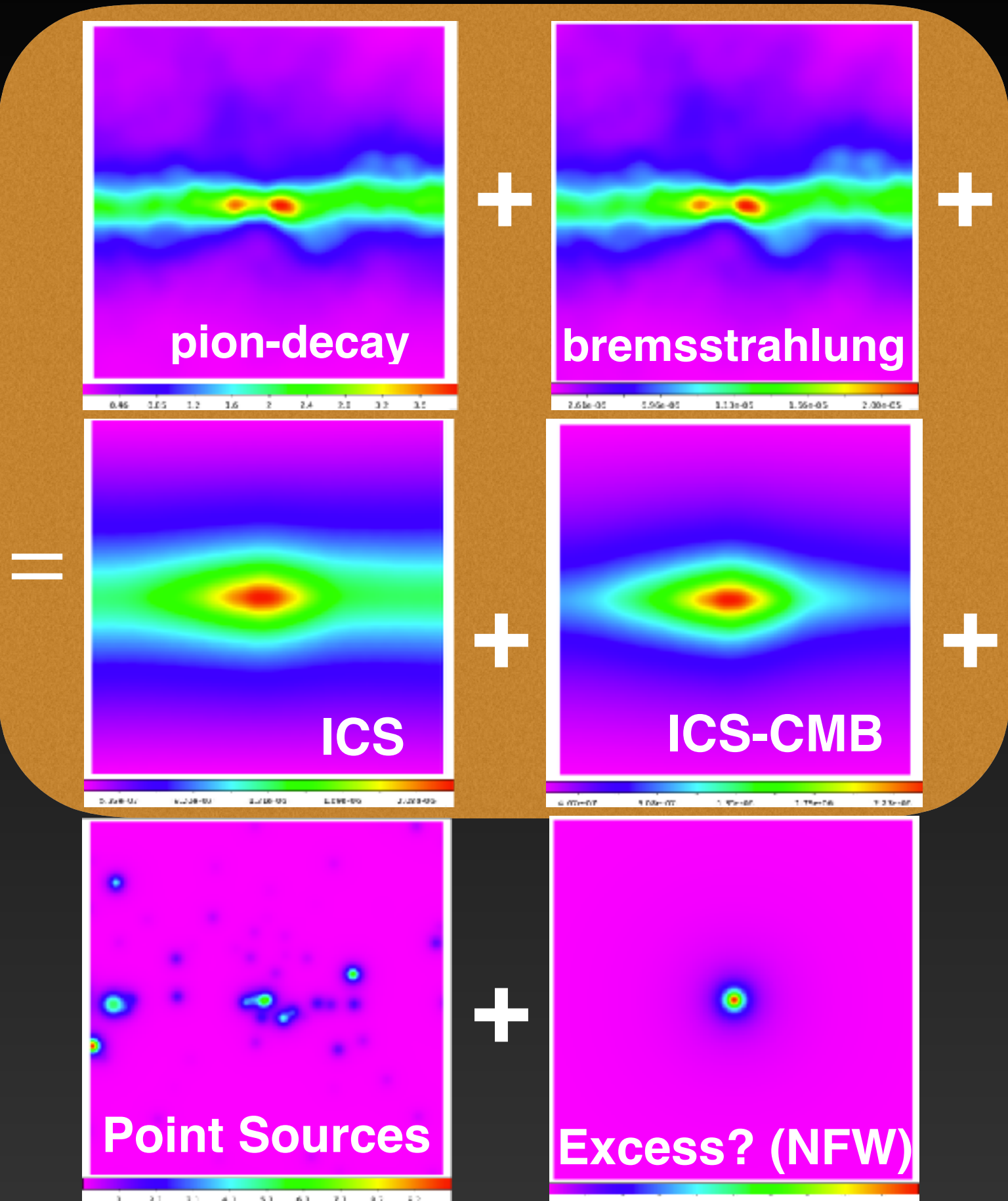


Data

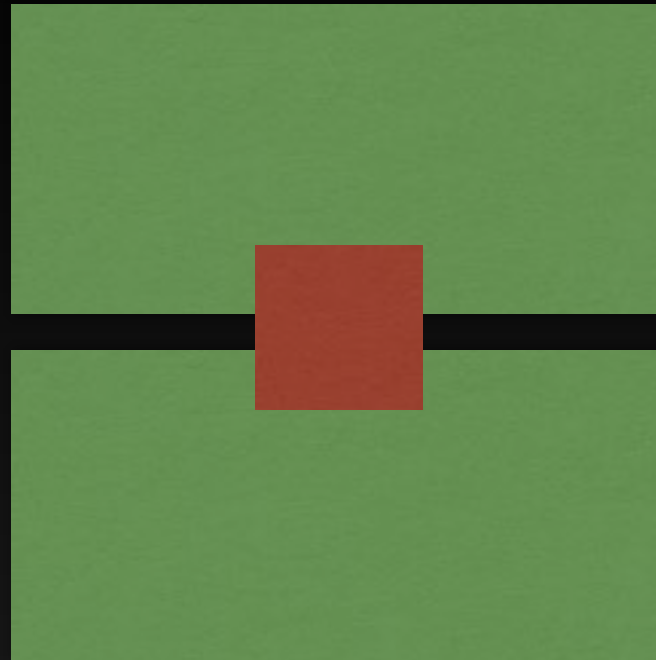
750 — 950 MeV

Best Angular Resolution Cut

$10^\circ \times 10^\circ$ ROI



Two Analyses of the Gamma-Ray Excess



INNER GALAXY

- Mask galactic plane (e.g. $|b| > 1^\circ$), and consider $40^\circ \times 40^\circ$ box
- Bright point sources masked at 2°
- Use likelihood analysis, allowing the diffuse templates to float in each energy bin
- Background systematics controlled

GALACTIC CENTER

- Box around the GC ($10^\circ \times 10^\circ$)
- Include and model all point sources
- Use likelihood analysis to calculate the spectrum and intensity of each source
- Bright Signal

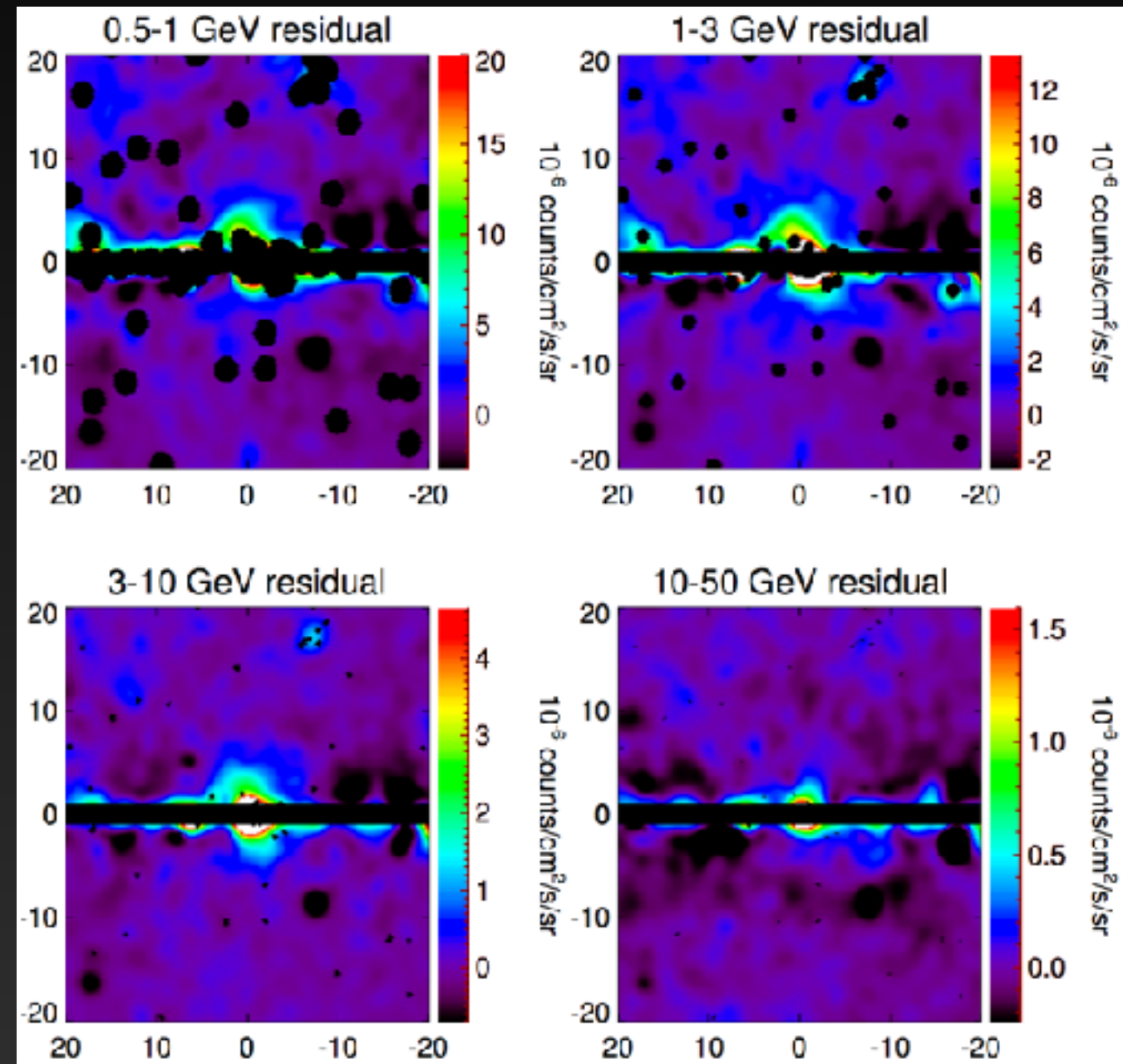
The Galactic Center Excess

Utilizing different models for removing astrophysical and point source foregrounds. Multiple studies have consistently observed a gamma-ray excess.

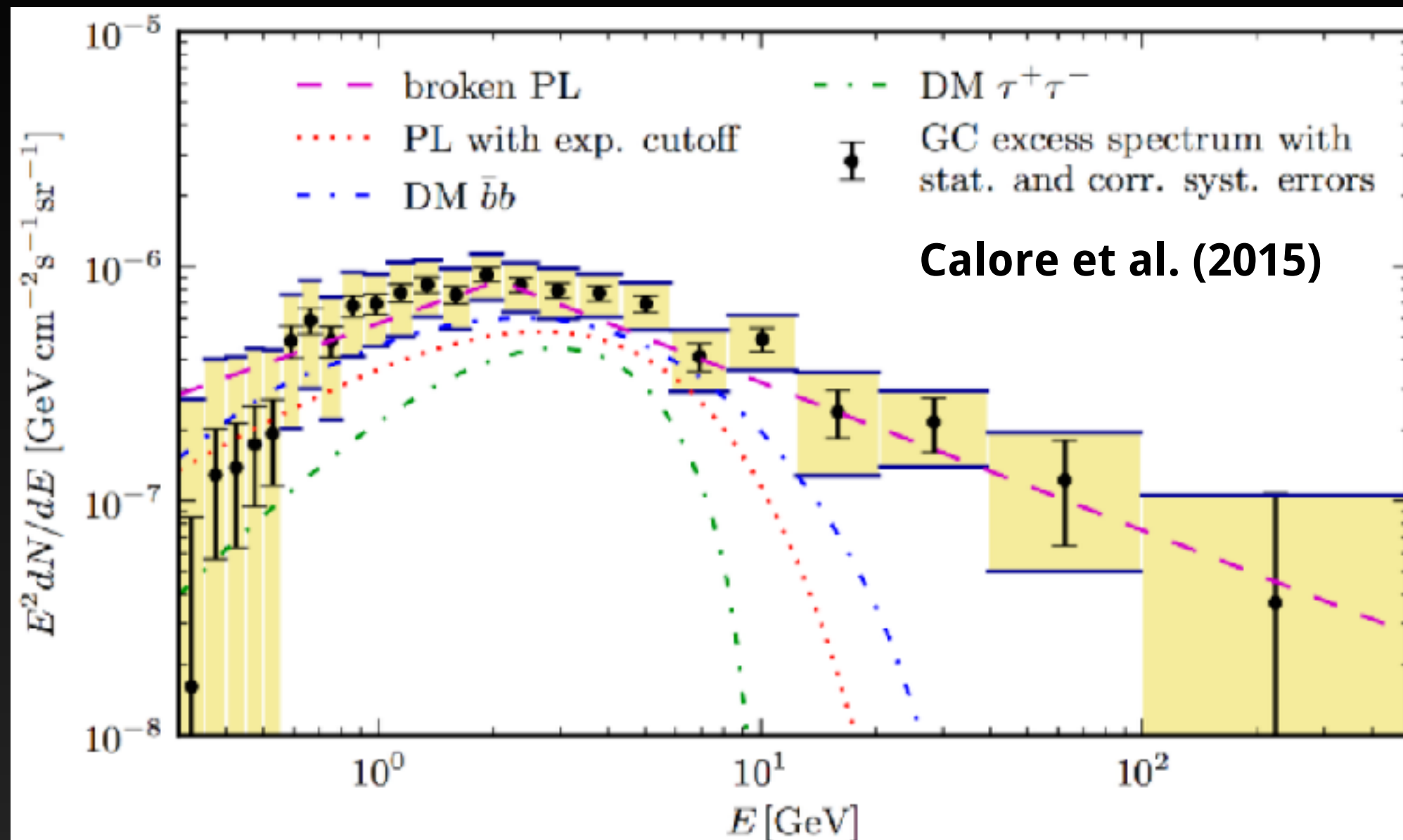
Goodenough & Hooper (2009, 0910.2998)
Hooper & Goodenough (2010, 1010.2752)
Hooper & Linden (2011, 1110.0006)
Abazajian & Kaplinghat (2012, 1207.6047)
Gordon & Macias (2013, 1306.5725)
Gordon & Macias (2013, 1312.6671)
Abazajian et al. (2014, 1402.4090)
Daylan et al. (2014, 1402.6703)
Calore et al. (2014, 1409.0042)
Abazajian et al. (2014, 1410.6168)
Bartels et al. (2015, 1506.05104)
Lee et al. (2015, 1506.05124)
Gaggero et al. (2015, 1507.06129)
Carlson et al. (2015, 1510.04698)
The Fermi-LAT Collaboration (2015, 1511.02938)
Yang & Aharonian (2016, 1602.06764)
Carlson et al. (2016, 1603.06584)
Linden et al. (2016, 1604.01026)
Horiuchi et al. (2016, 1604.01402)

IG

Daylan et al. (2014)



Observational Results



IG

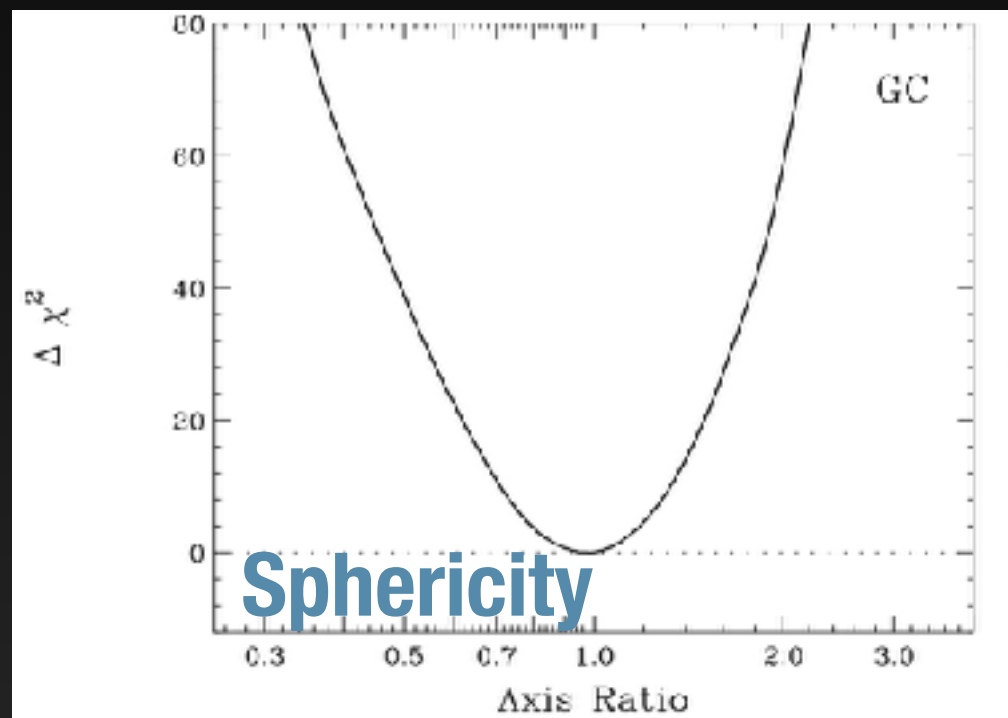
The excess has an unusual spectrum - highly peaked at an energy of ~ 2 GeV.

This spectrum is significantly harder than expected from astrophysical diffuse emission.

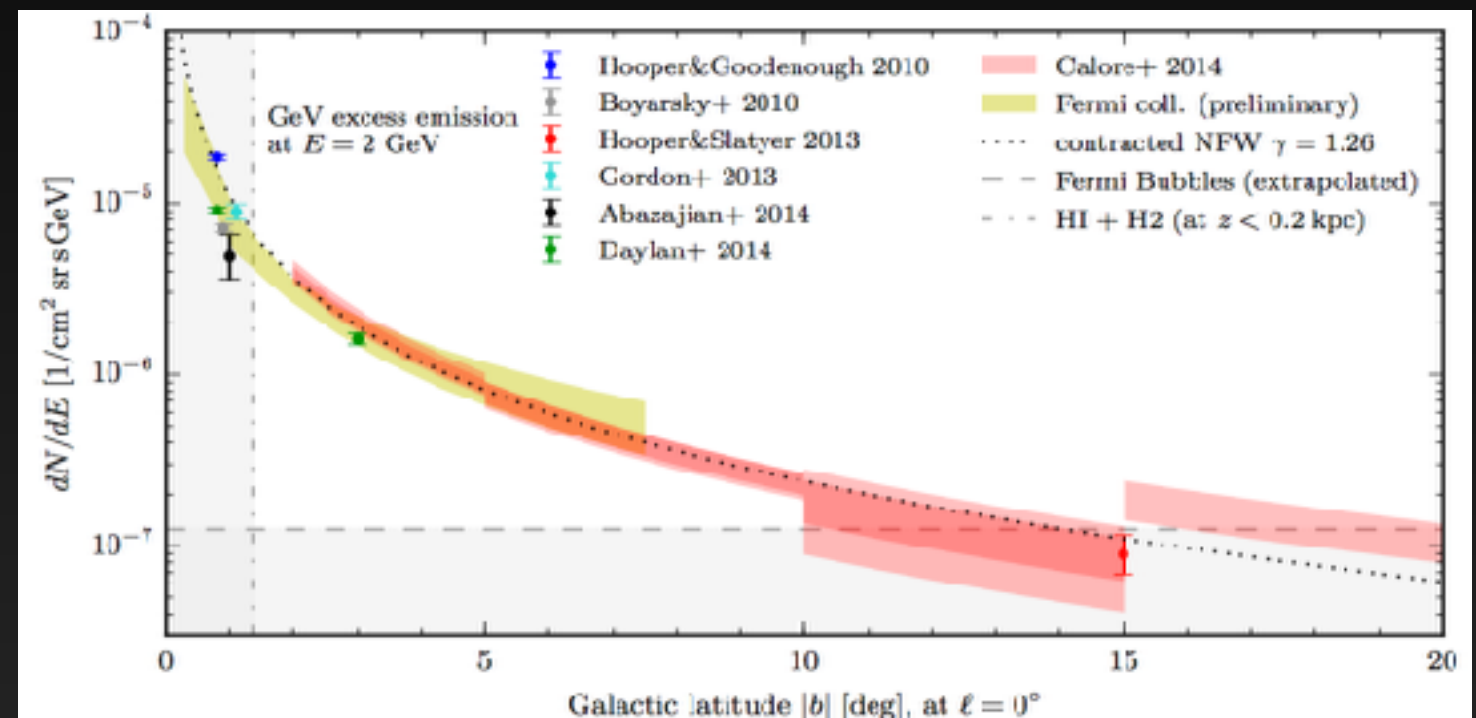
Observational Results



Daylan et al. (2014)



Calore et al. (2014b)



The GeV excess spherically symmetric, and is statistically significant from $0.1^\circ - 10^\circ$ from the Galactic Center.

Observational Results

These are the three resilient features of the GeV Excess:

- 1.) Hard Gamma-Ray Spectrum peaking at ~ 2 GeV
- 2.) Spherically Symmetric Emission Morphology
- 3.) Extension to $>10^\circ$ from the GC.

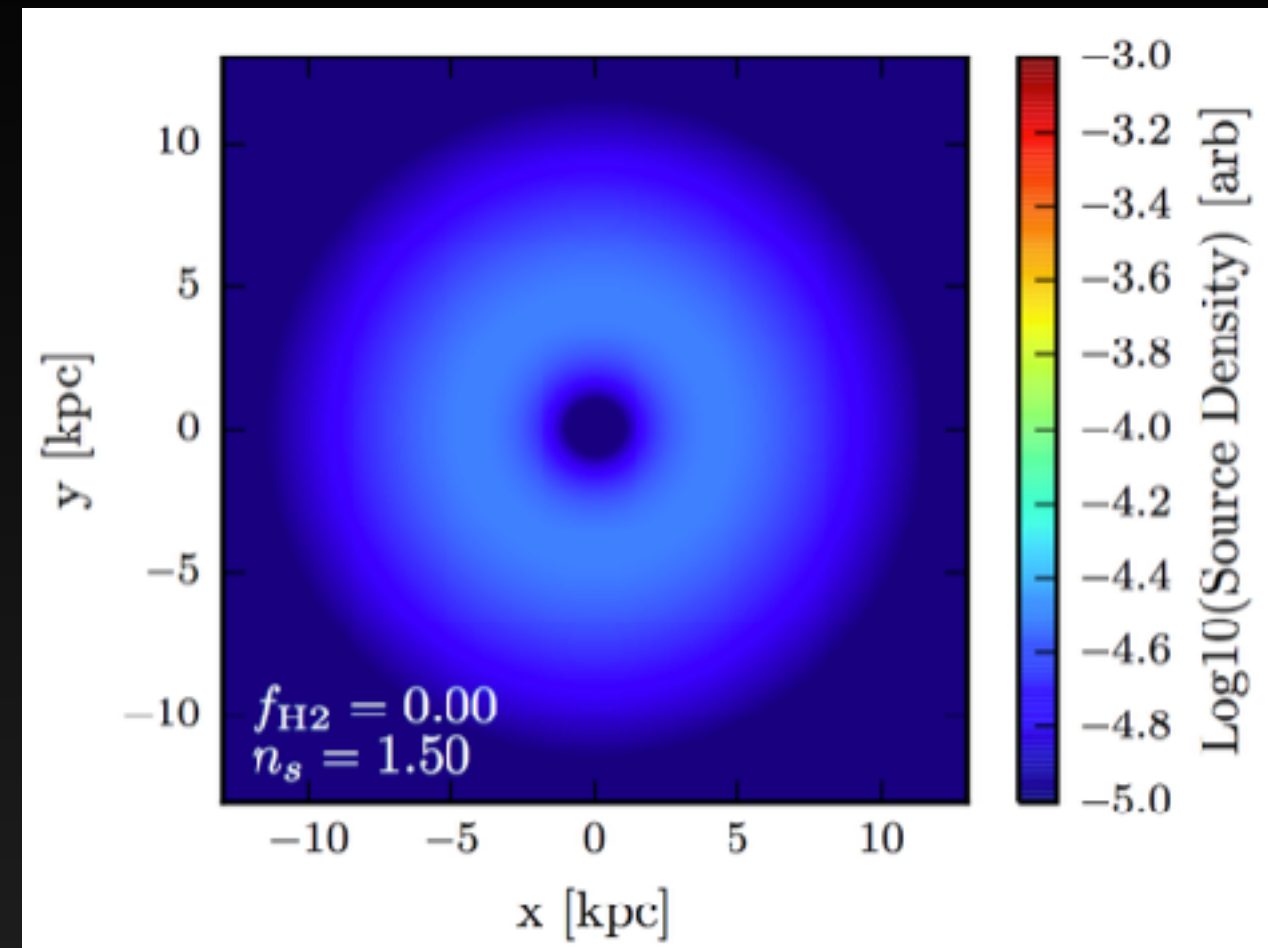
How could we model this with:

- 1.) Dark Matter annihilation
- 2.) Millisecond Pulsars
- 3.) Leptonic Outbursts from Sgr A*
- 4.) Changes in Diffuse Emission Modeling

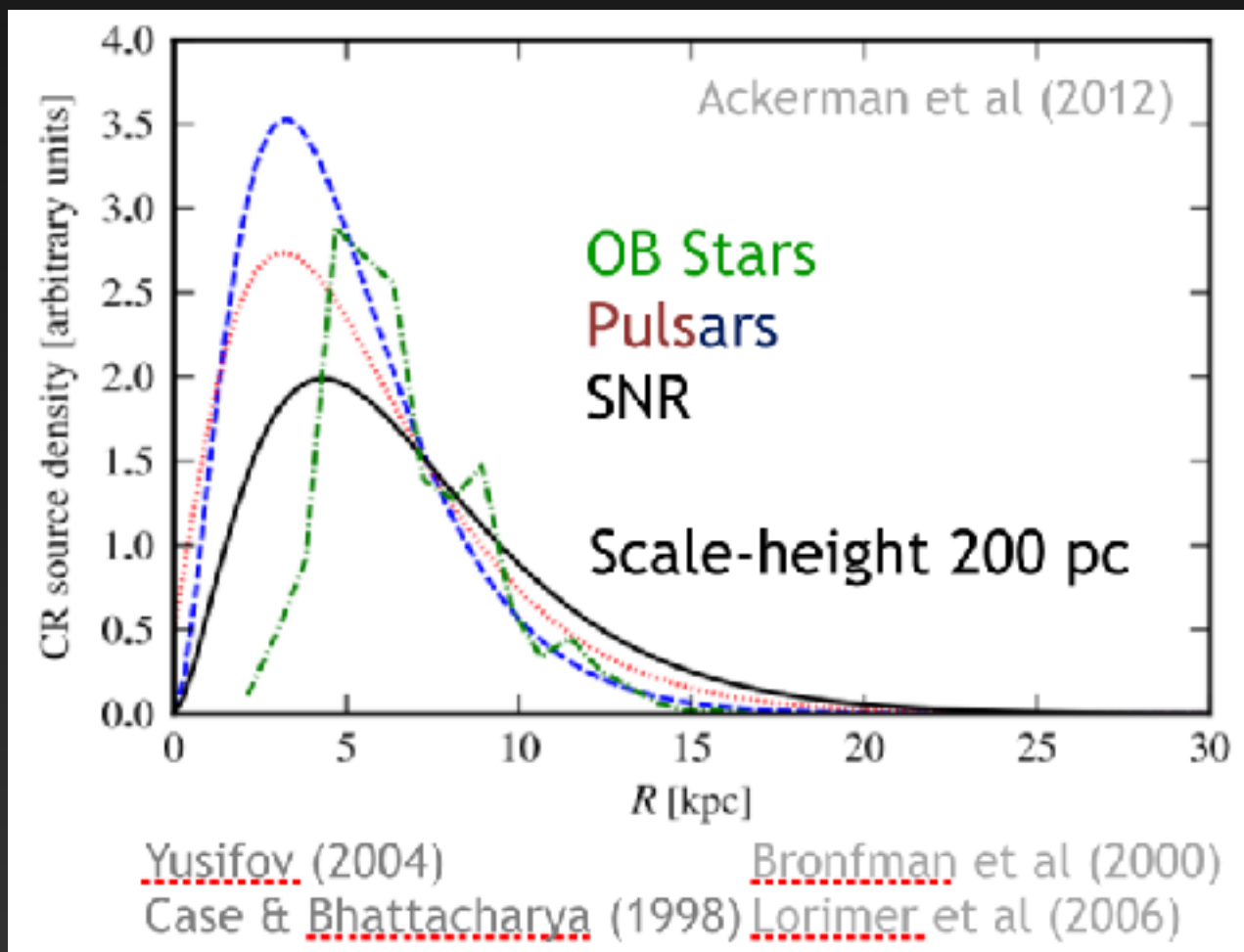
An Excess Compared to What?

Cosmic-Ray Propagation Codes (e.g. Galprop), generally utilize a cosmic-ray injection rate at the Galactic center that is identically 0.

These models were not produced to study the very center of the Galaxy!



Results from these cosmic-ray propagation codes are used in many analyses of the Galactic center region.



Carlson et al. (2016a, 2016b)
1510.04698
1603.06584

The Solution

Solution: Add a new cosmic-ray injection morphology tracing the molecular gas density.

Observationally Resilient: Several tracers of molecular gas are sensitive to the galactic center region.

Theoretically Motivated: Molecular Gas is the seed of star formation, the Schmidt Law gives

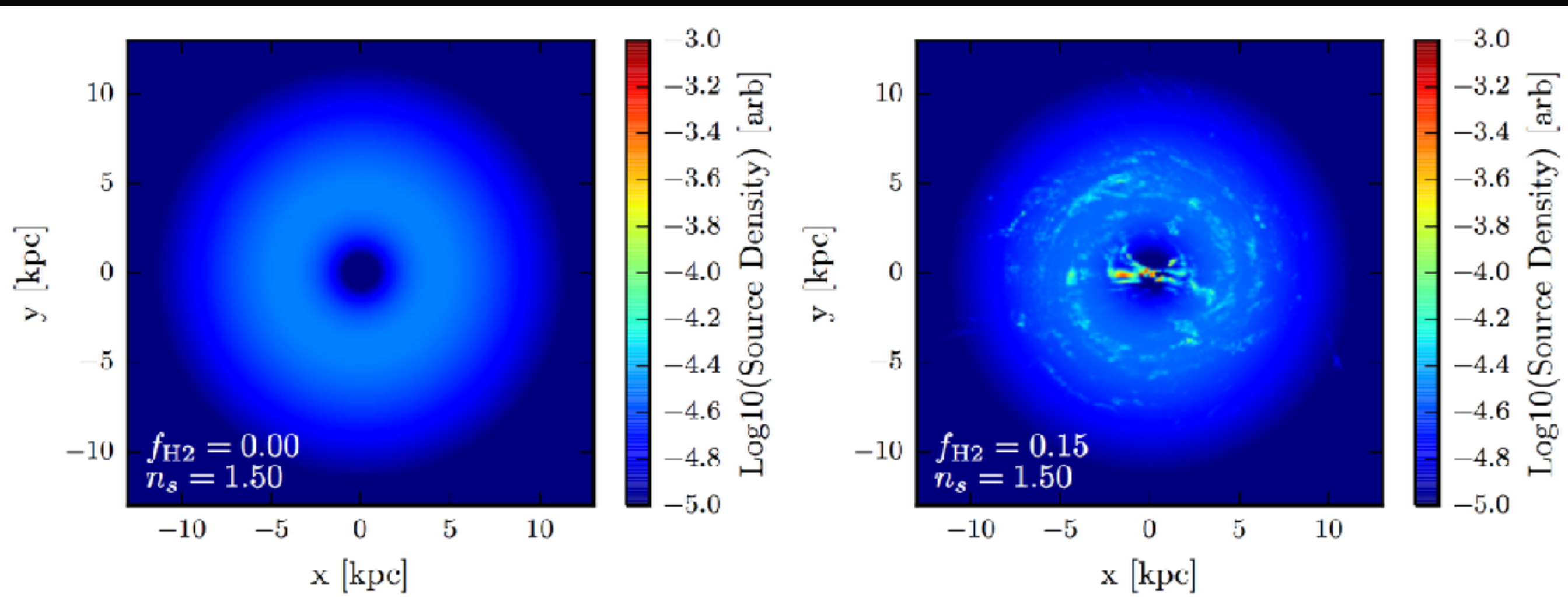
$$\Sigma_{\text{SFR}} \propto \Sigma_{\text{Gas}}^{1.4 \pm .15}$$

Specifically we inject a fraction of cosmic-rays ($0 < f_{\text{H}_2} < 1$) following:

$$Q_{\text{CR}}(\vec{r}) \propto \begin{cases} 0 & \rho_{\text{H}_2} \leq \rho_s \\ \rho_{\text{H}_2}^{n_s} & \rho_{\text{H}_2} > \rho_s \end{cases}$$

1510.04698

The Solution

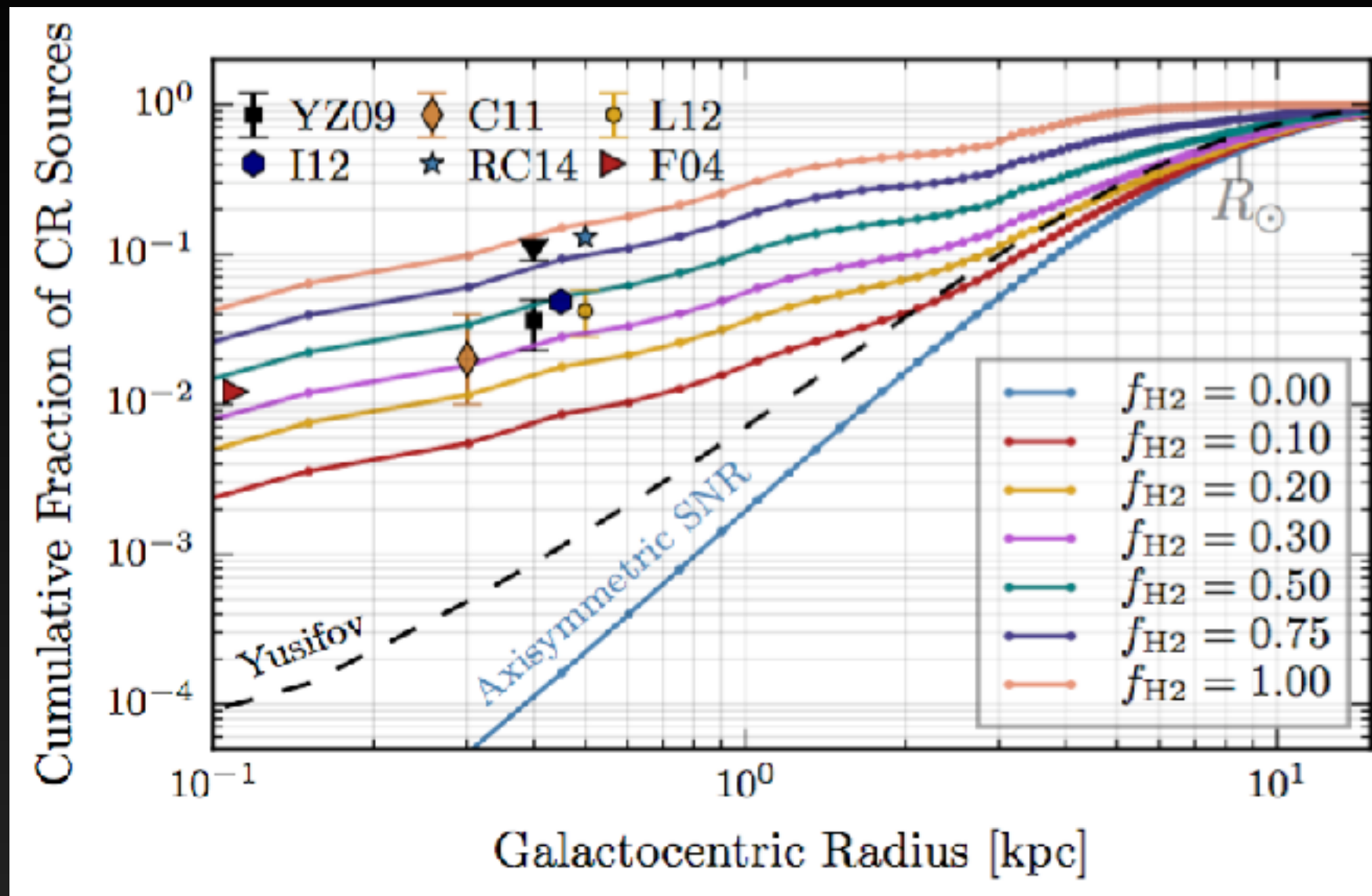


Two features leap out immediately:

1.) Spiral Arms

2.) A bright bar in the Galactic Center

The Solution



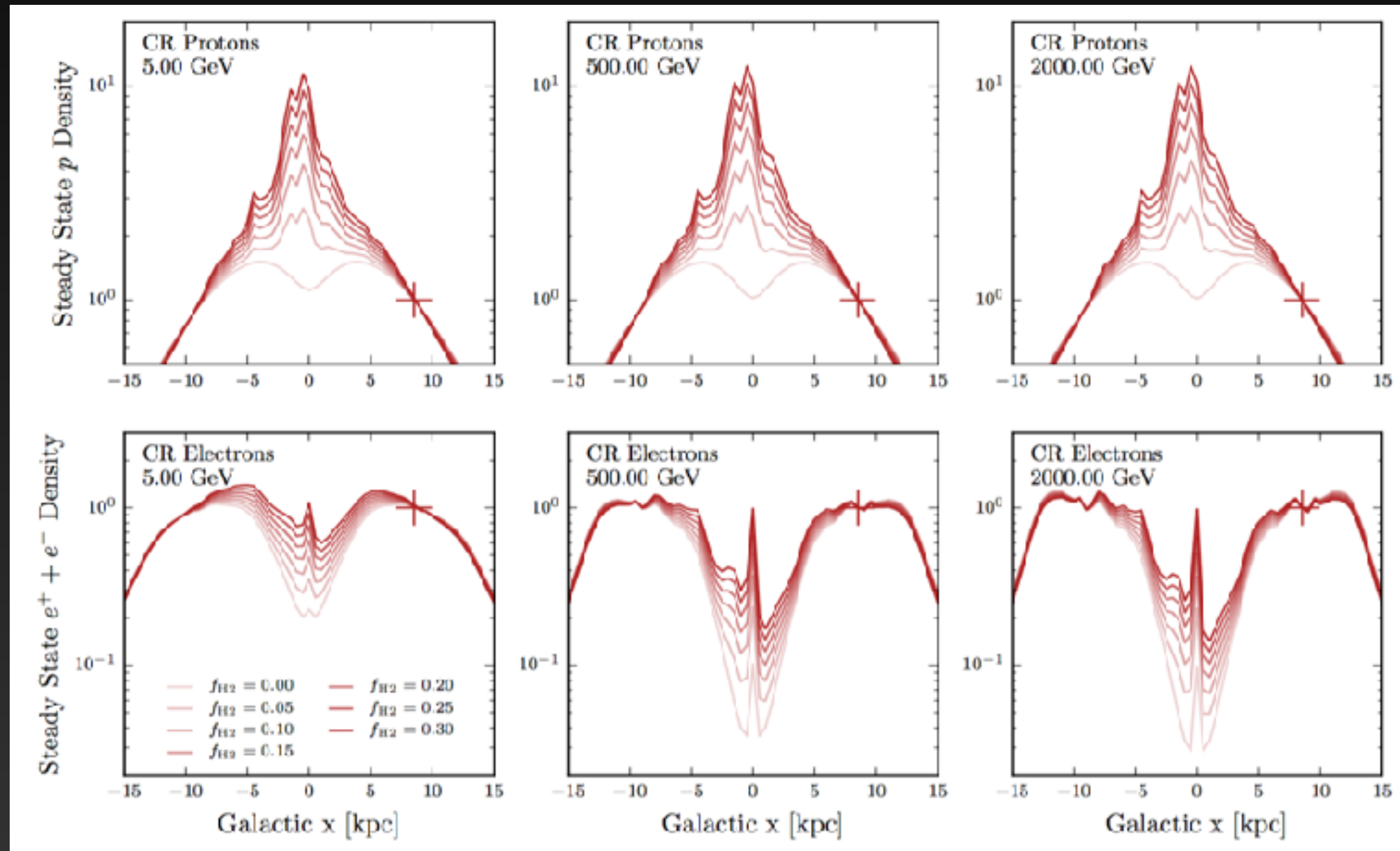
Adds a new, and significant, cosmic-ray injection component, in particular near the Galactic Center.

The cosmic-ray injection rate now matches observational constraints.

Simulations!

Add the new cosmic-ray injection models into Galprop to produce a new steady-state cosmic-ray distribution.

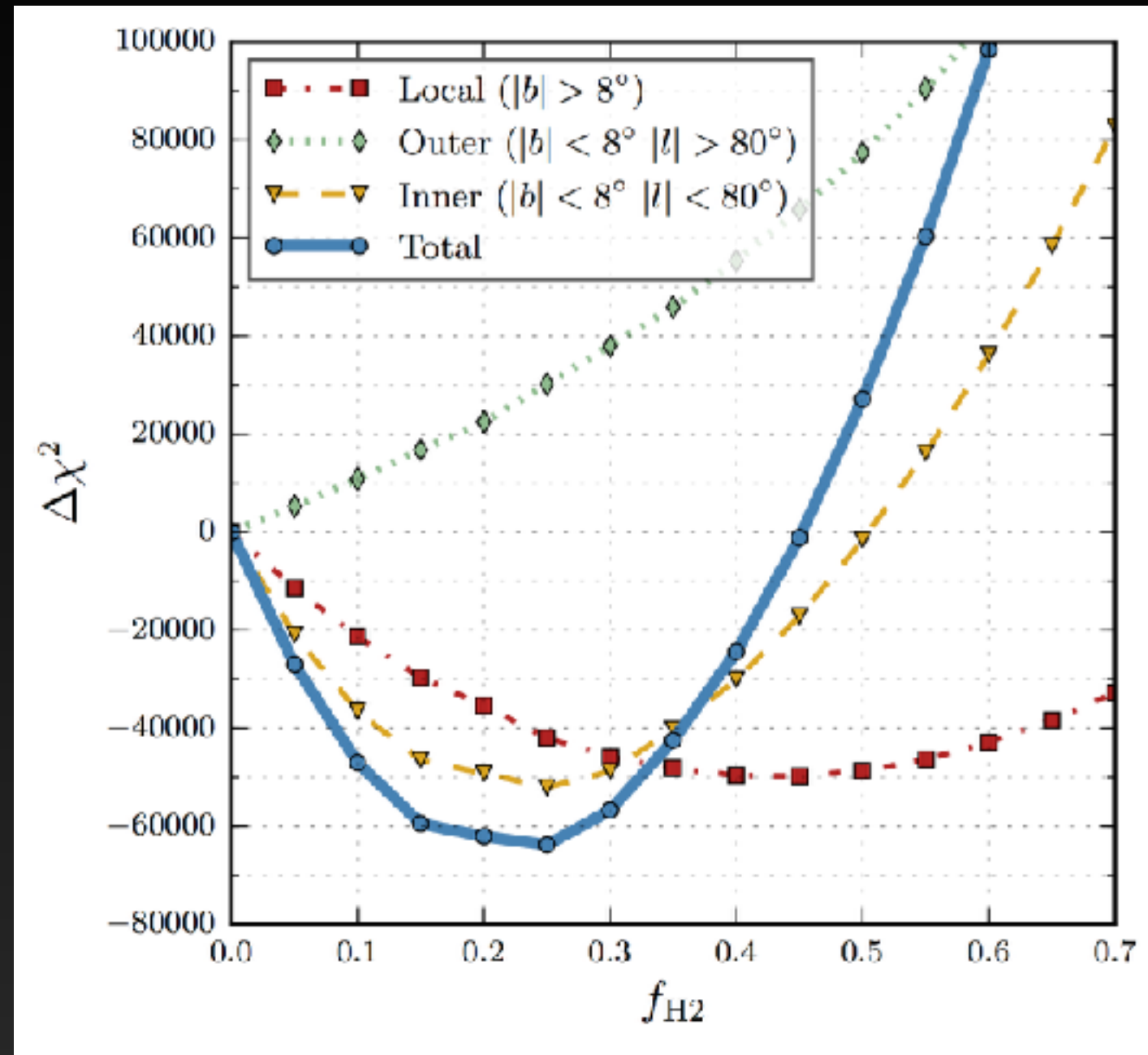
Parameter	Units	Canonical	Mod A	Description
D_0	$\text{cm}^2 \text{s}^{-1}$	7.2×10^{28}	5.0×10^{28}	Diffusion constant at $\mathcal{R} = 4$ GV
δ	—	0.33	0.33	Index of diffusion constant energy dependence
z_{halo}	kpc	3	4	Half-height of diffusion halo
R_{halo}	kpc	20	20	Radius diffusion halo
v_0	km s^{-1}	35	32.7	Alfvén velocity
dv/dz	$\text{km s}^{-1} \text{kpc}^{-1}$	0	50	Vertical convection gradient
α_p	—	1.88 (2.39)	1.88 (2.47)	p injection index below (above) $\mathcal{R} = 11.5$ GV
α_e	—	1.6 (2.42)	1.6 (2.43)	e^- injection index below (above) $\mathcal{R} = 2$ GV
Source	—	SNR	SNR	Distribution of $(1 - f_{\text{H2}})$ primary sources*
f_{H2}	—	.20	N/A	Fraction of sources in star formation model*
n_s	—	1.5	N/A	Schmidt Index*
ρ_c	cm^{-3}	0.1	N/A	Critical H_2 density for star formation*
B_0	μG	7.2	9.0	Local ($r = R_\odot$) magnetic field strength
r_B, z_B	kpc	5, 1	5, 2	Scaling radius and height for magnetic field
ISRF	—	(1.0,.86,.86)	(1.0,.86,.86)	Relative CMB, Optical, FIR density
dx, dy	kpc	0.5, 0.5	1 (2D)	x, y (3D) or radial (2D) cosmic-ray grid spacing
dz	kpc	0.125	.1	z -axis cosmic-ray grid spacing



A Better fit to the Gamma-Ray Sky

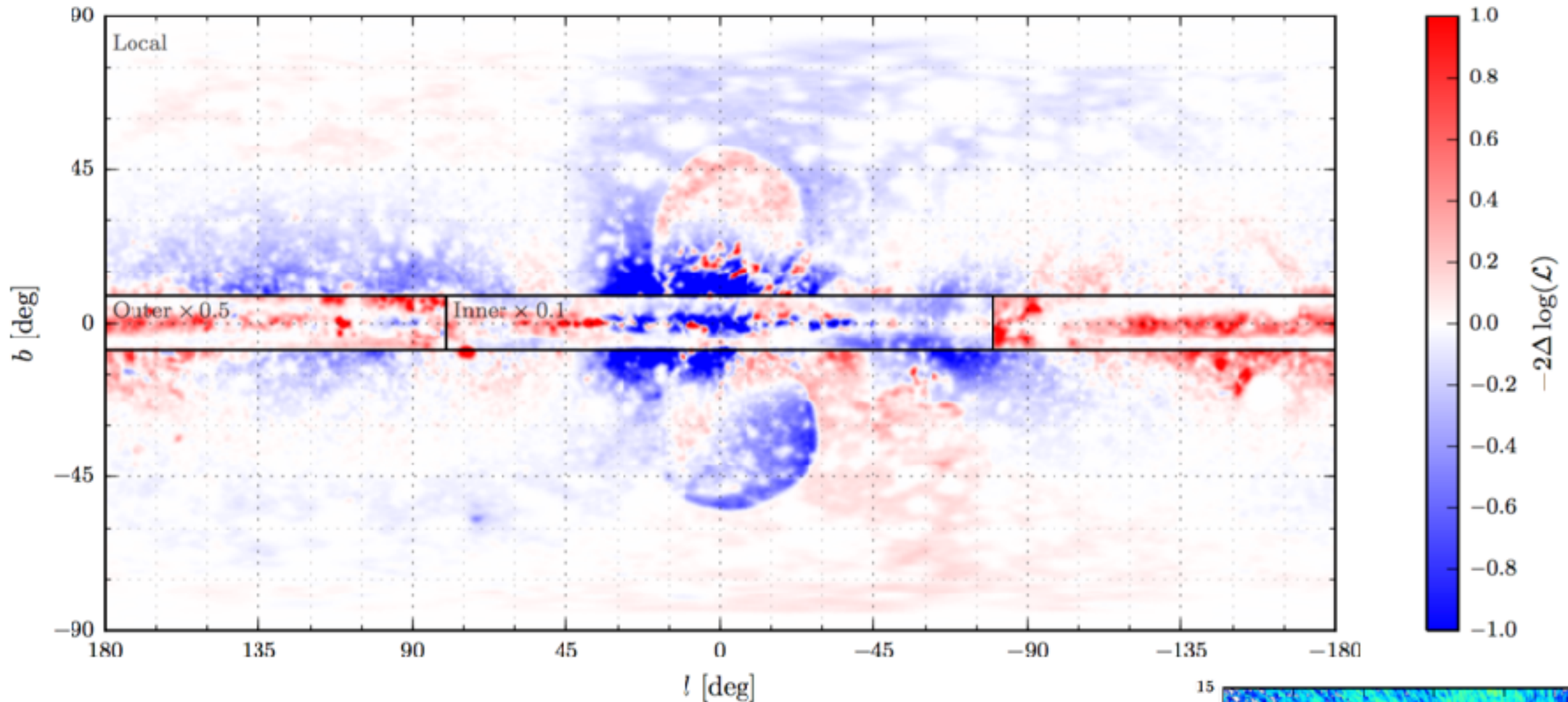
1.) Adding a cosmic-ray injection component tracing f_{H_2} improves the full-sky fit to the gamma-ray data.

2.) The best fit value over the full sky is $f_{\text{H}_2} = 0.25$

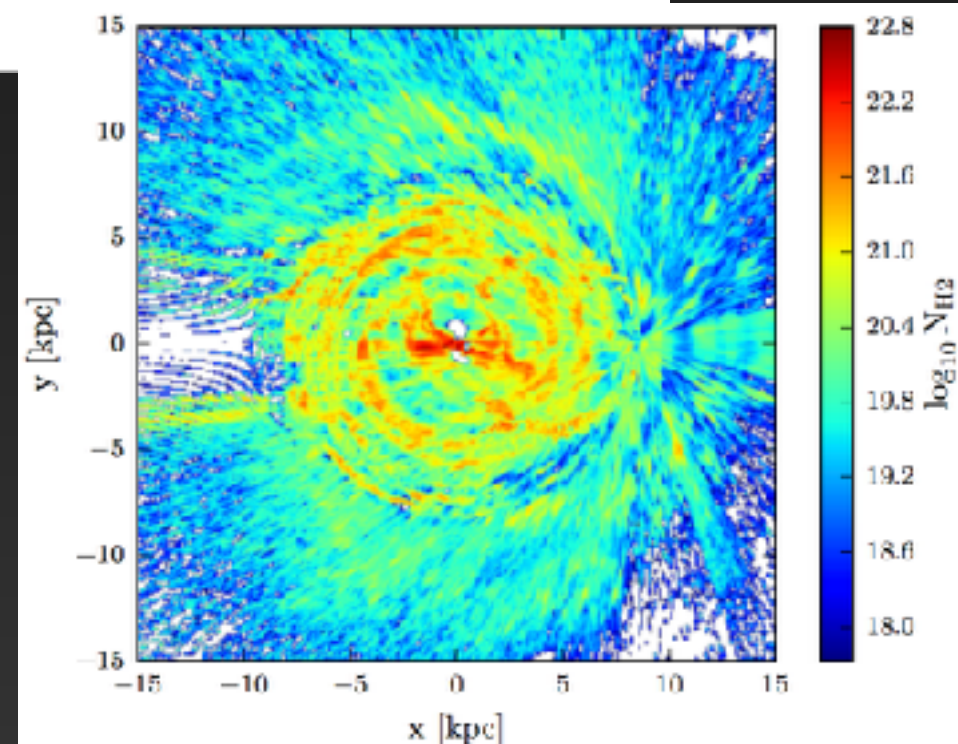


3.) Technique will become more powerful with the introduction of 3D gas and dust maps in the near future.

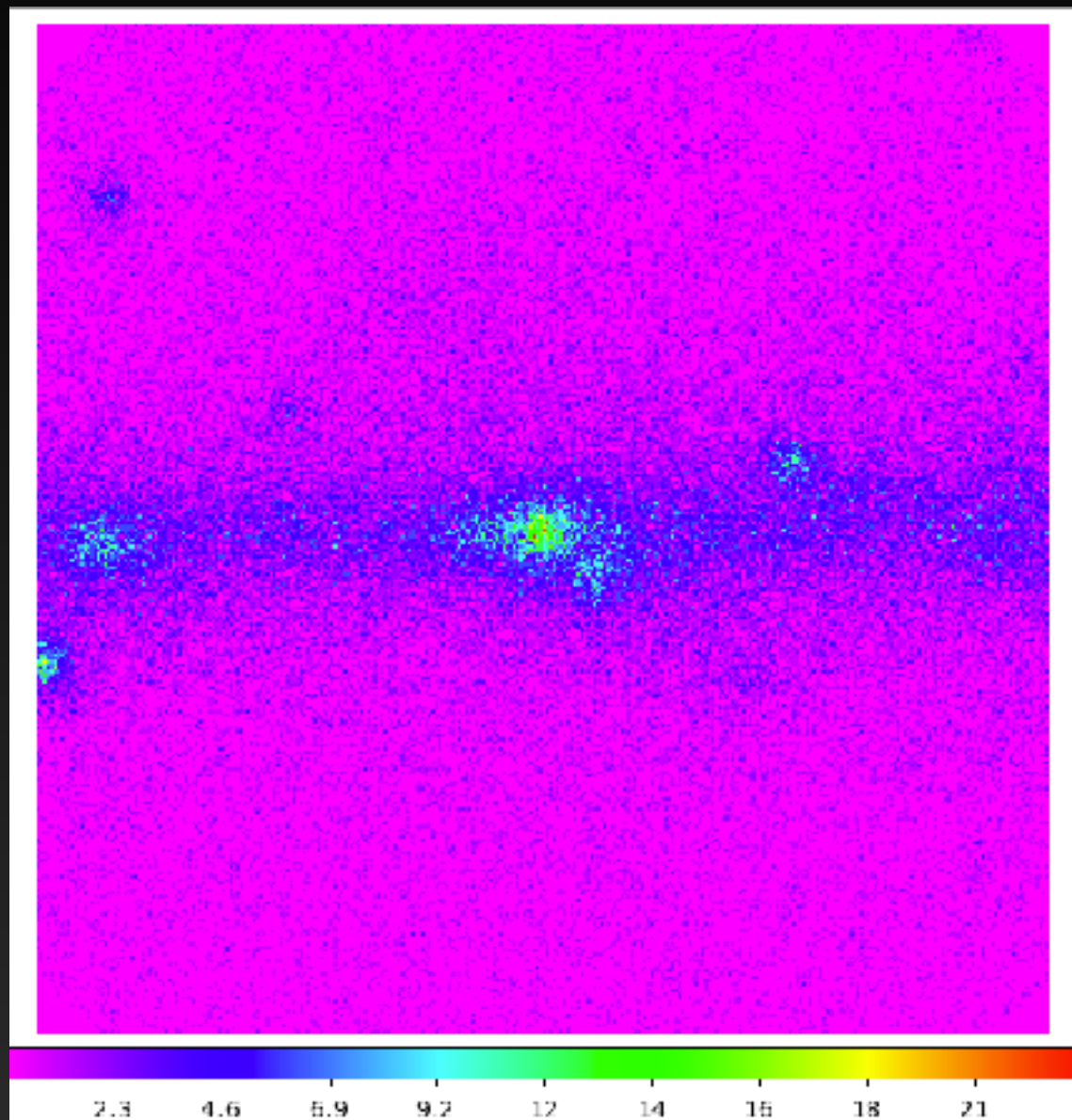
A Better fit to the Gamma-Ray Sky



Fits are significantly improved, in particular in regions near the Galactic Center where there is significant kinematic gas information.



Application to the Galactic Center

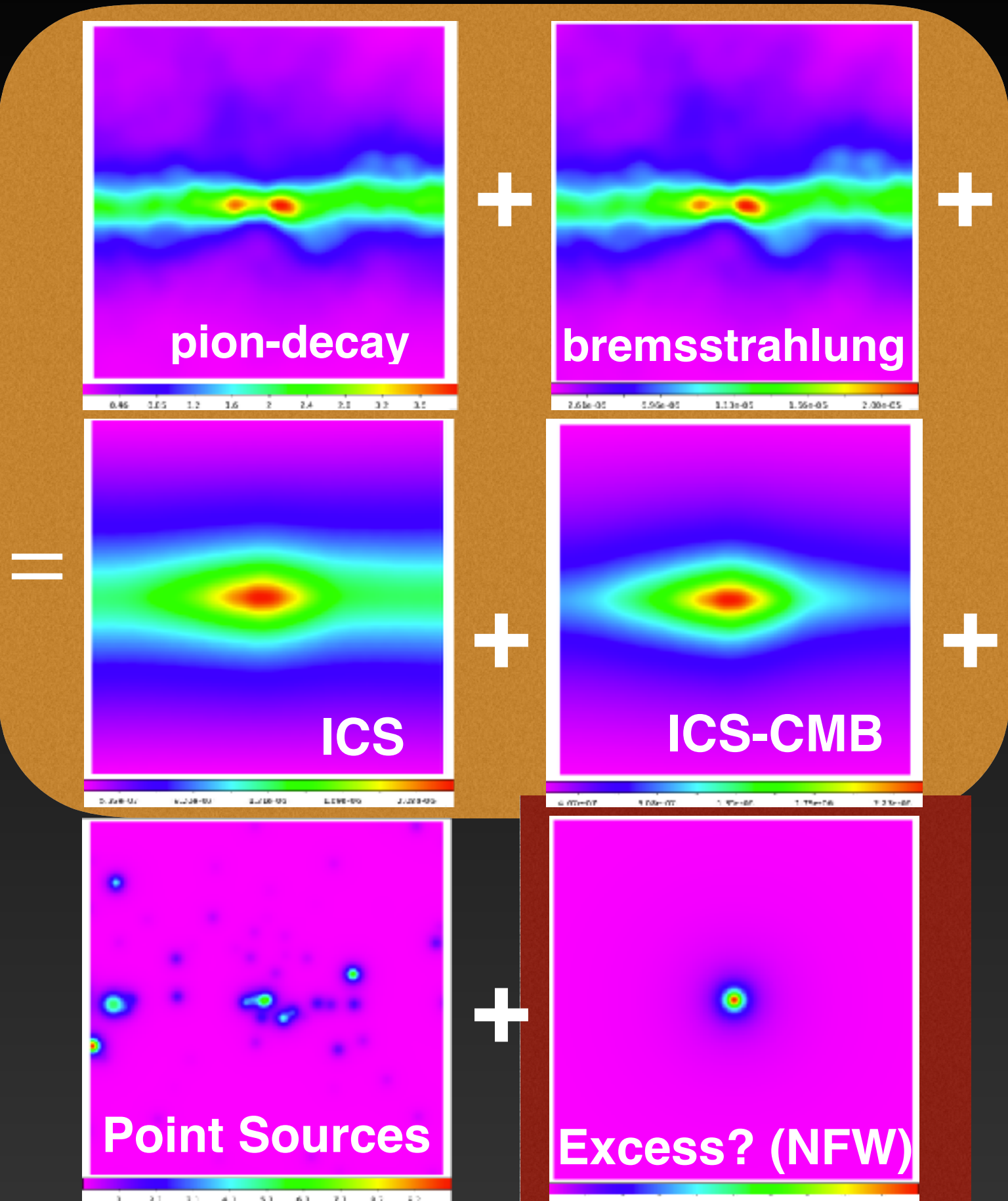


Data

750 — 950 MeV

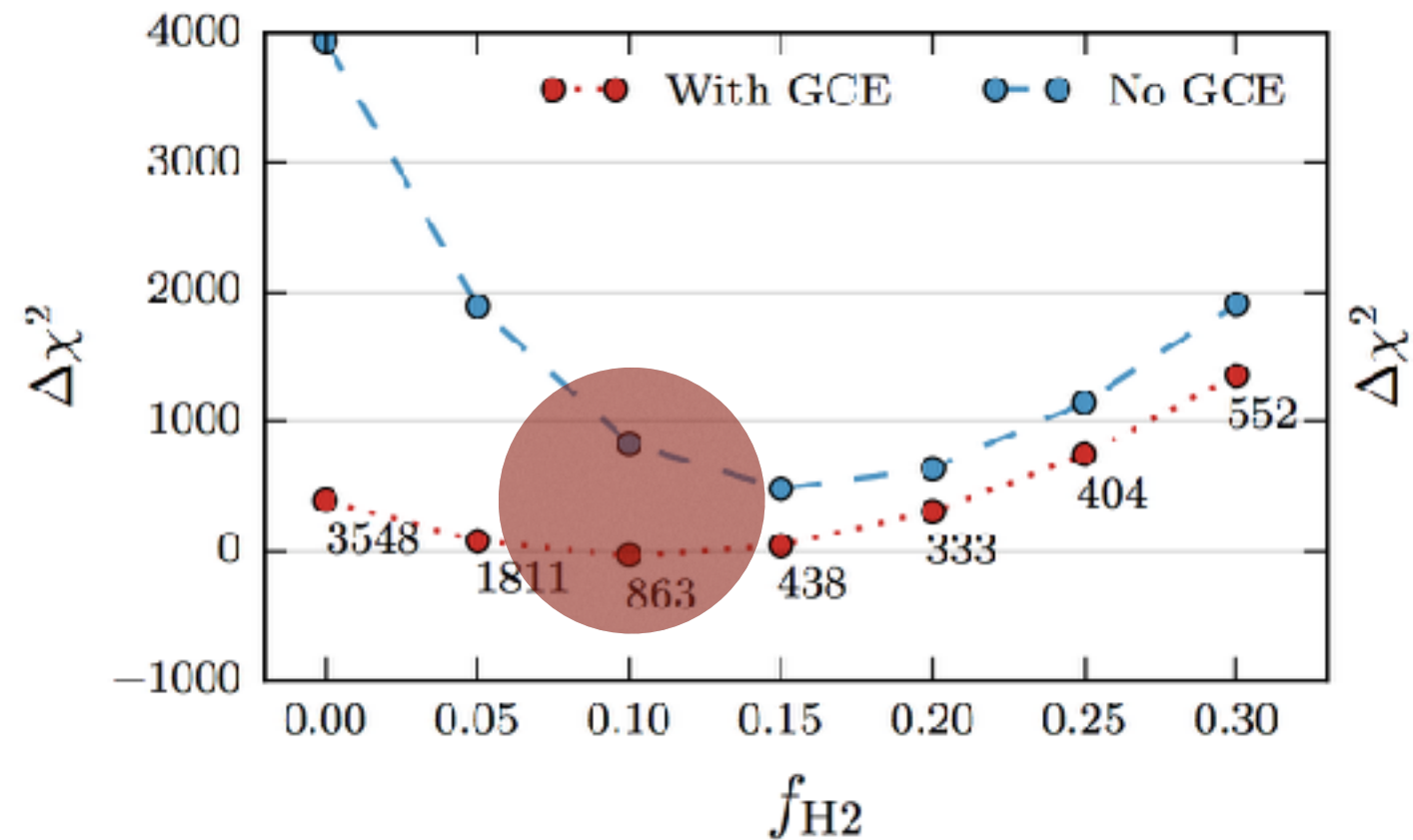
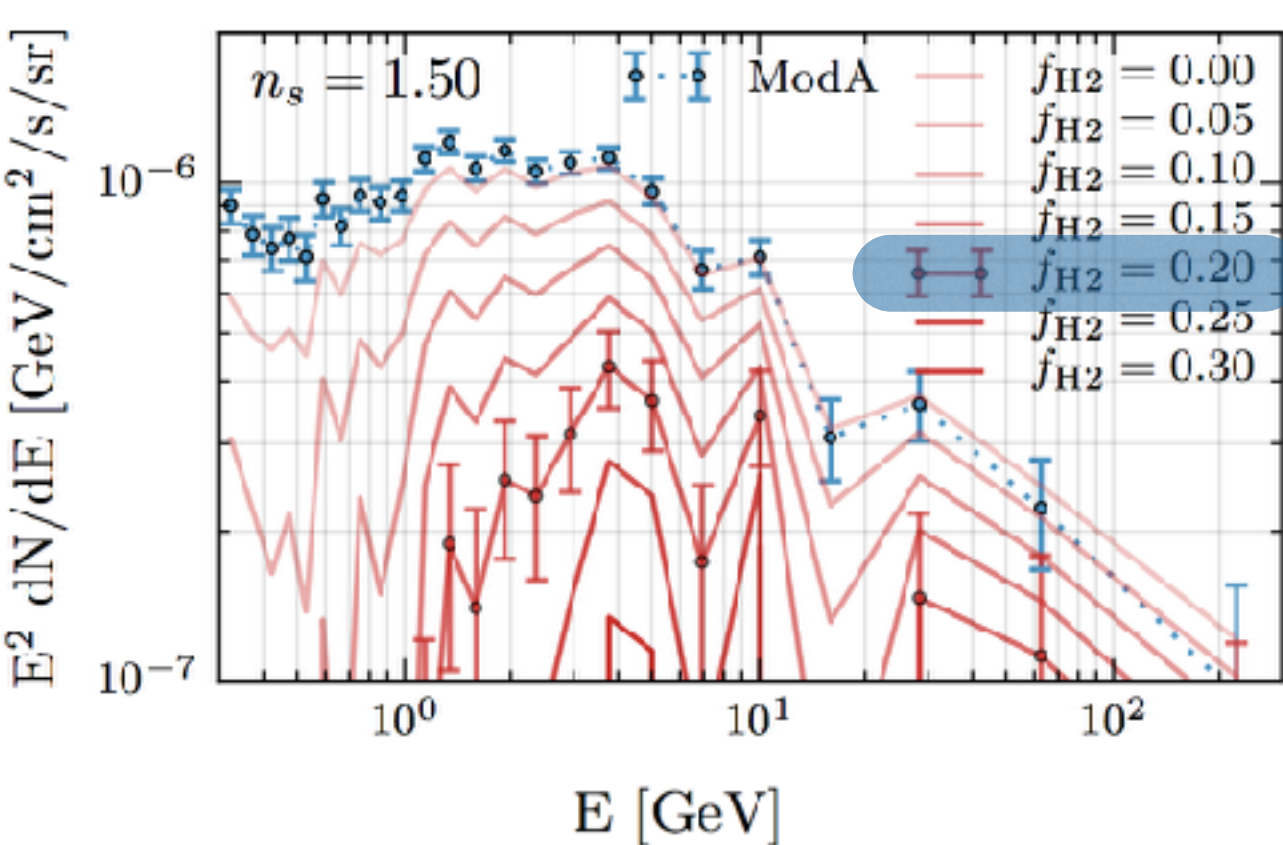
Best Angular Resolution Cut

$10^\circ \times 10^\circ$ ROI



Effect on the GC Excess

IG

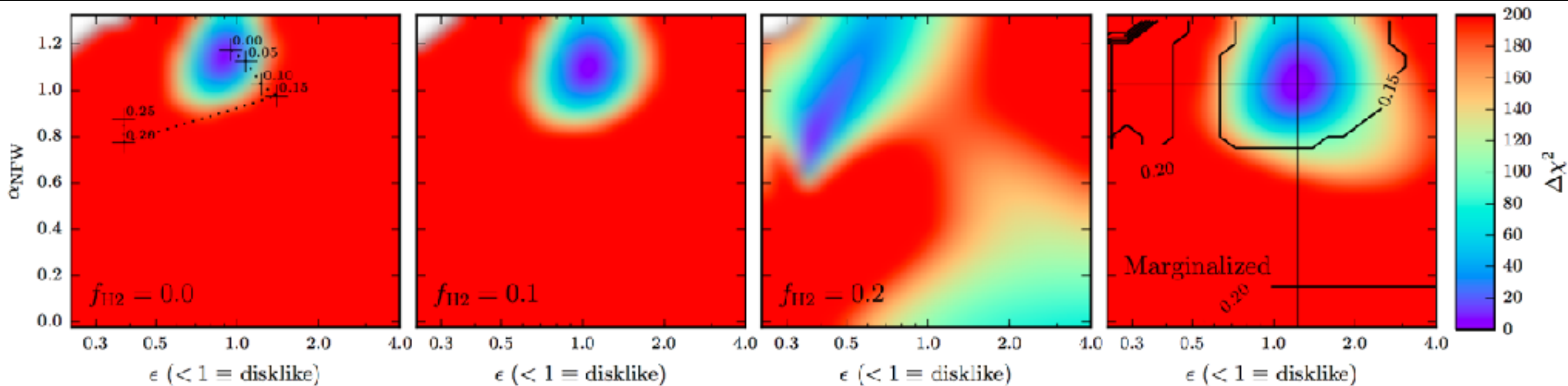


Increasing the value of f_{H2} decreases the intensity of the gamma-ray excess.

However, the best global fit is $f_{H2} = 0.1$, with a GC excess intensity that decreases by only $\sim 30\%$.

Effect on the Excess Morphology

IG



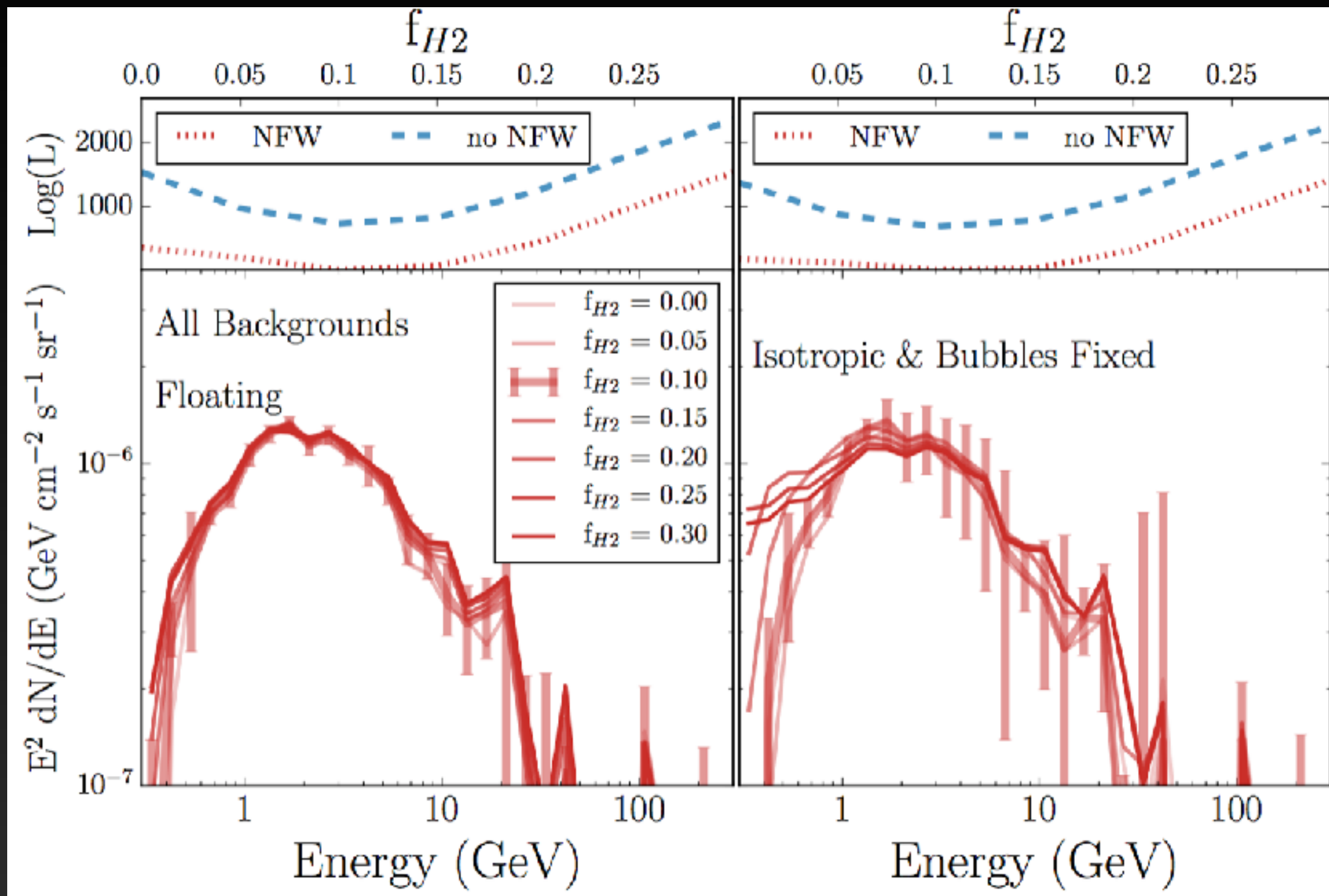
The morphology of the excess is also degenerate with f_{H2} .

As f_{H2} is increased, the best-fit morphology becomes stretched perpendicular to the galactic plane.

However, marginalized over all values of f_{H2} , the standard NFW template is still consistent with the data.

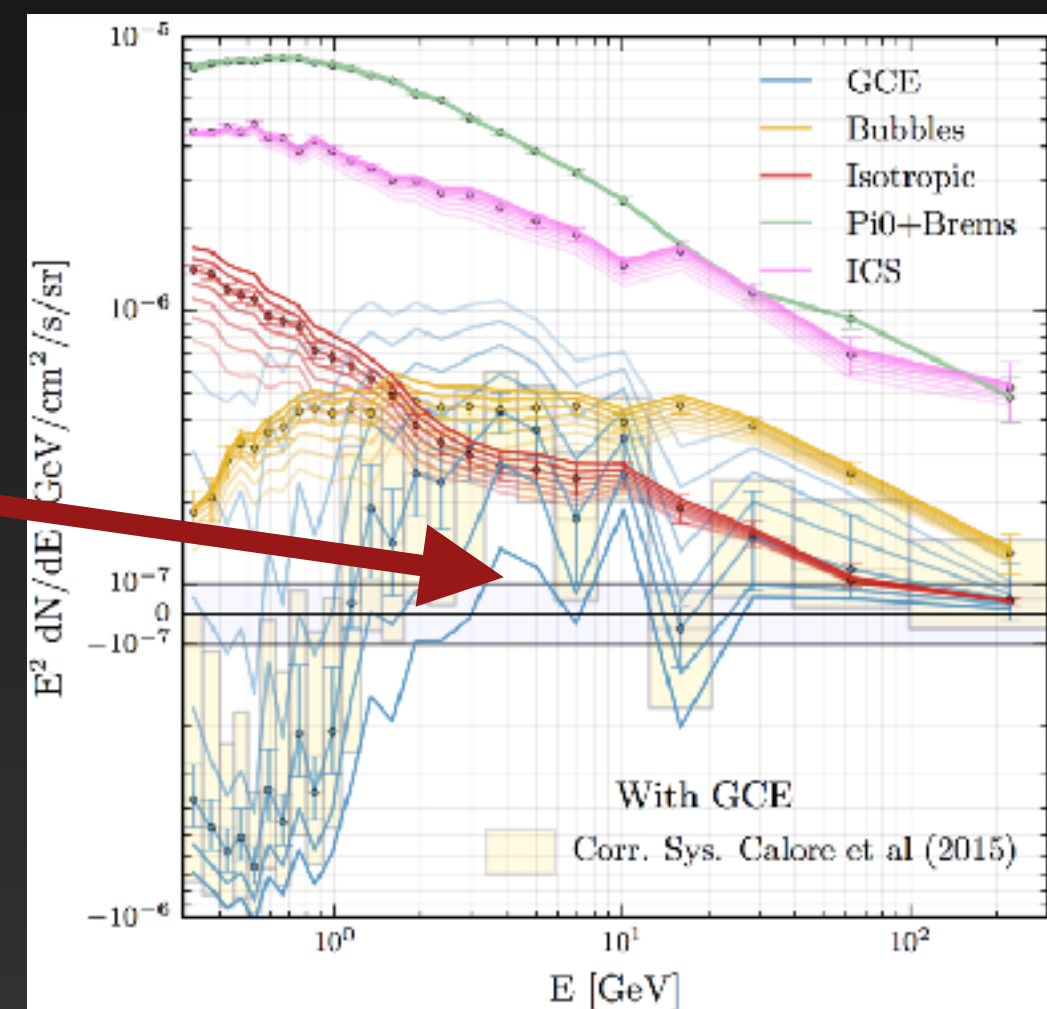
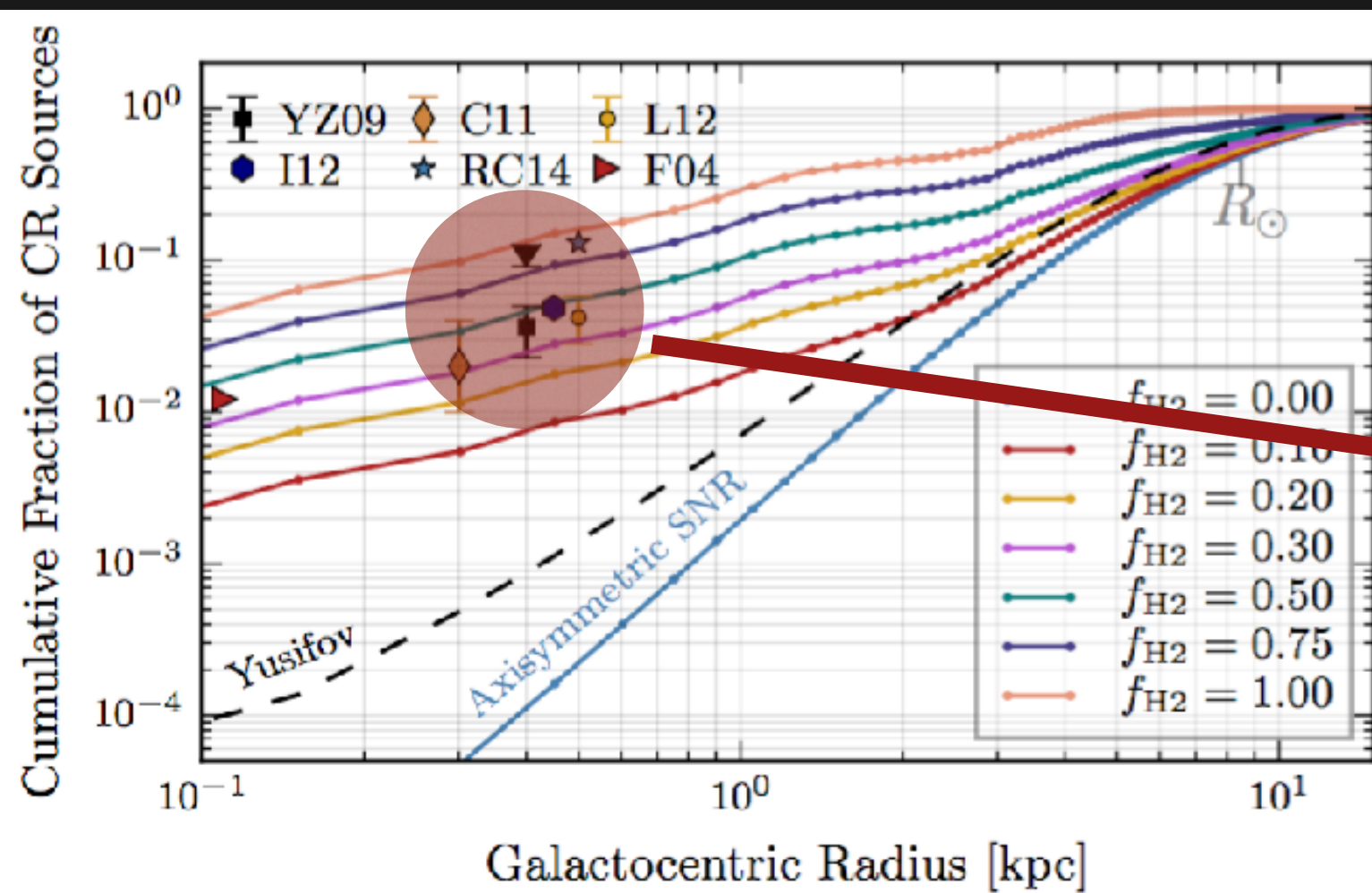
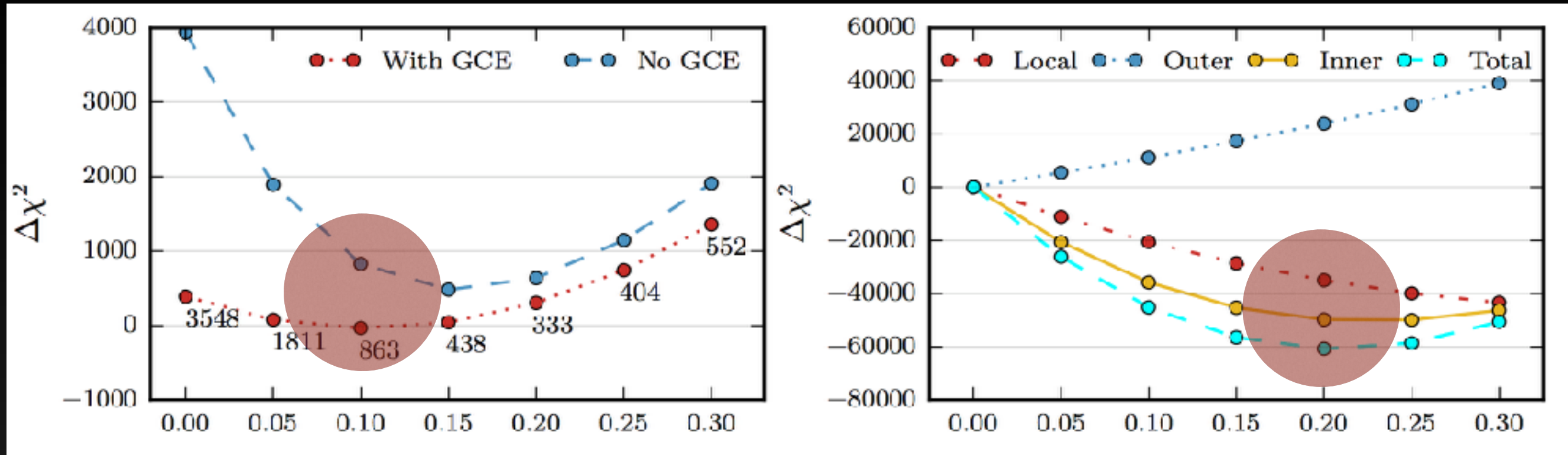
Analysis in the Galactic Center

GC



In this smaller region, the excess remains resilient to changes in diffuse emission modeling.

The Galactic Center Deficit?

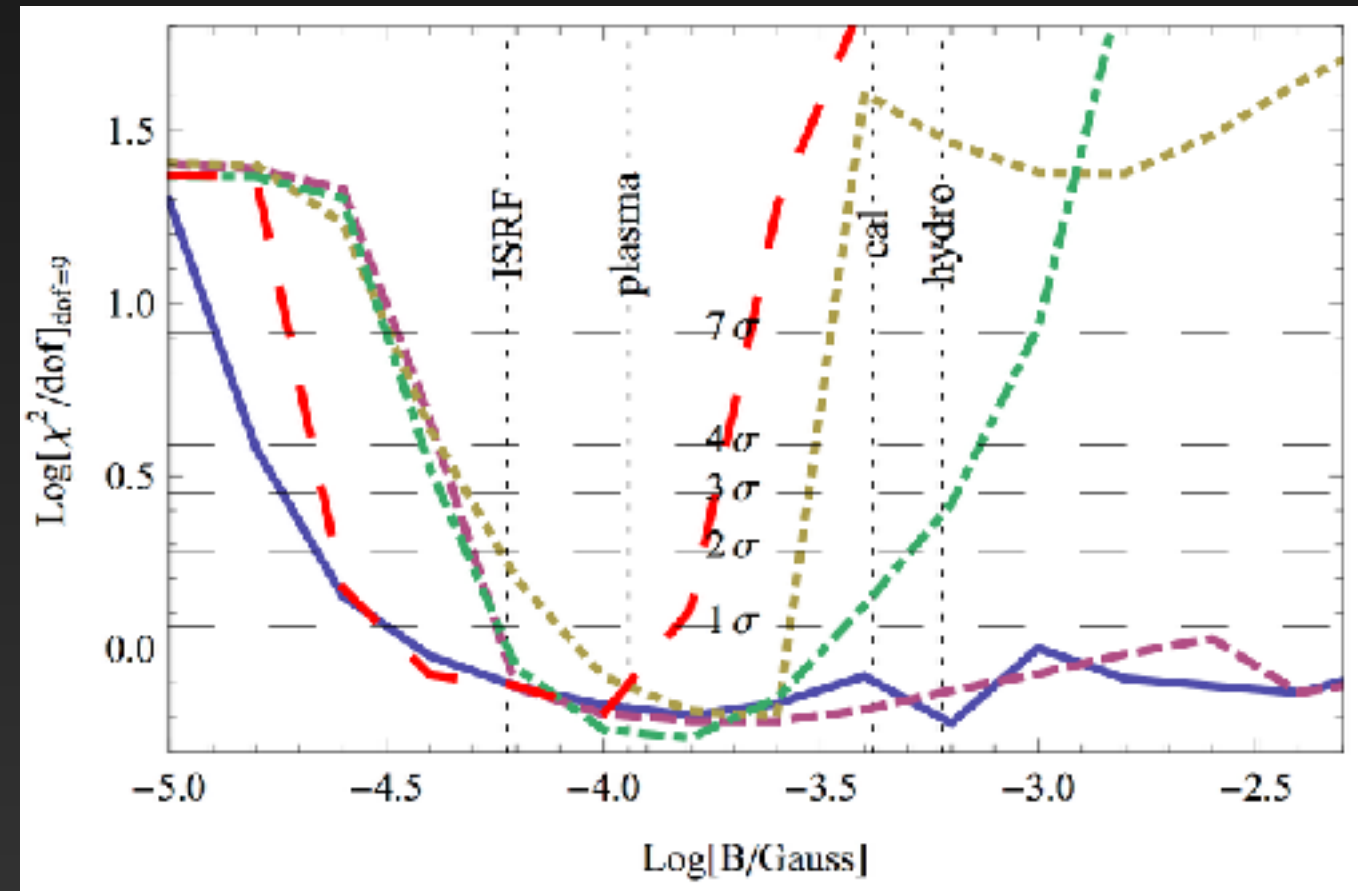
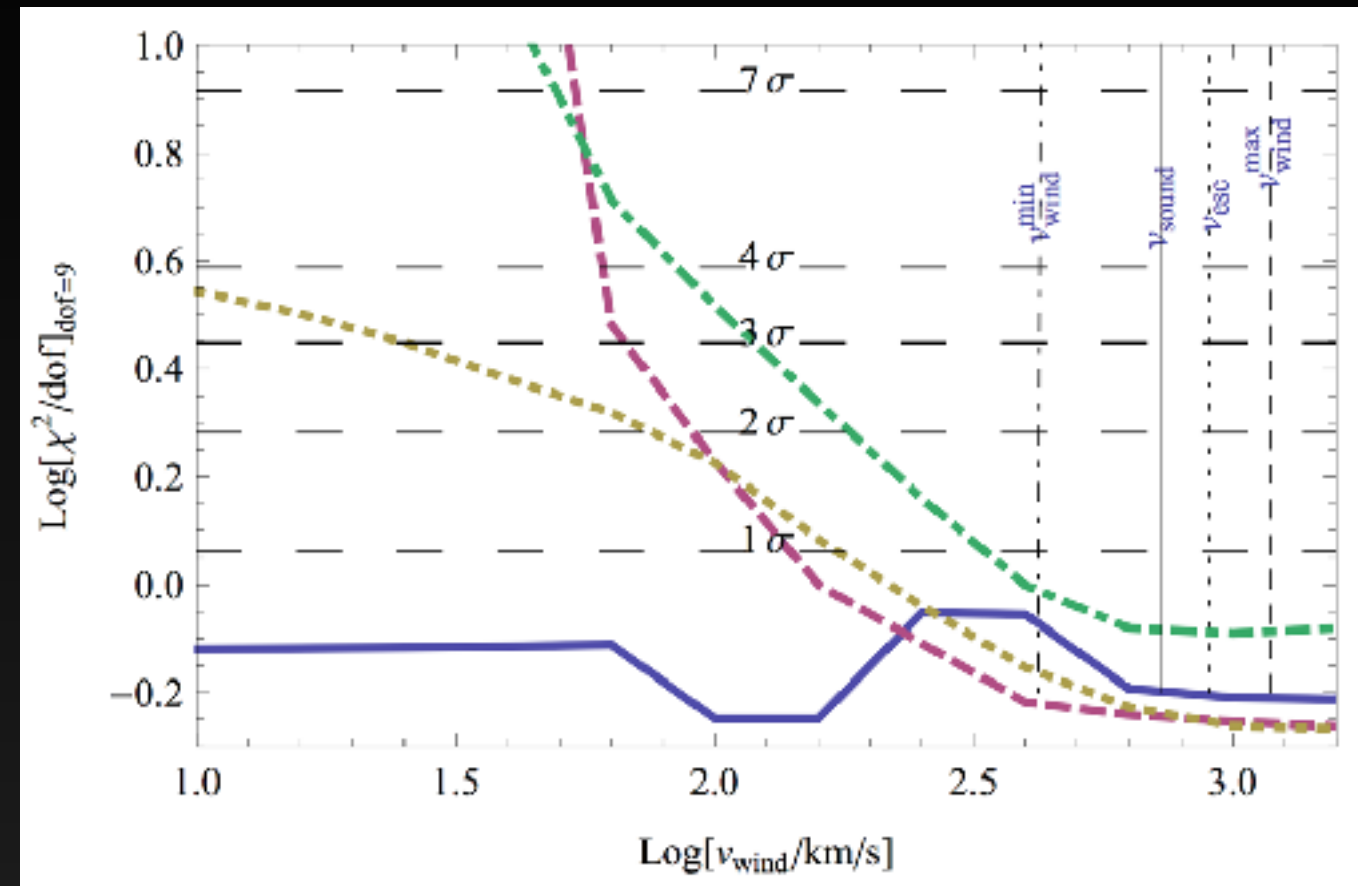


Advection and Convection in the Galactic Center

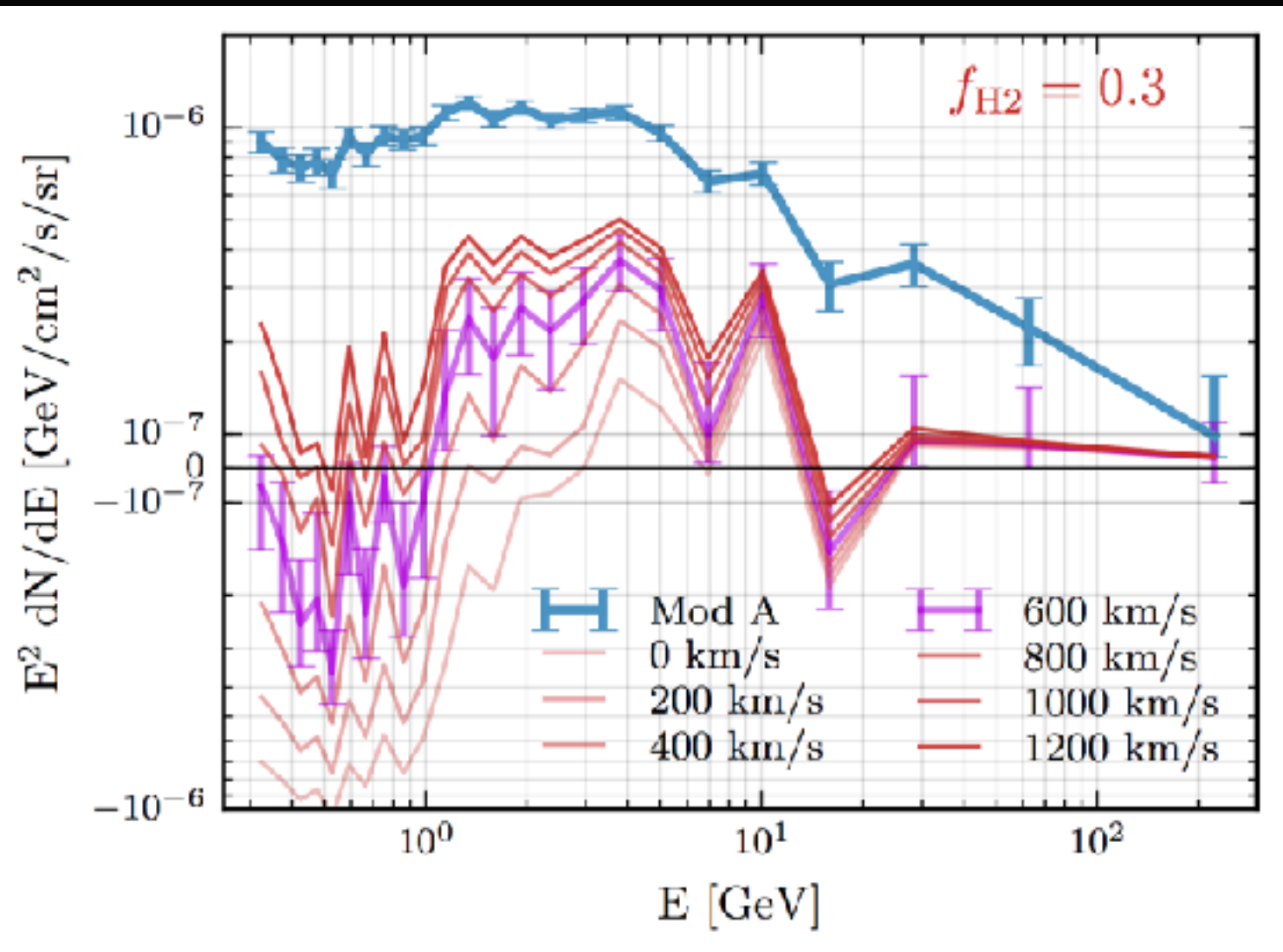
Crocker et al. (2011) demonstrated that the break in the GC synchrotron spectrum is best fit in the regime with:

- a.) Large Magnetic Fields
- b.) Large Convective Winds

Very different from typical Galprop diffusion scenario.



The Low Energy Spectrum



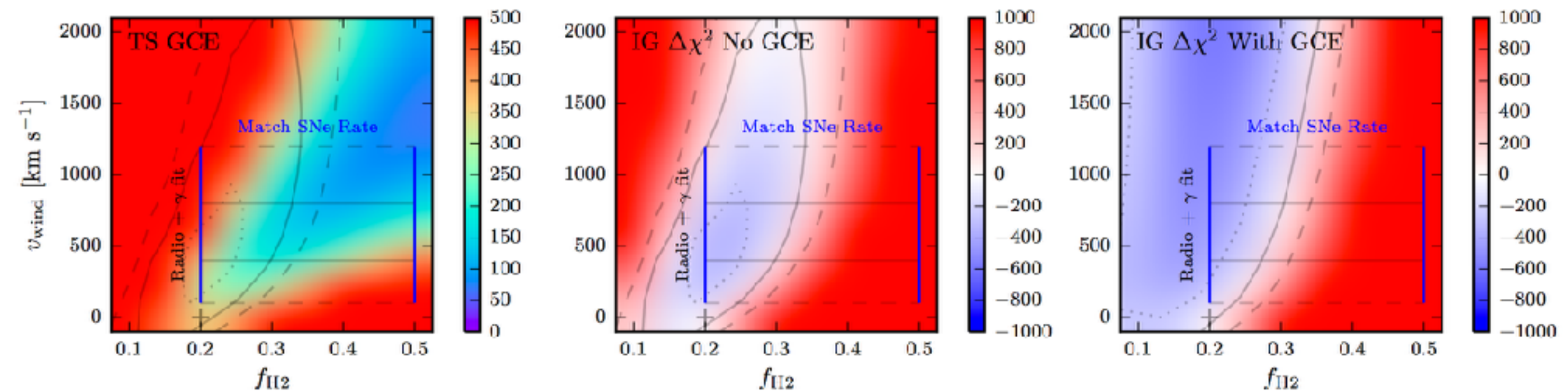
IG

Applying strong convective winds to the diffuse emission model fixes the low-energy over subtraction.

The intensity of the excess near the spectral peak also increases, up to ~50% of its nominal value.

The model produces a significantly better fit to the gamma-ray sky dataset - and also coincides better with multi wavelength data.

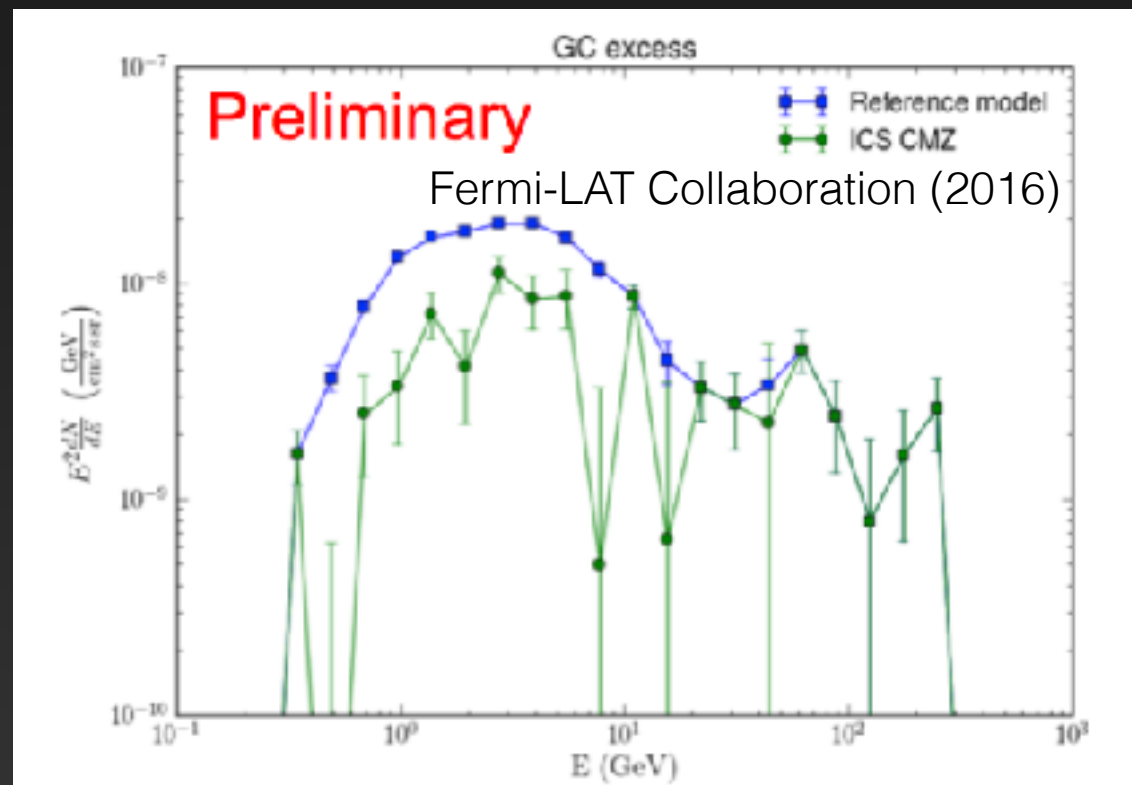
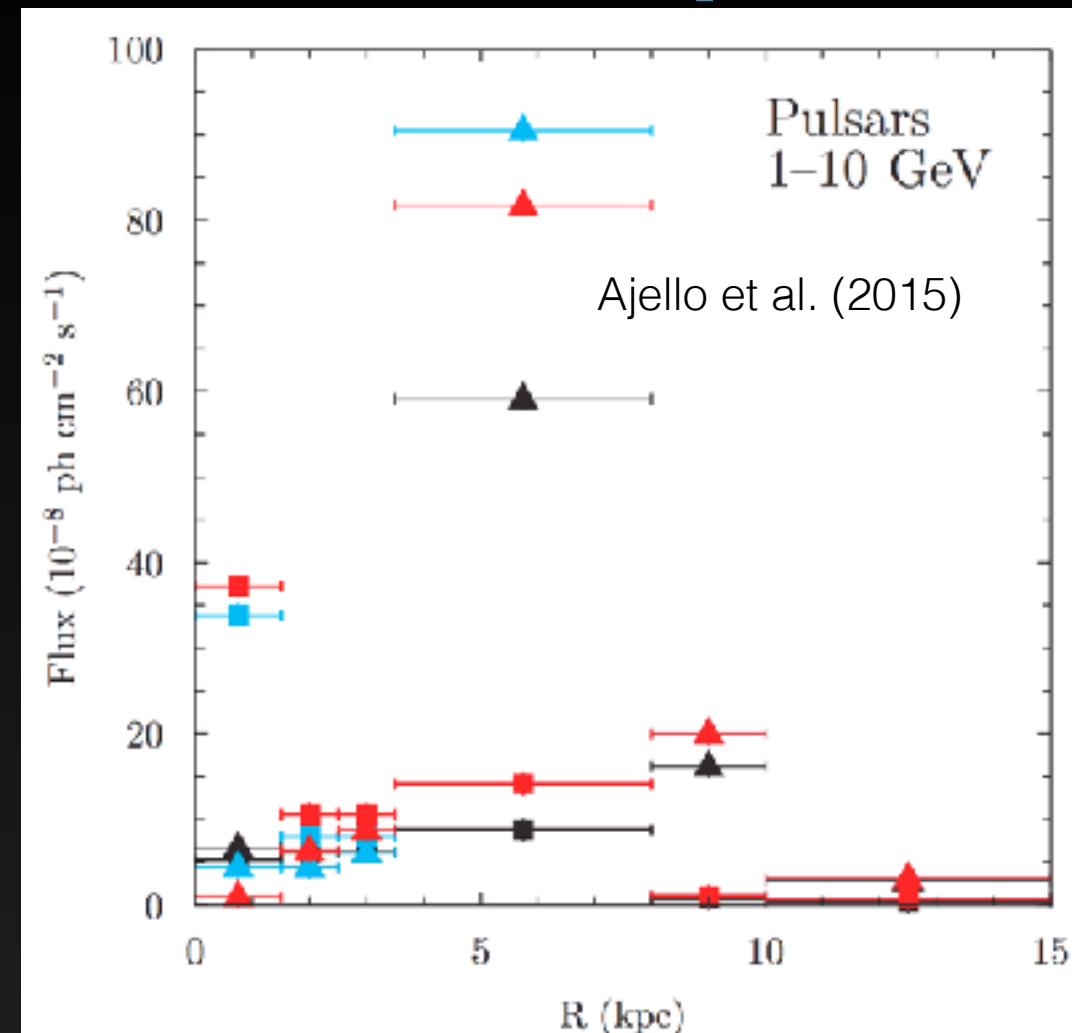
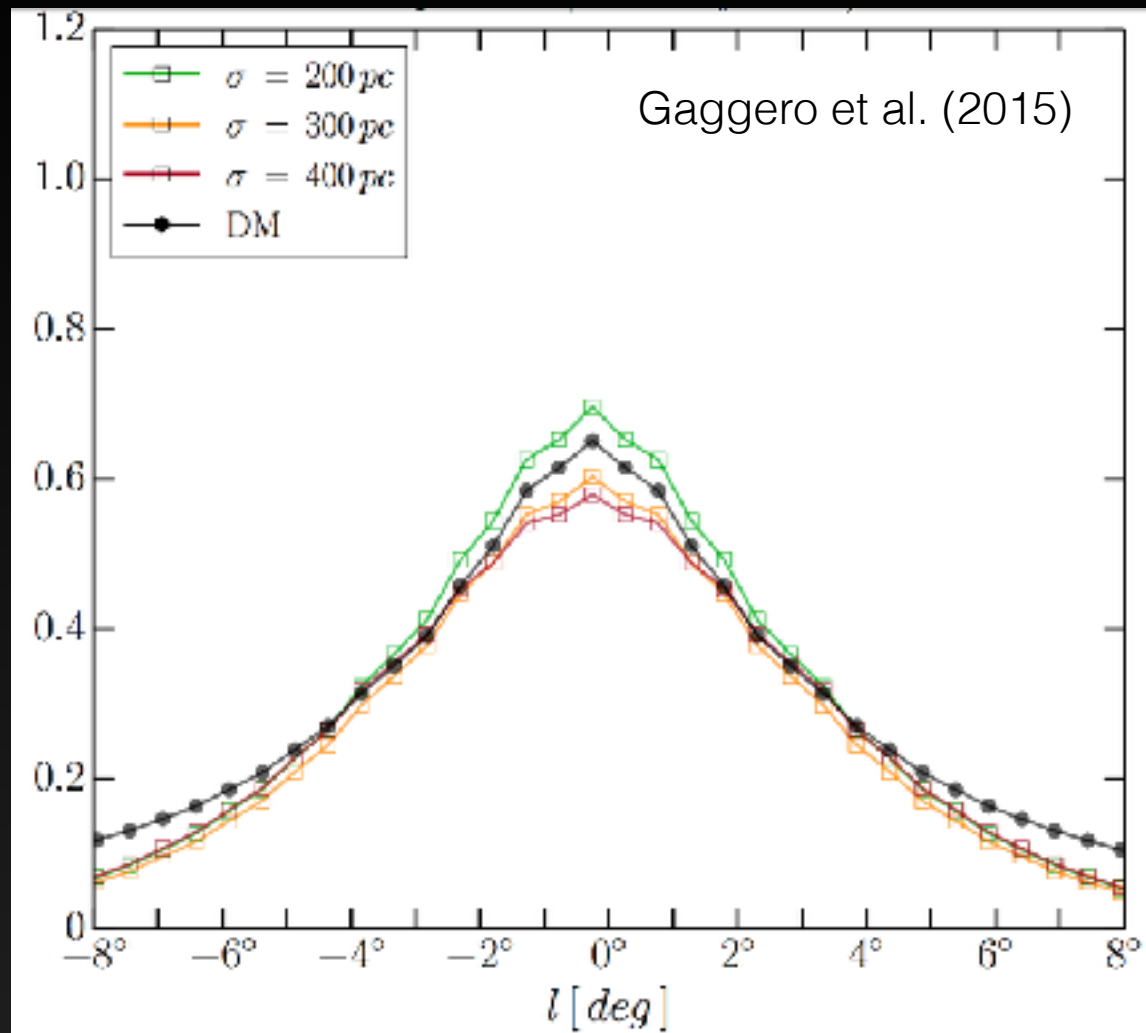
Convection in the Galactic Center



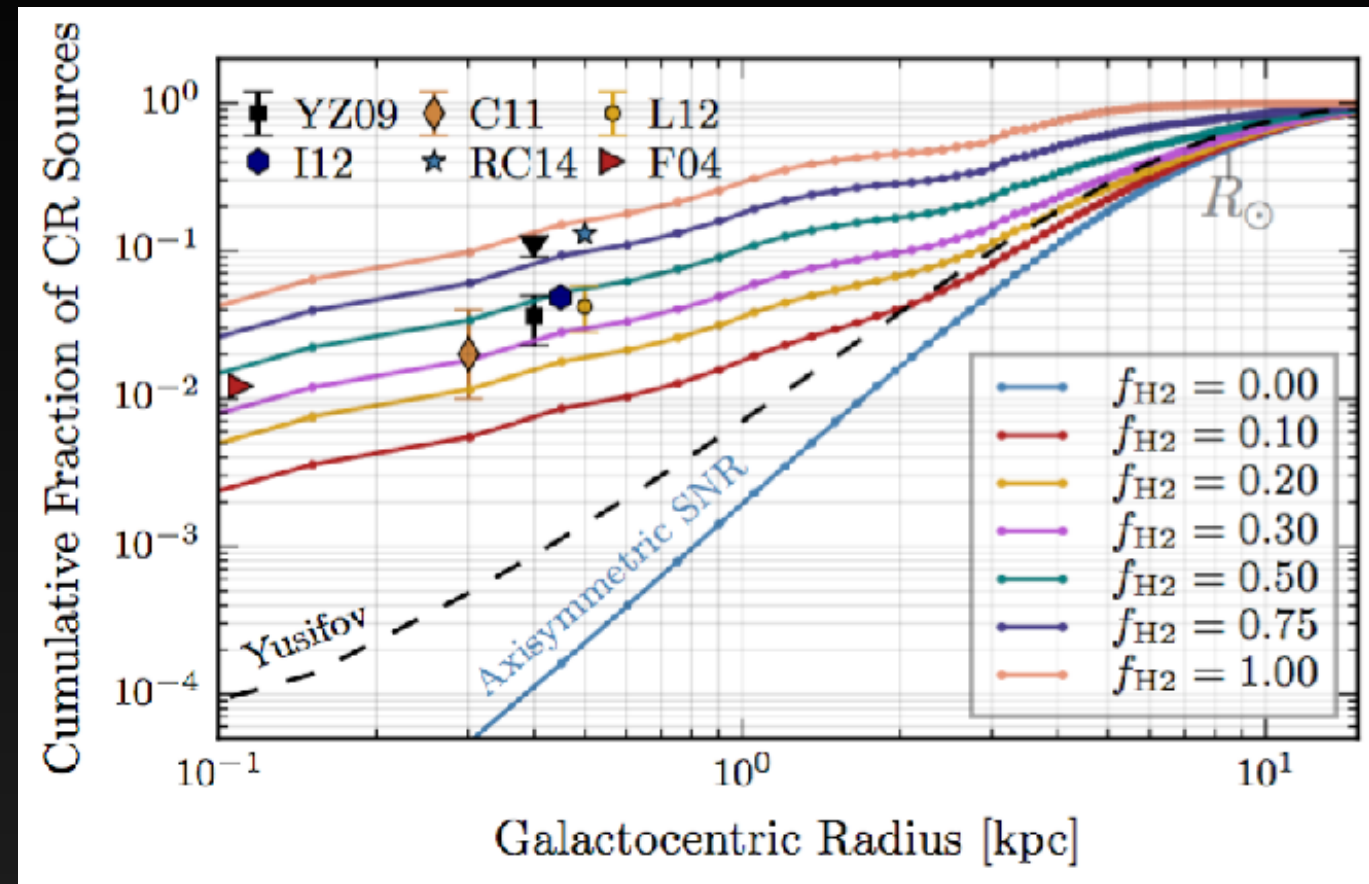
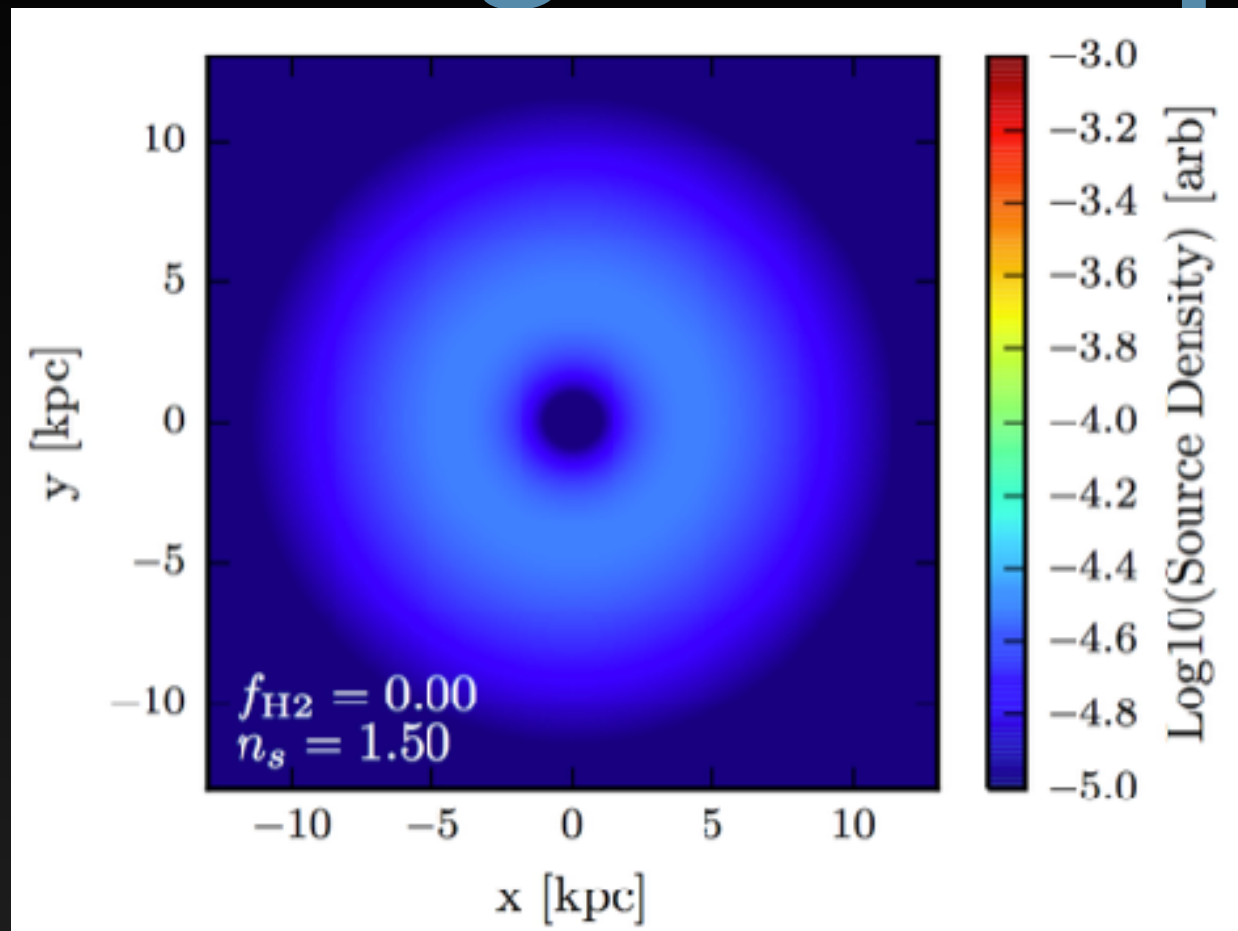
This increases the best fit value of f_{H_2} for the GC data, bringing this value into agreement with the global best fit value.

Models with a GCE component still prefer slightly lower values of f_{H_2} , but these have increased to 0.2 as well.

A Similar Result with Different Techniques



Waxing Philosophical.....

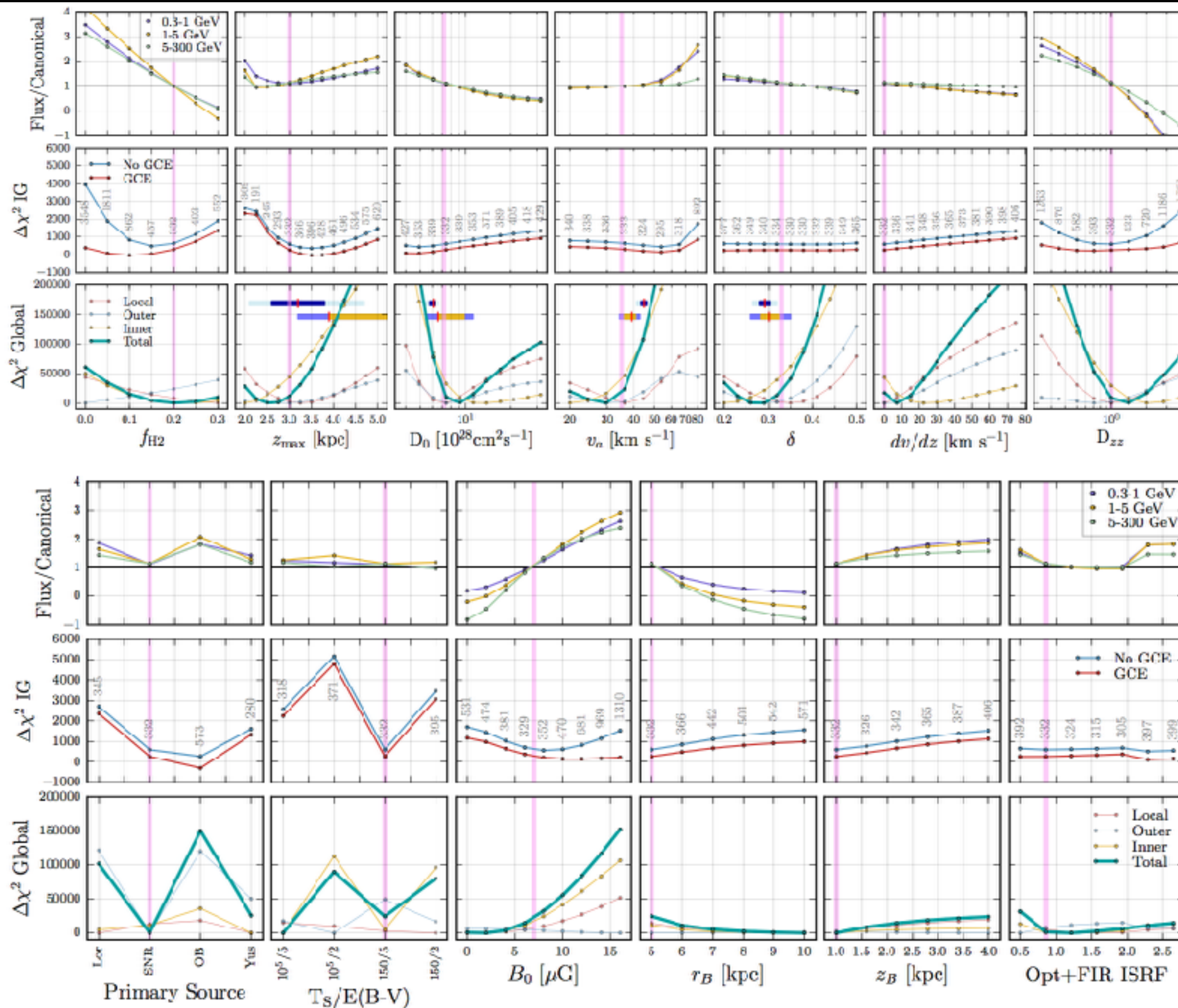


The lack of cosmic-ray injection in the GC should still be slightly disturbing. Especially when we try to answer the question: “excess compared to what?”

Our models indicate a degeneracy between cosmic-ray injection and the existence of a Galactic center excess template tracing an NFW profile. However, at present the best fit models still include a significant NFW component.

Many other checks still show an excess...

IG

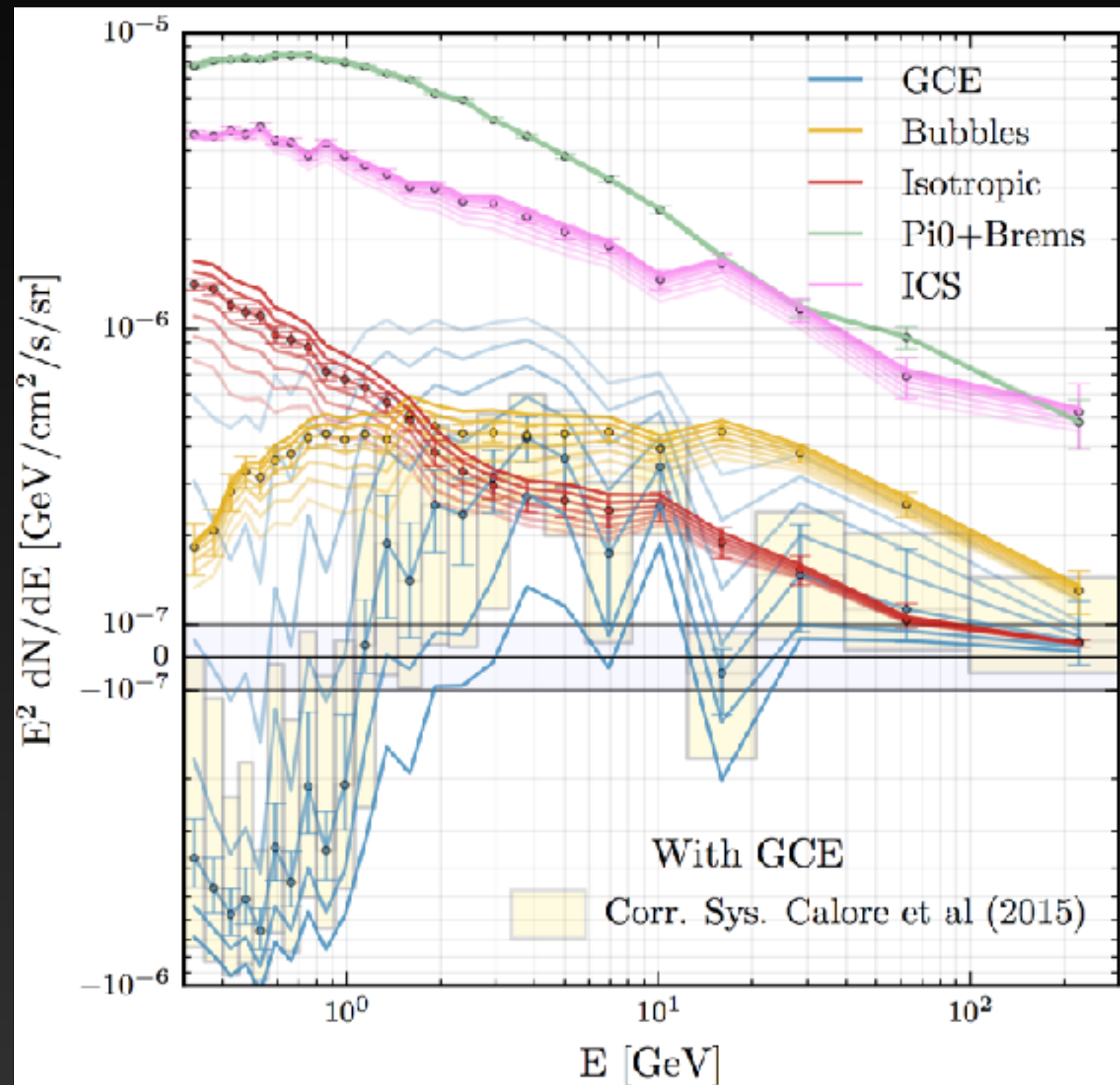


And the excess still appears spectrally unique....

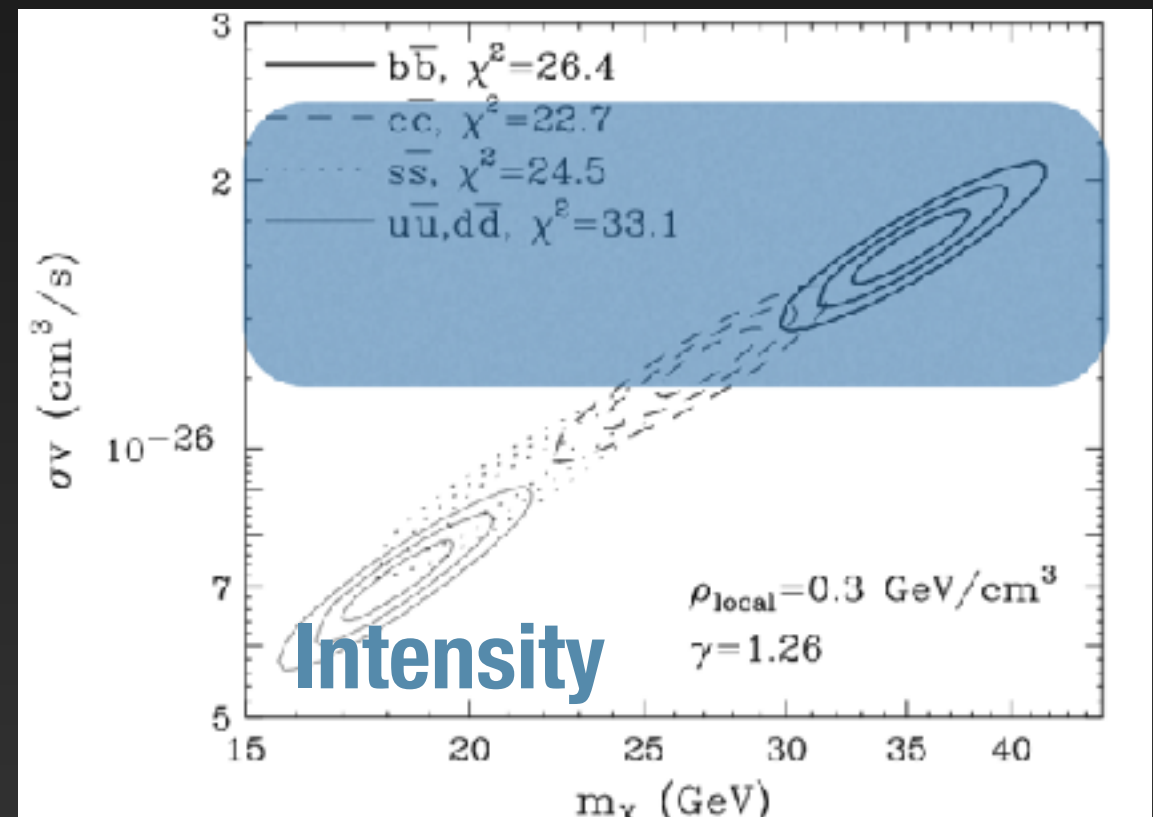
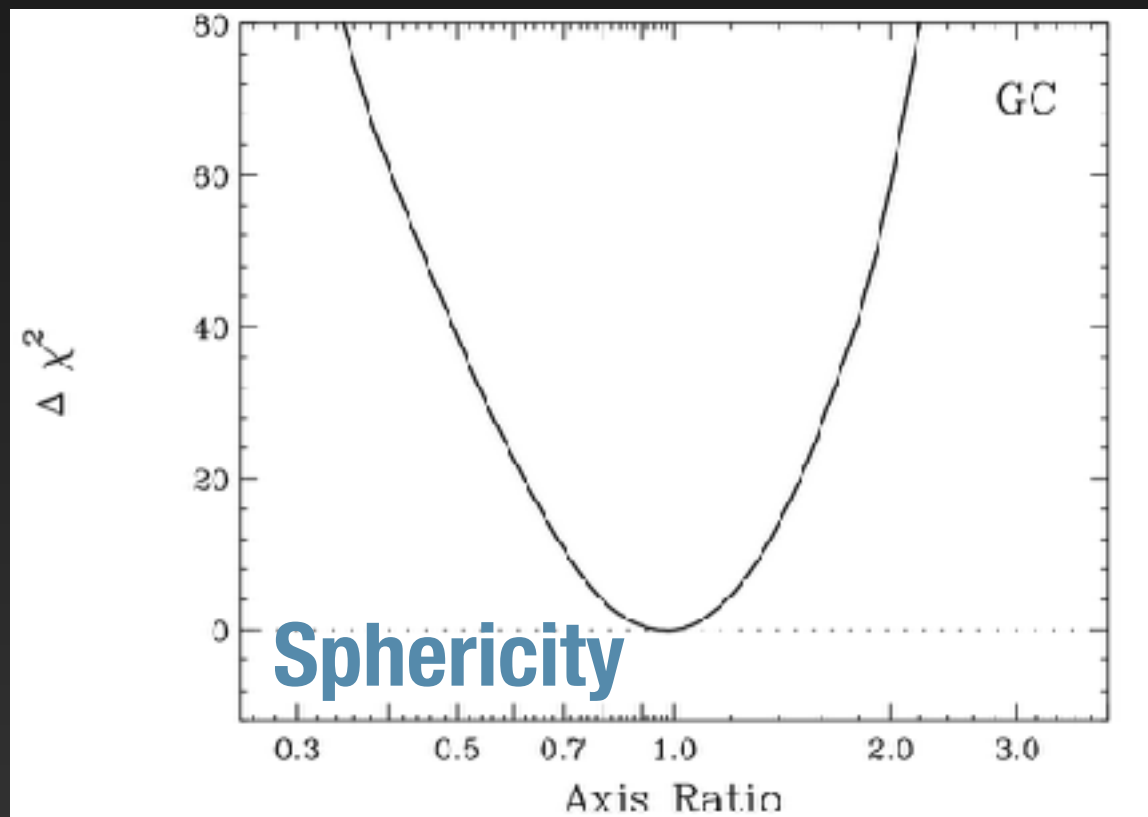
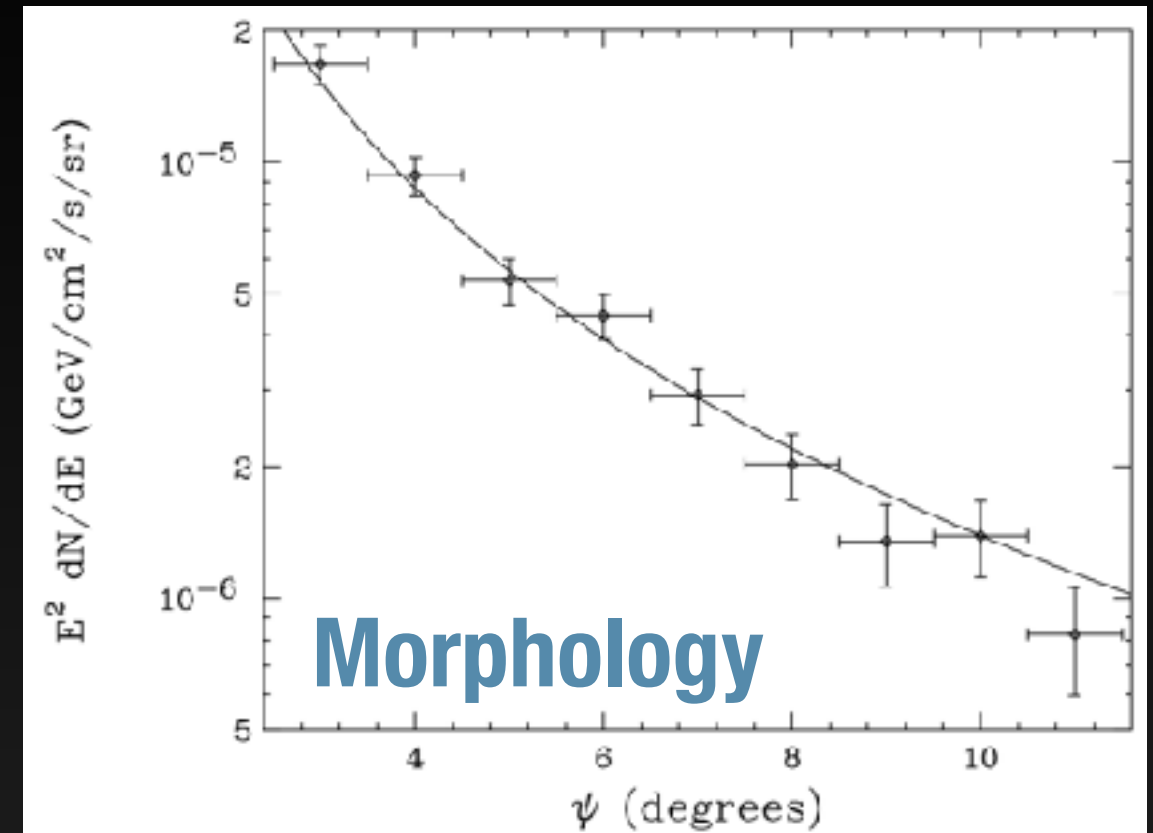
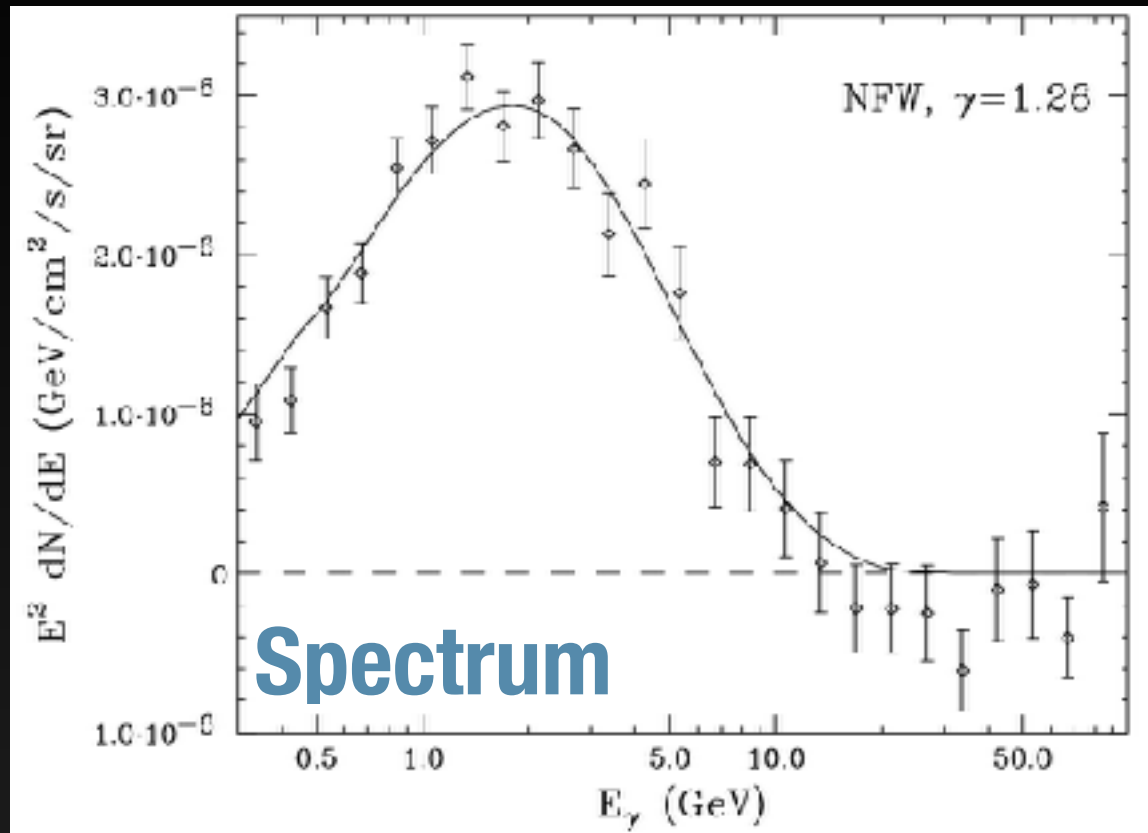
IG

Even as the fraction of emission from diffuse models increases — and the total amplitude of the excess decreases, a spectral component remains.

Note: The spectrum of the diffuse model is allowed to change on a bin to bin basis. We do not force the spectrum of the diffuse model.



Dark Matter Model Fitting?

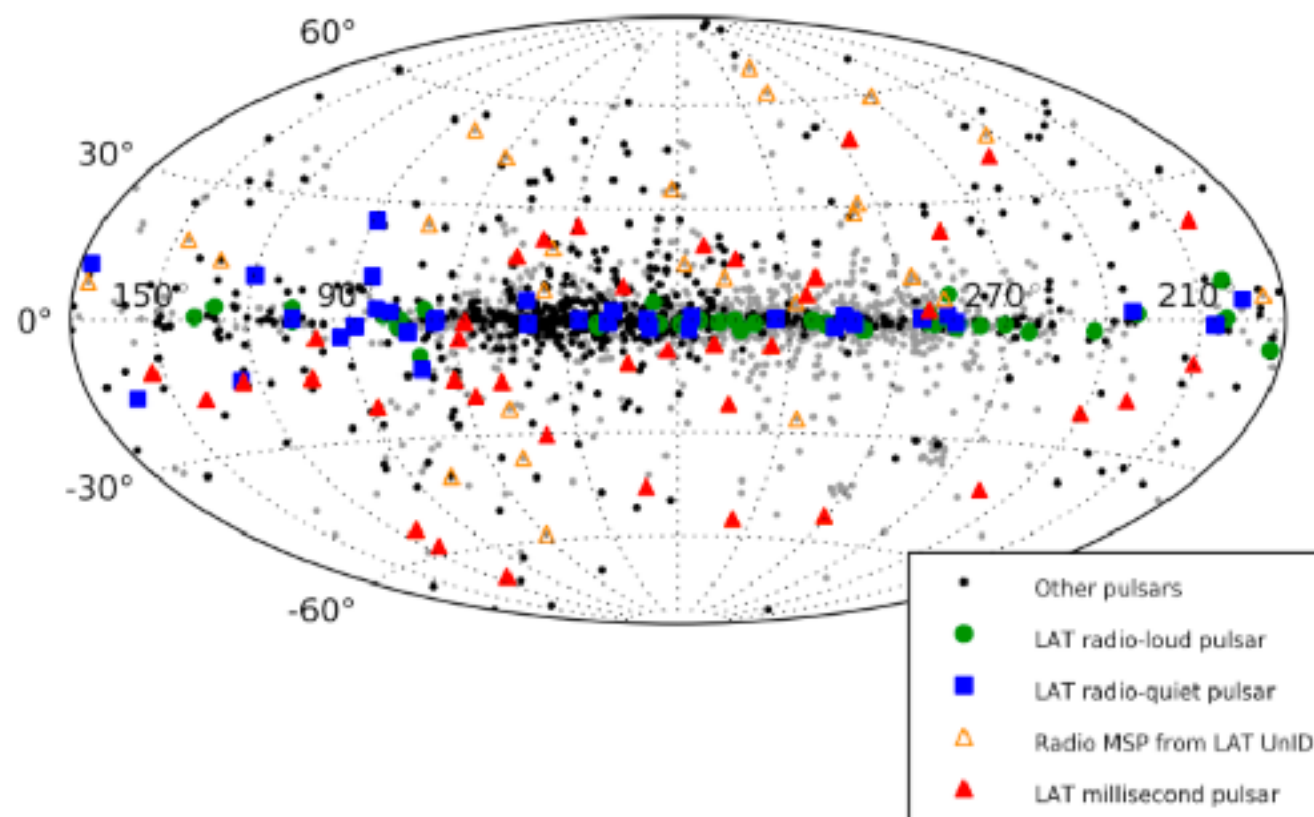
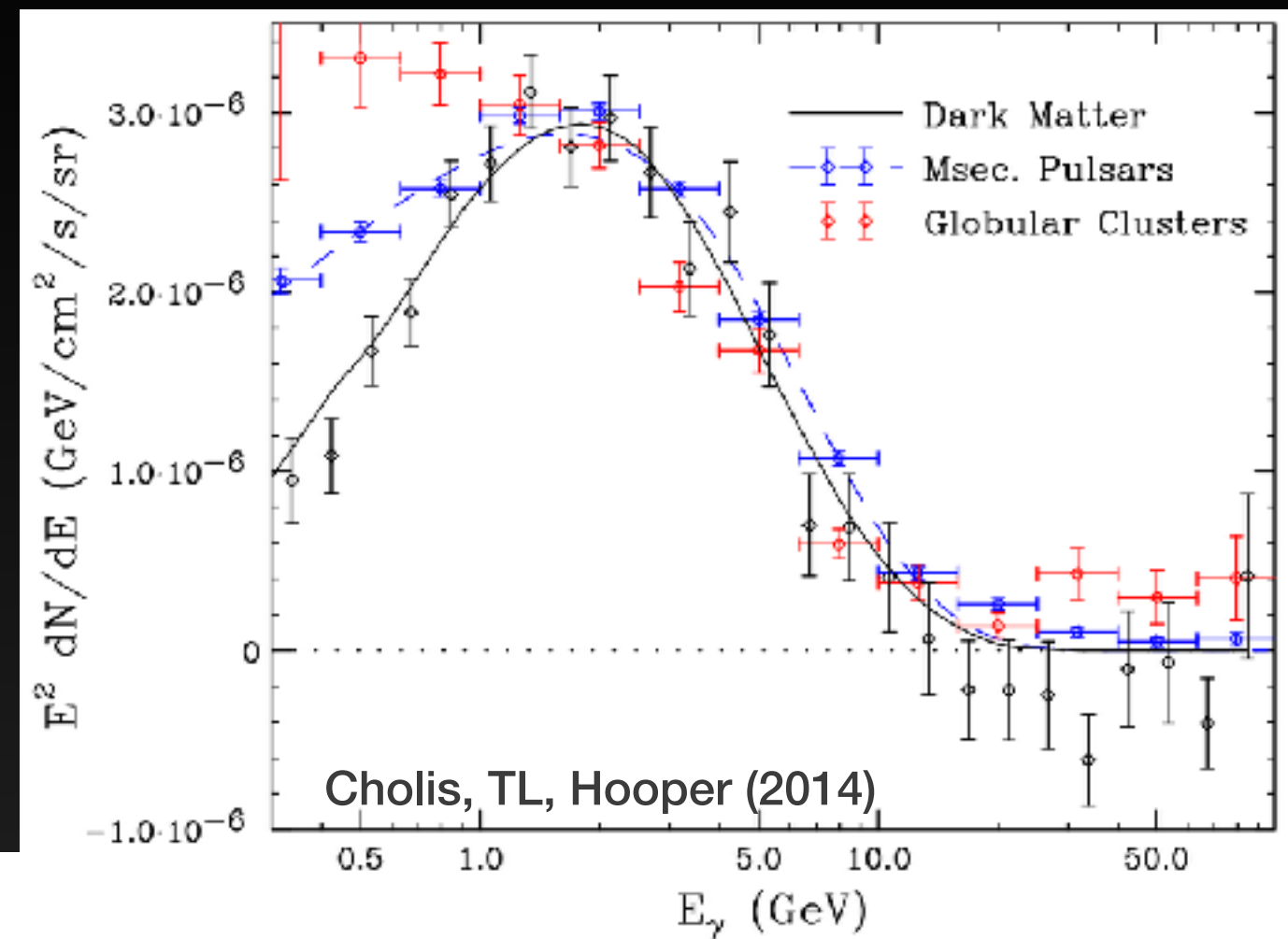


Particle Physics Models Exist...

Chan (1607.02246)	Butter et al. (1507.02288)	Buckley et al. (1410.6497)	Alves et al. (1312.5281)
Jia (1607.00737)	Mondal et al. (1507.01793)	Heikinheimo & Spethmann (1410.4842)	Fortes et al. (1312.2837)
Barrau et al. (1606.08031)	Cao et al. (1506.06471)	Freytsis et al. (1410.3818)	Banik et al. (1311.0126)
Huang et al. (1605.09018)	Banik et al. (1506.05665)	Yu et al. (1410.3347)	Arhrib et al. (1310.0358)
Cui et al. (1605.08138)	Ipek (1505.07826)	Cao et al. (1410.3239)	Kelso et al. (1308.6630)
Krauss et al. (1605.05327)	Buchmueller et al. (1505.07826)	Guo et al. (1409.7864)	Kozaczuk et al. (1308.5705)
Kumar et al. (1605.00611)	Balazs et al. (1505.06758)	Yu (1409.3227)	Kumar (1308.4513)
Biswas et al. (1604.06566)	Medina (1505.05565)	Cahill-Rowley et al. (1409.1573)	Demir et al. (1308.1203)
Sage et al. (1604.04589)	Kim et al. (1505.04620)	Banik & Majumdar (1408.5795)	Buckley et al. (1307.3561)
Choquette et al. (1604.01039)	Ko et al. (1504.06944)	Bell et al. (1408.5142)	Cline et al. (1306.4710)
Cuoco et al. (1603.08228)	Ko & Tang (1504.03908)	Ghorbani (1408.4929)	Cannoni et al. (1205.1709)
Chao et al. (1602.05192)	Ghorbani & Ghorbani (1504.03610)	Okada & Seto (1408.2583)	An et al. (1110.1366)
Horiuchi et al. (1602.04788)	Fortes et al. (1503.08220)	Frank & Mondal (1408.2223)	Buckley et al. (1106.3583)
Hektor et al. (1602.00004)	Cline et al. (1503.08213)	Baek et al. (1407.6588)	Boucenna et al. (1106.3368)
Freytsis et al. (1601.07556)	Rajaraman et al. (1503.05919)	Tang (1407.5492)	Ellis et al. (1106.0768)
Kim et al. (1601.05089)	Bi et al. (1503.03749)	Balazs & Li (1407.0174)	Cheung et al. (1104.5329)
Huang et al. (1512.08992)	Kopp et al. (1503.02669)	Huang et al. (1407.0038)	Marshall et al. (1102.0492)
Kulkarni et al. (1512.06836)	Elor et al. (1503.01773)	McDermott (1406.6408)	Abada et al. (1101.0365)
Tang et al. (1512.02899)	Gherghetta et al. (1502.07173)	Cheung et al. (1406.6372)	Tytgat (1012.0576)
Cox et al. (1512.00471)	Berlin et al. (1502.06000)	Arina et al. (1406.5542)	Logan (1010.4214)
Cai et al. (1511.09247)	Achterberg et al. (1502.05703)	Chang & Ng (1406.4601)	Barger et al. (1008.1796)
Agrawal et al. (1511.06293)	Modak et al. (1502.05682)	Wang & Han (1406.3598)	Raklev et al. (0911.1986)
Duerr et al. (1510.07562)	Guo et al. (1502.00508)	Cline et al. (1405.7691)	
Drozd et al. (1510.07053)	Chen & Nomura (1501.07413)	Berlin et al. (1405.5204)	
Arcadi et al. (1510.02297)	Kozaczuk & Martin (1501.07275)	Mondal & Basak (1405.4877)	
Williams (1510.00714)	Berlin et al. (1501.03496)	Martin et al. (1405.0272)	
Cai & Spray (1509.08481)	Kaplinghat et al. (1501.03507)	Ghosh et al. (1405.0206)	
Freese et al. (1509.05076)	Alves et al. (1501.03490)	Abdullah et al. (1404.5503)	
Bhattacharya et al. (1509.03665)	Biswas et al. (1501.02666)	Park & Tang (1404.5257)	
Algeri et al. (1509.01010)	Biswas et al. (1501.02666)	Cerdeno et al. (1404.2572)	
Fox & Tucker-Smith (1509.00499)	Ghorbani & Ghorbani (1501.00206)	Izaguirre et al. (1404.2018)	
Dutta et al. (1509.05989)	Cerdeno et al. (1501.01296)	Agrawal et al. (1404.1373)	
Liu et al. (1508.05716)	Liu et al. (1412.1485)	Berlin et al. (1404.0022)	
Berlin et al. (1508.05390)	Hooper (1411.4079)	Alves et al. (1403.5027)	
Fan et al. (1507.06993)	Arcadi et al. (1411.2985)	Finkbeiner & Weiner (1402.6671)	
Hektor et al. (1507.05096)	Cheung et al. (1411.2619)	Boehm et al. (1401.6458)	
Achterbeg et al. (1507.04644)	Agrawal et al. (1411.2592)	Kopp et al. (1401.6457)	
Biswas et al. (1507.04543)	Kile et al. (1411.1407)	Modak et al. (1312.7488)	

Millisecond Pulsar Fits

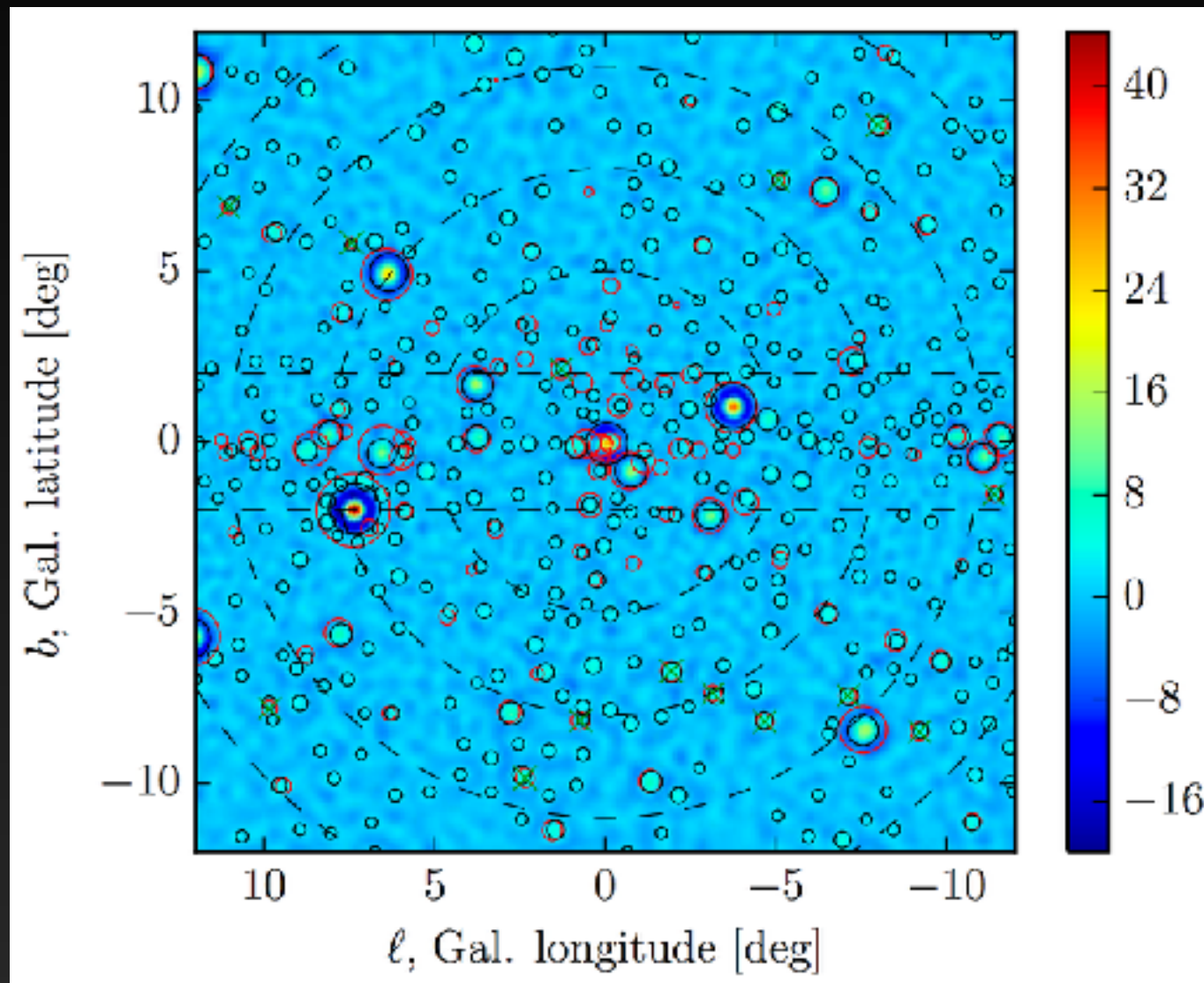
- The peak of the MSP energy spectrum matches the peak of the GeV excess



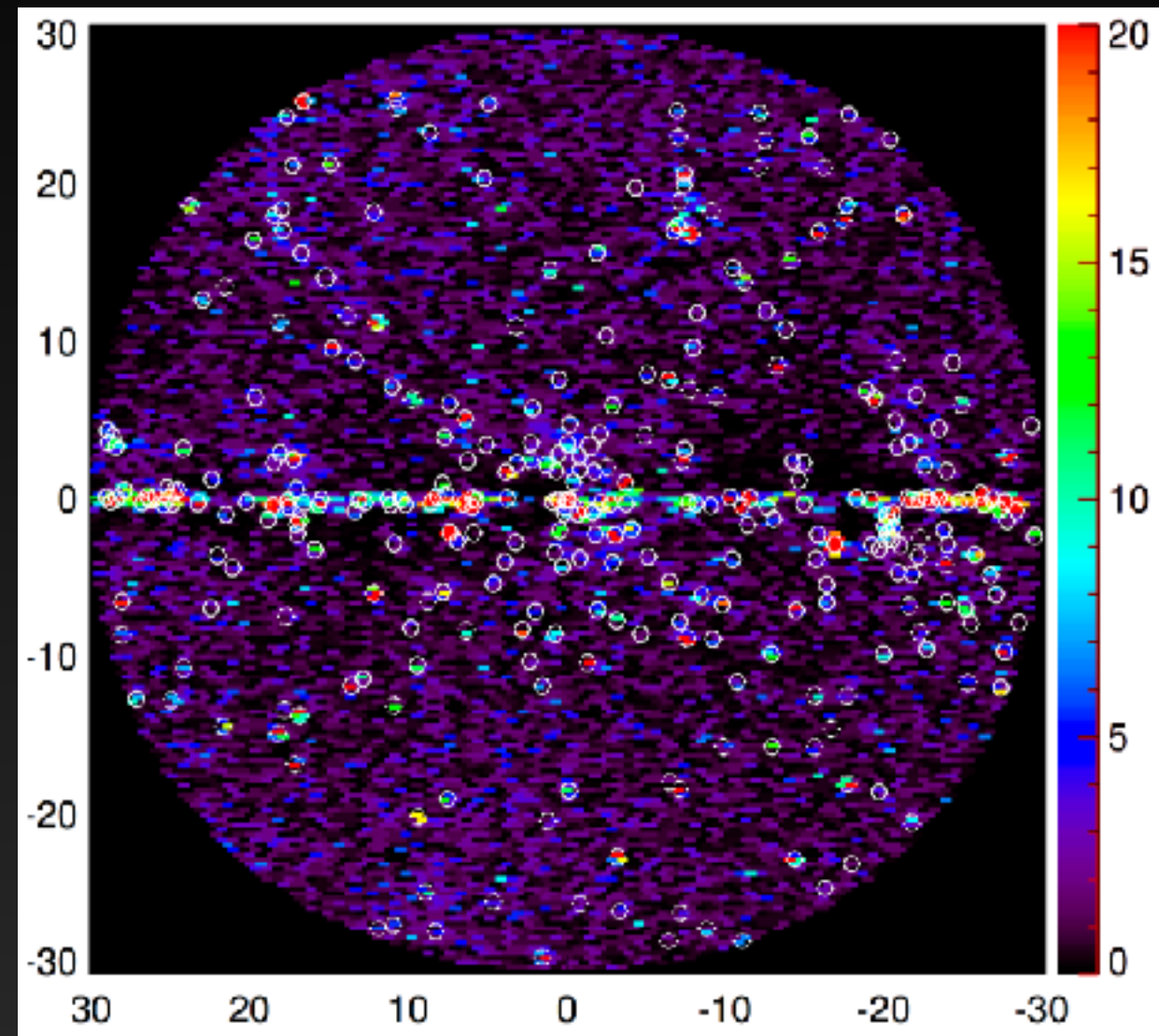
- MSPs are thought to be overabundant in dense star-forming regions like the Galactic Center

Millisecond Pulsar Fits

Bartels et al. (2015)



Lee et al. (2015)



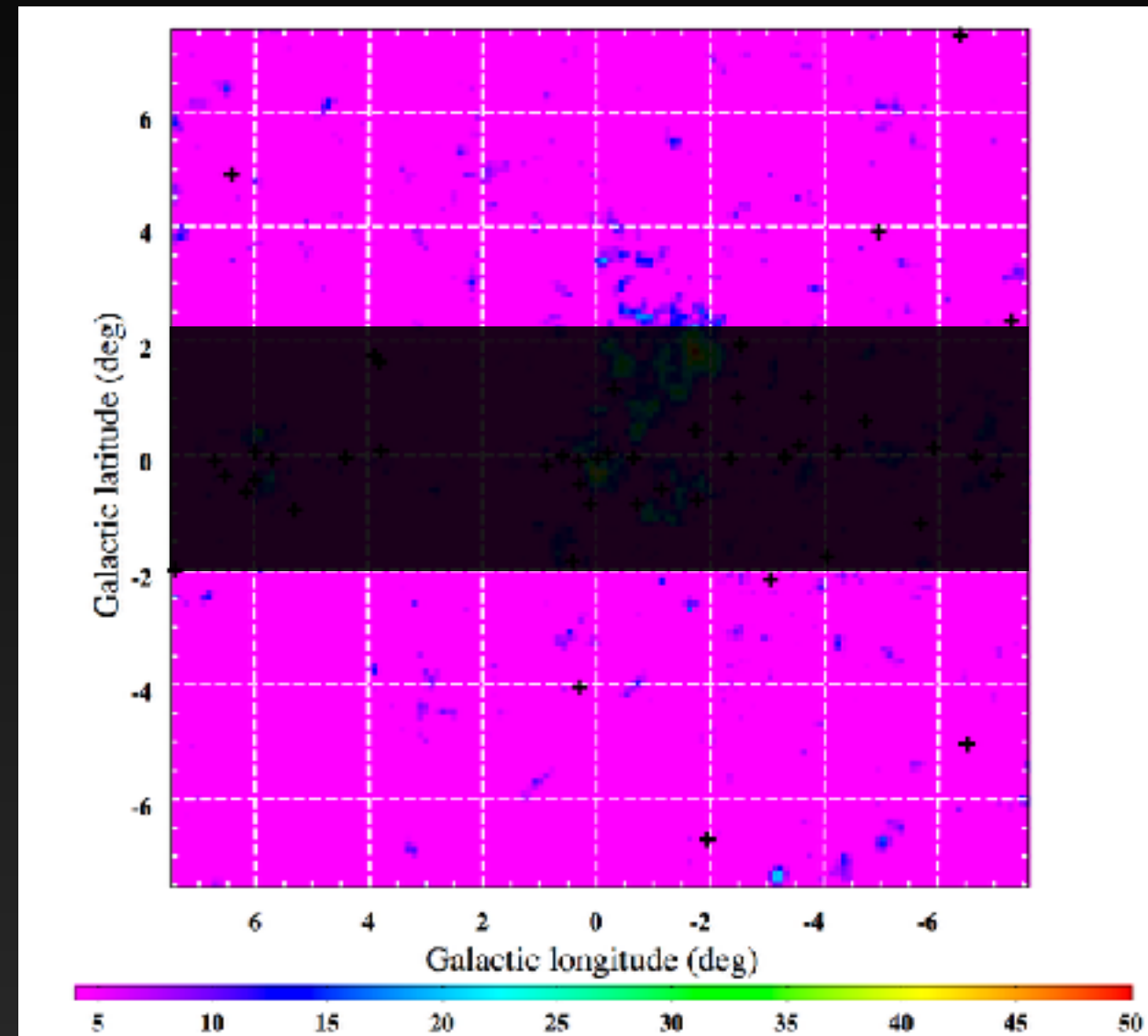
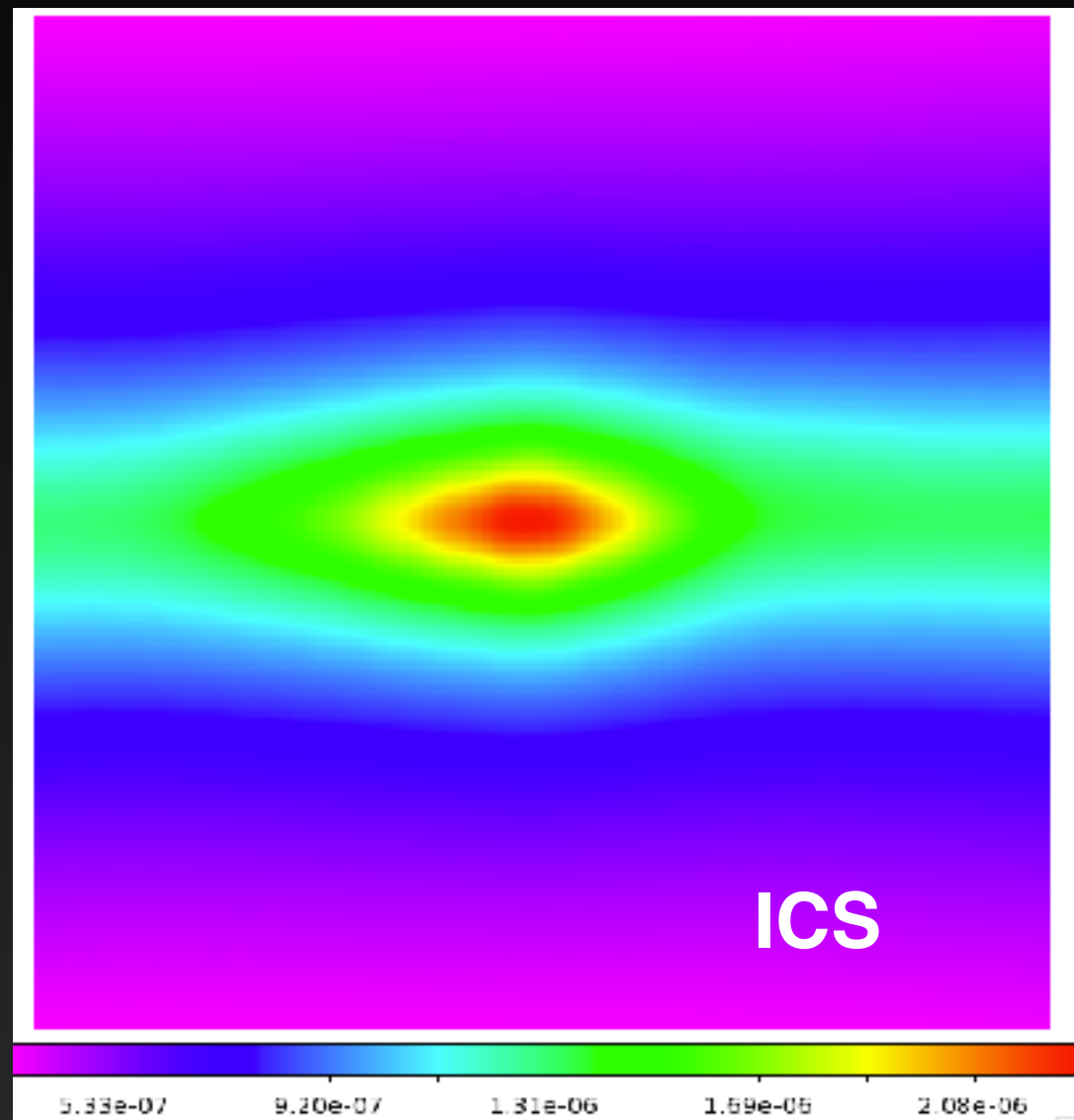
IG

- Recent analyses of hot-spots and cold spots in the GC region find evidence for the presence of a population of sub-threshold point sources.

Millisecond Pulsar Fits

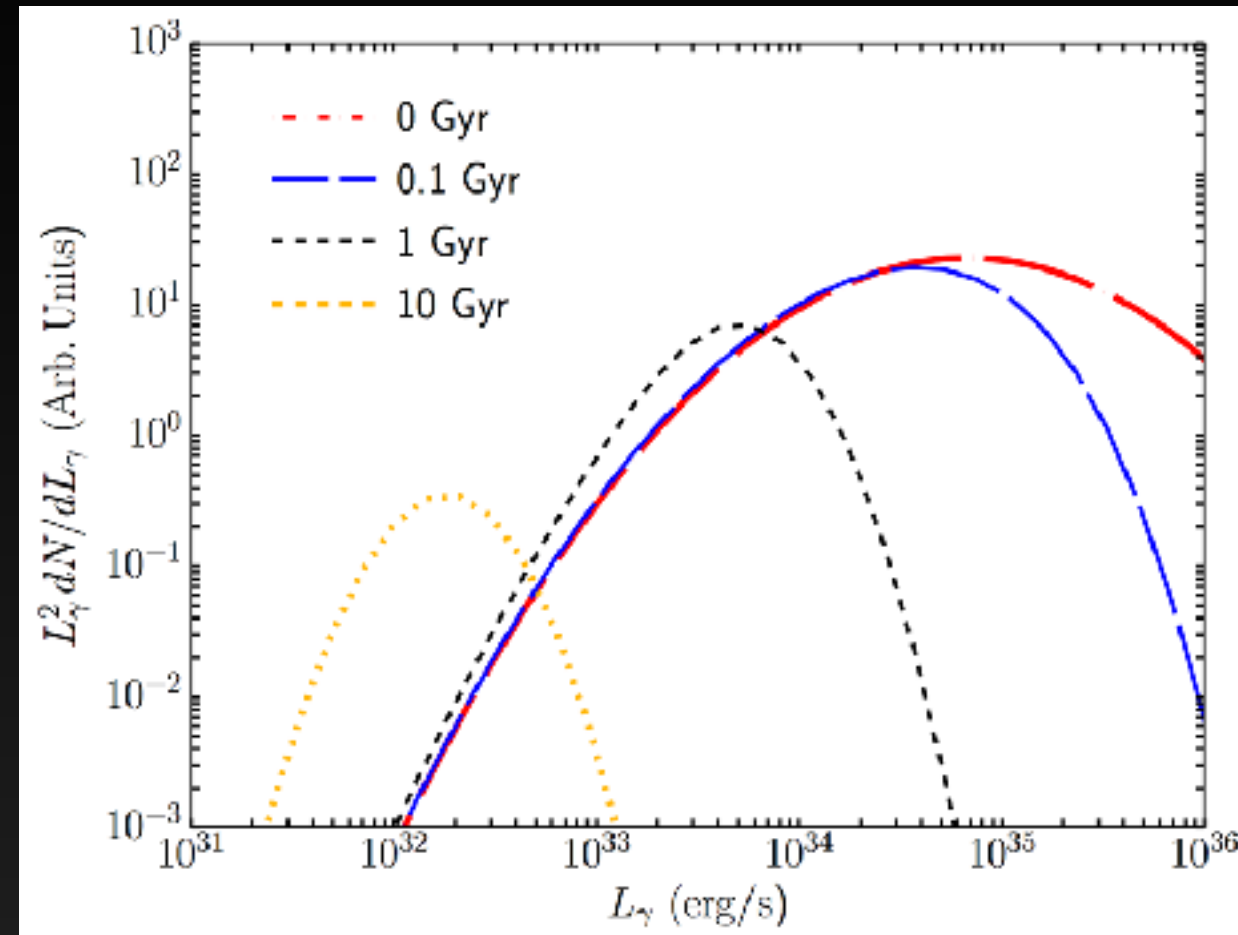
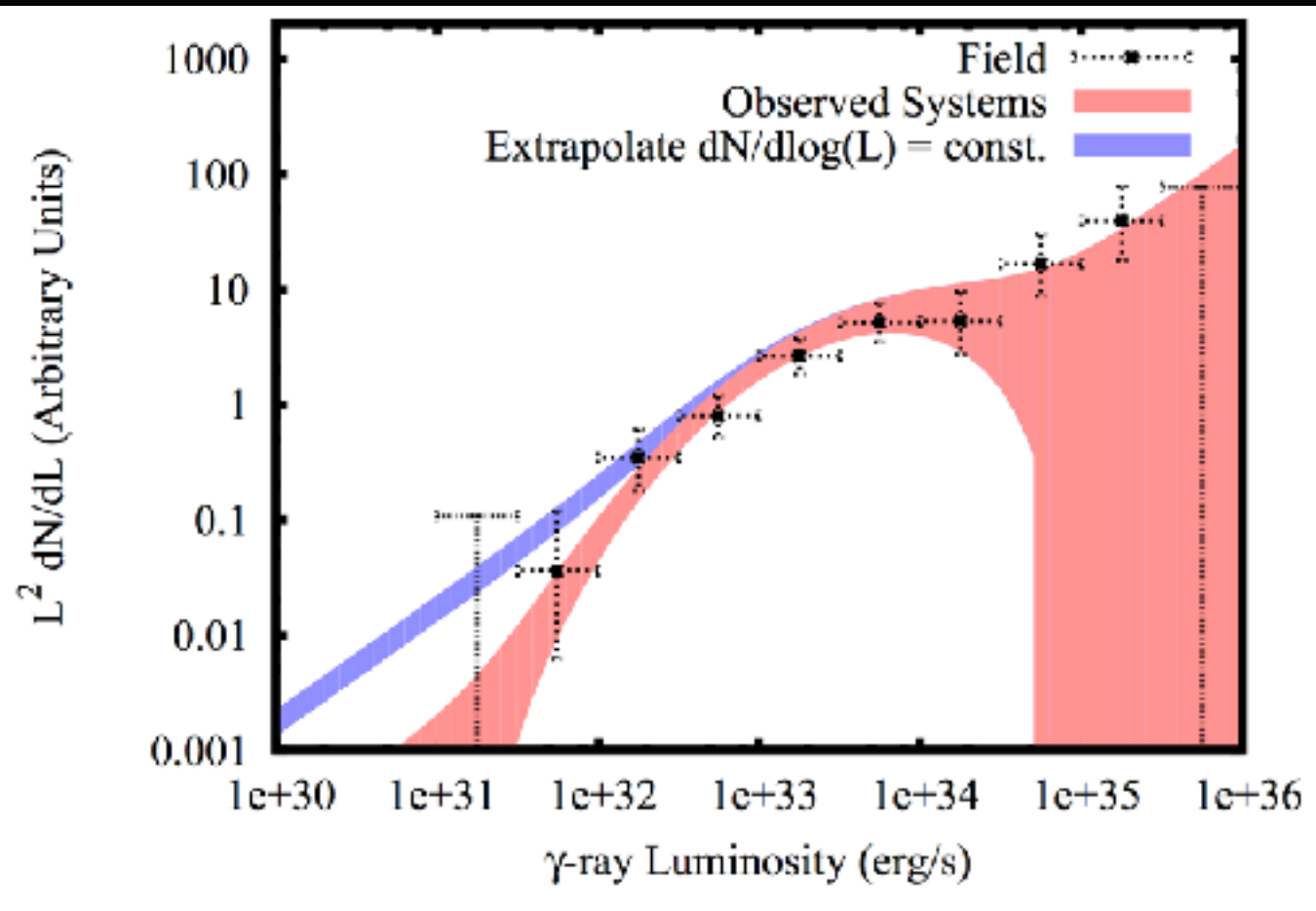
IG

Ajello et al. (2015)



- However, these residuals are found once an extremely smooth diffuse emission model is subtracted - it remains to be seen whether the residuals are resilient to diffuse model changes.

Too Bright or Too Many?



- Utilizing the luminosity distribution of pulsars in the field produces too many bright (detectable) pulsars, compared to observations. (Hooper et al. 2013, 2015)
- Evolving the pulsars (compared to the replenished field population) decreases the number of bright pulsars, but requires too many systems to explain the total luminosity. (Hooper & TL 2016)

Leptonic Outbursts

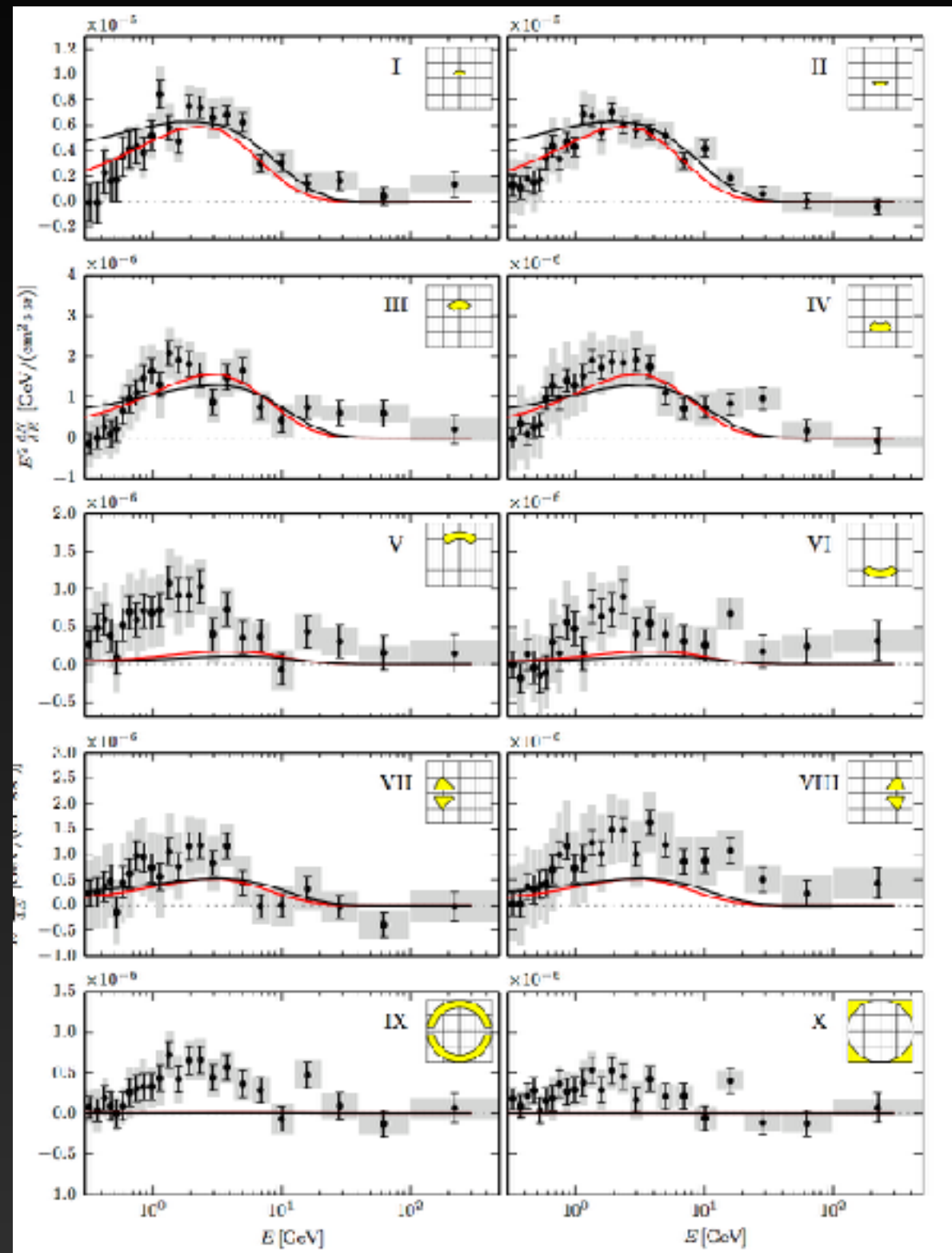
The Galactic center is unlikely to be in steady state (e.g. Fermi bubbles).

An outburst of leptonic origin can produce the gamma-ray excess, but only if the injected electron spectrum is extremely hard (compared to observed blazar spectra).

Petrovic et al. (2014, 1405.7928)

Cholis et al. (2015, 1506.05119)

Cholis et al. (2015, 1506.05119)



IG

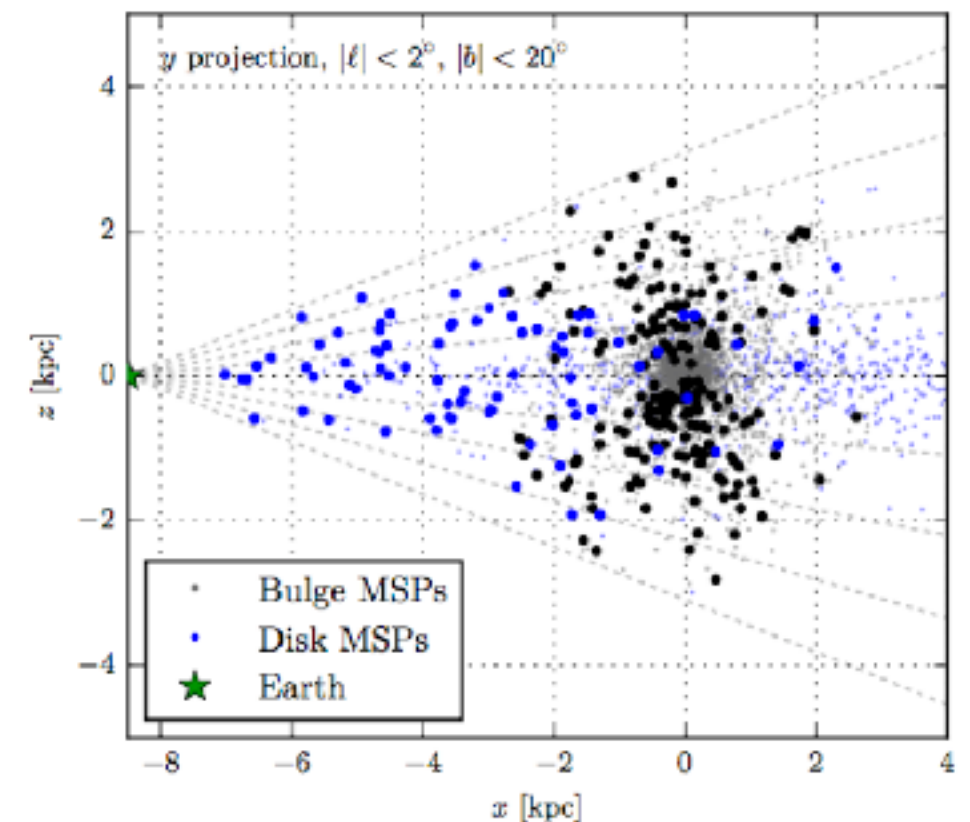
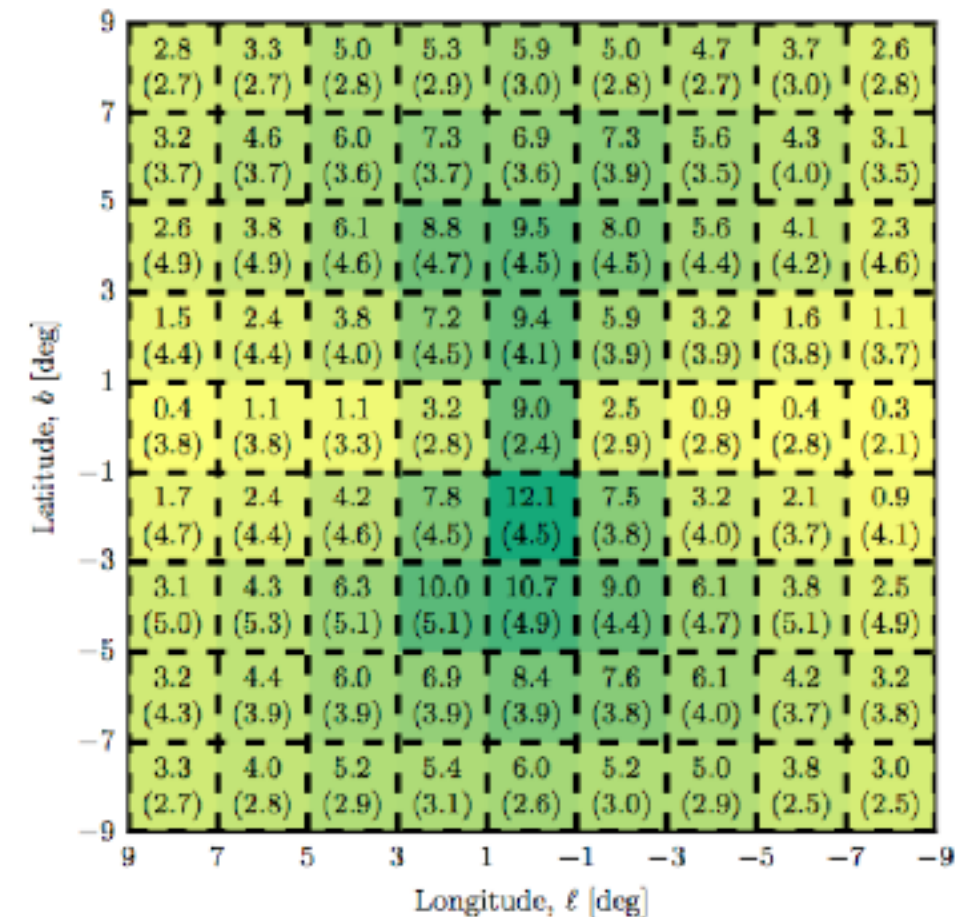
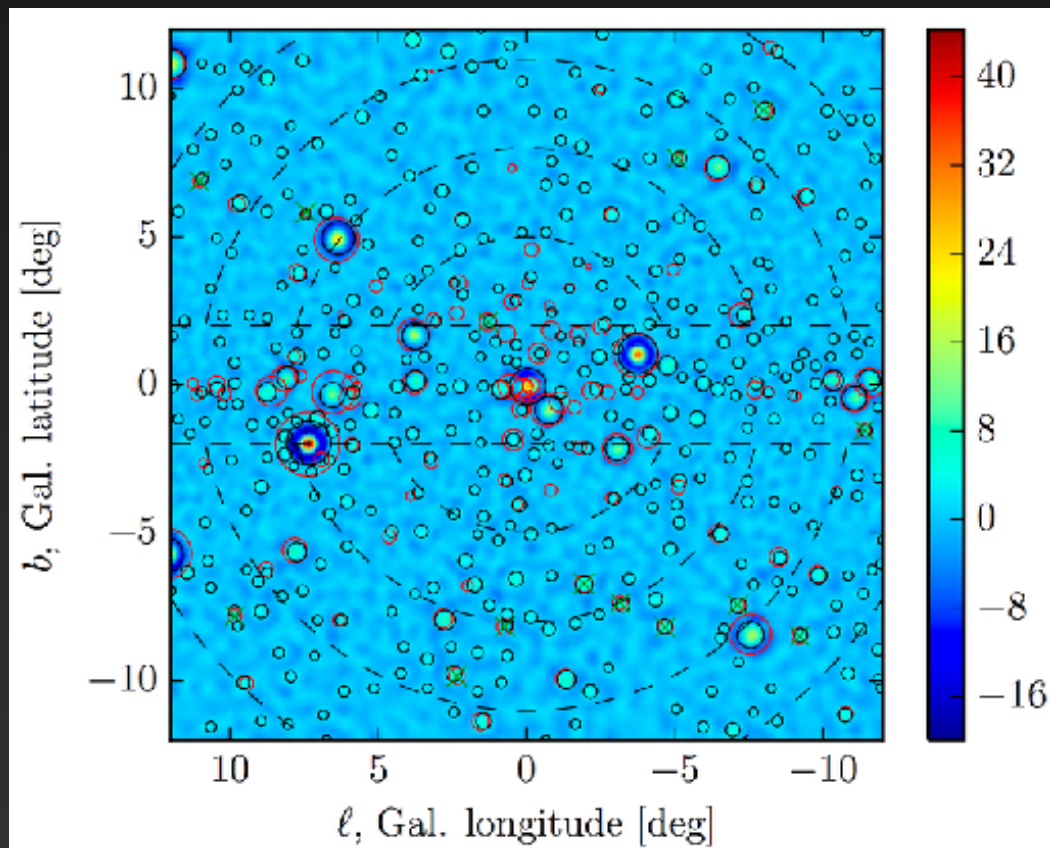
Not a Conclusion Yet...

- 1.) The Galactic Center is a complex, but exciting environment. Several significant excesses are tied to the dynamics of the Galactic center environment.
- 2.) The GeV excess is a robust component of the Galactic center emission profile. At present, no models have successfully eliminated the excess.
- 3.) Improving our diffuse emission modeling is imperative to understanding the properties of the excess.

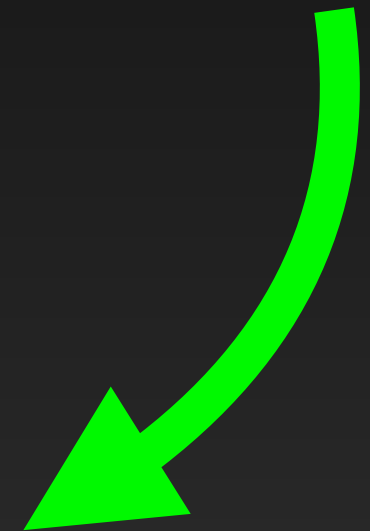
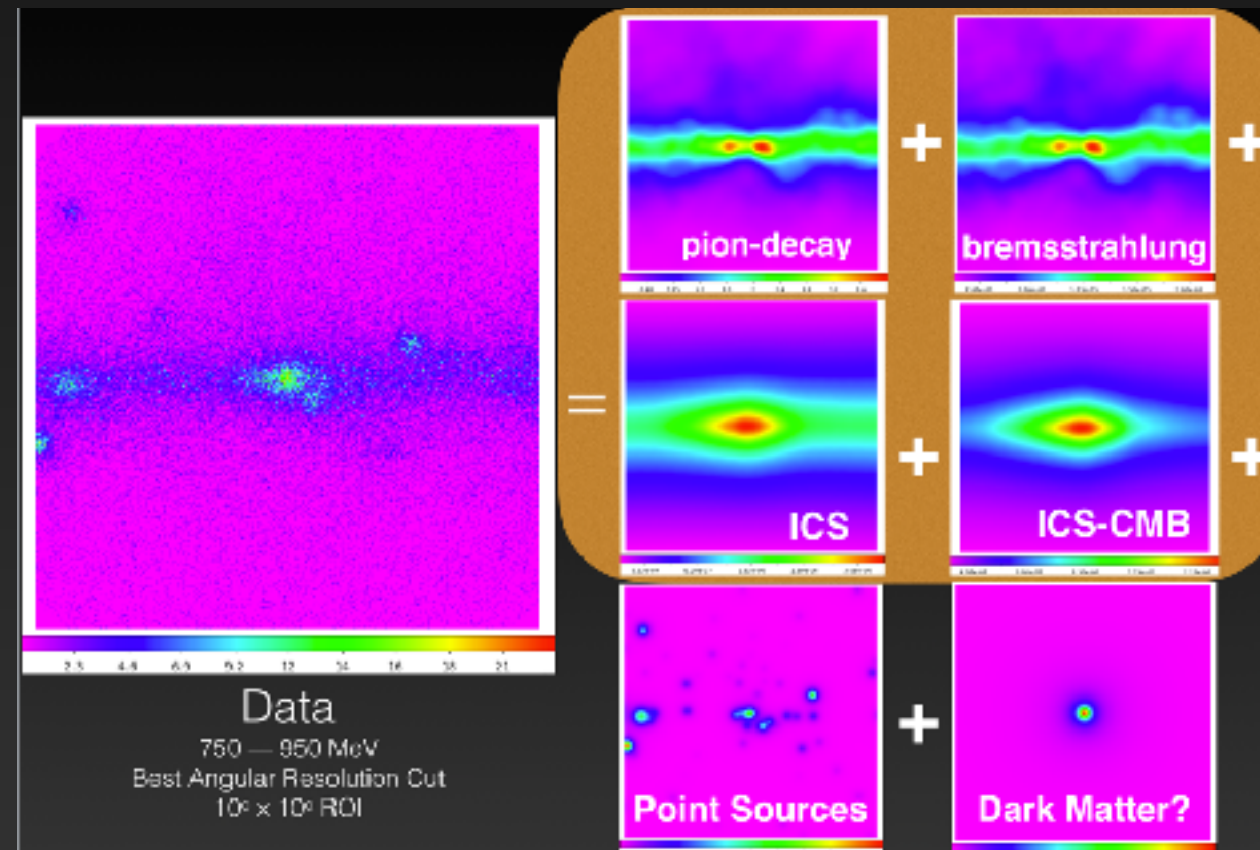
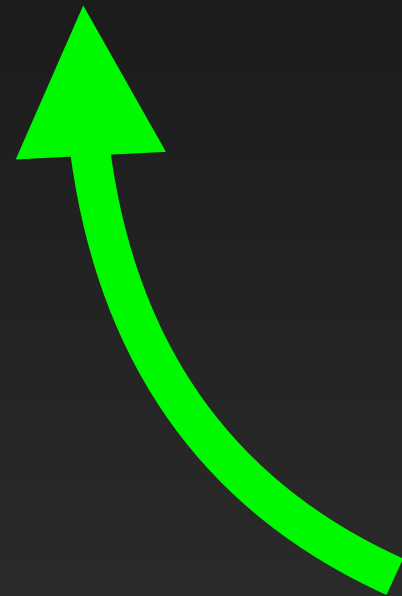
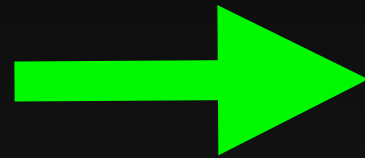
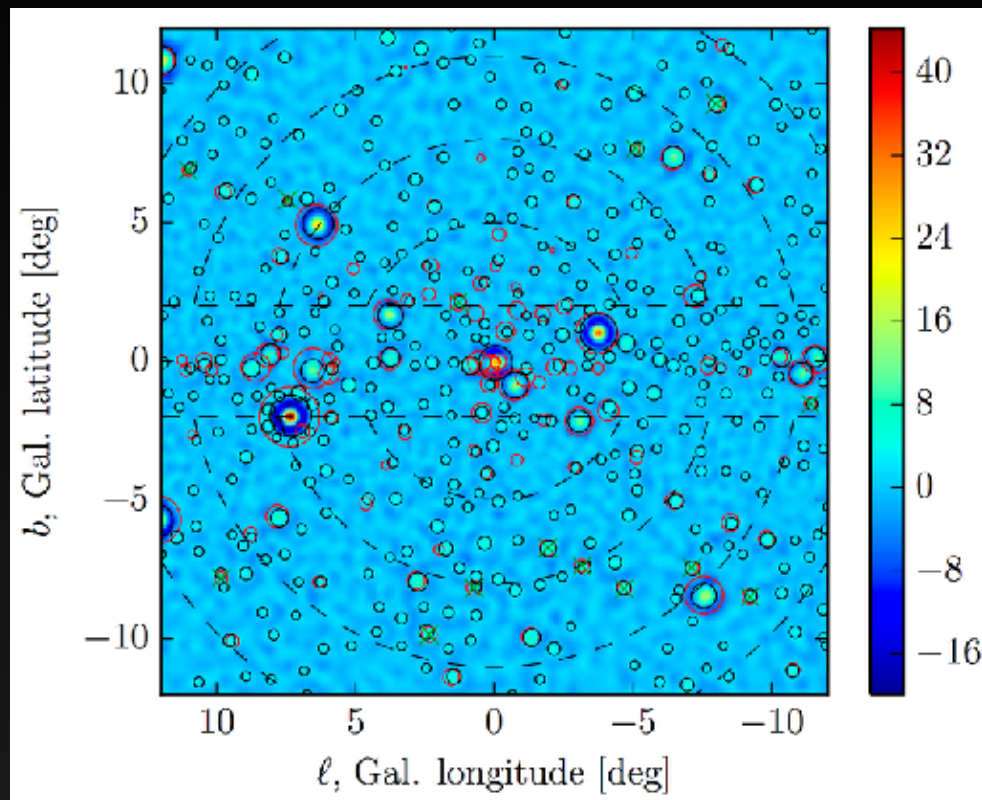
Stay Tuned!

Fortunately the Pulsar Hypothesis is Testable

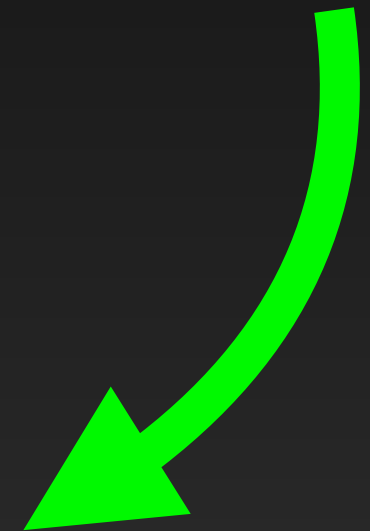
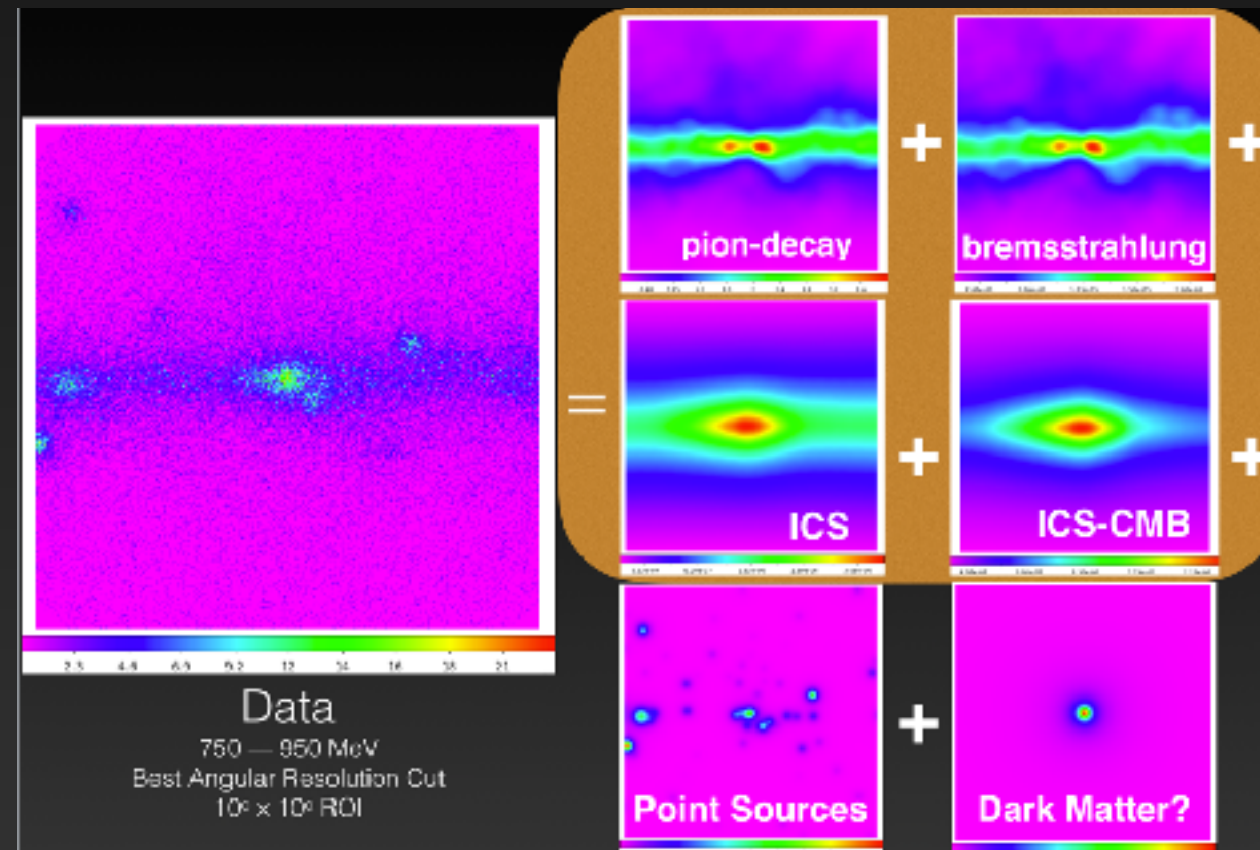
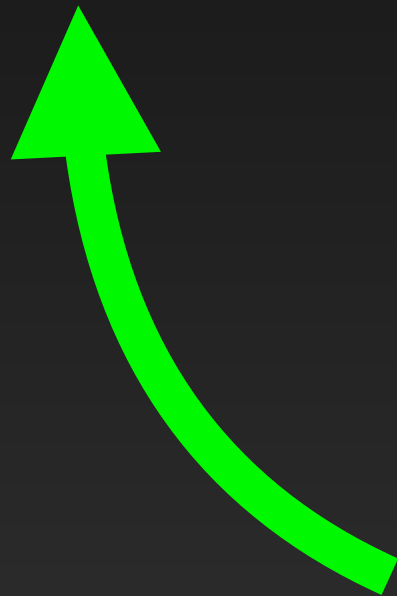
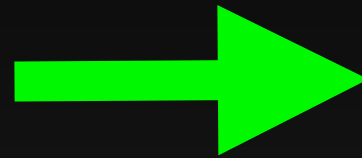
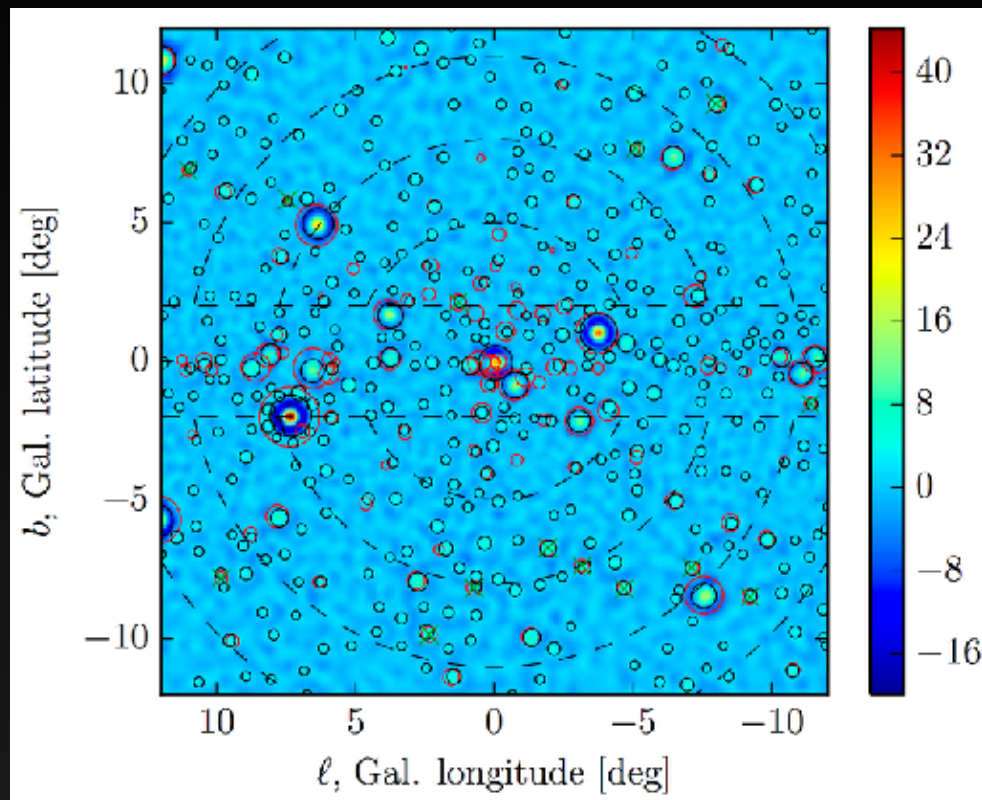
- Radio Observations with GBT targeted at gamma-ray hotspots would be expected to find ~5-10 MSPs with a 200 hr commitment.
- Fortunately, SKA observations are likely to conclusively find MSPs in the GC, or rule out this scenario.



Proving the Pulsar Interpretation



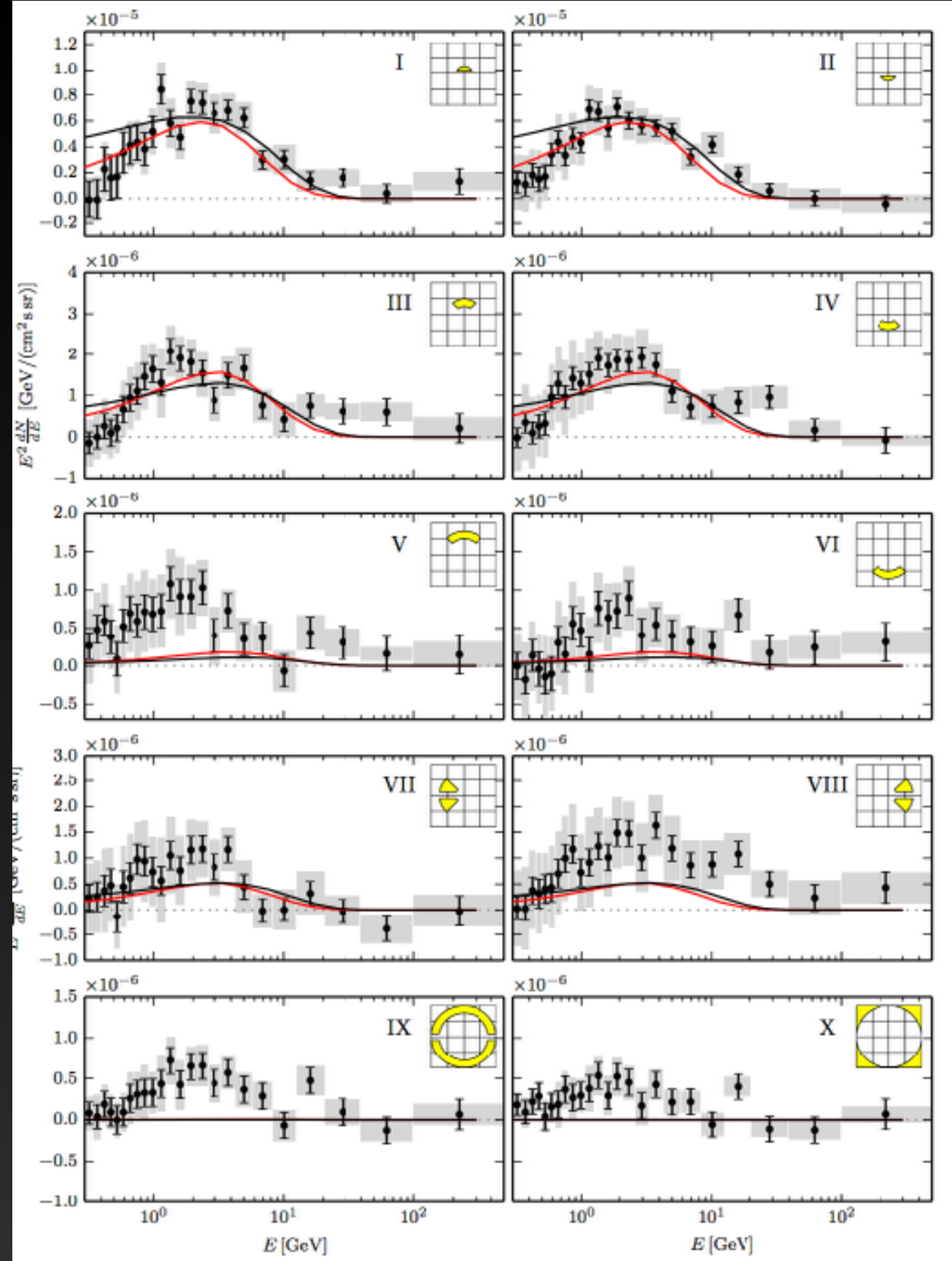
Can this be proven in the negative?



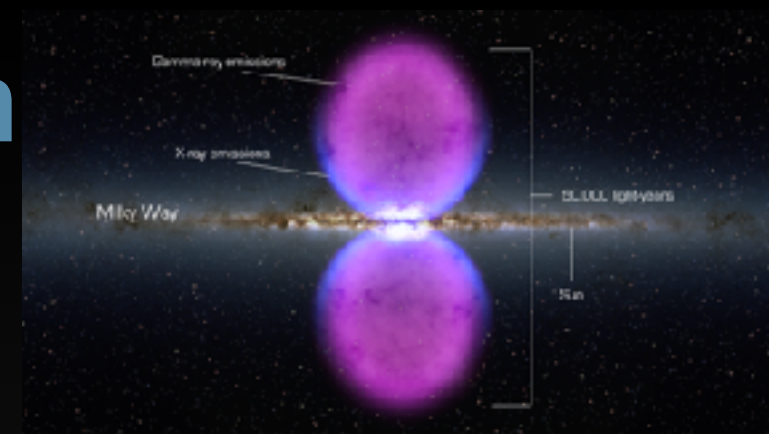
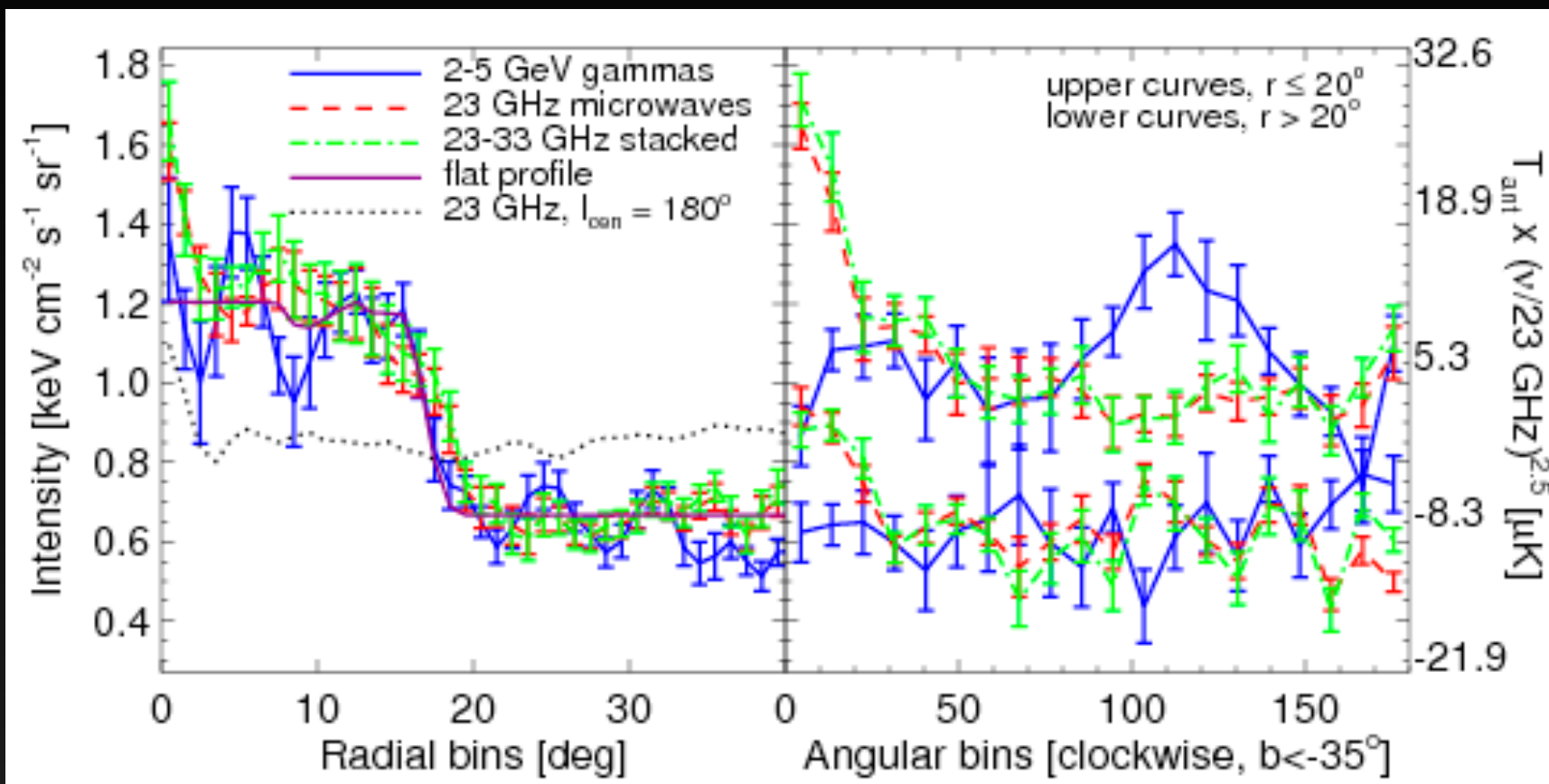
Leptonic Outbursts

So far, we have only considered steady-state diffuse emission scenarios - but the Galactic center is unlikely to be in steady state (e.g. Fermi bubbles).

An outburst of leptonic (or possibly hadronic) origin can also produce the gamma-ray excess, but only if the injected electron spectrum is extremely hard (compared to observed blazar spectra).

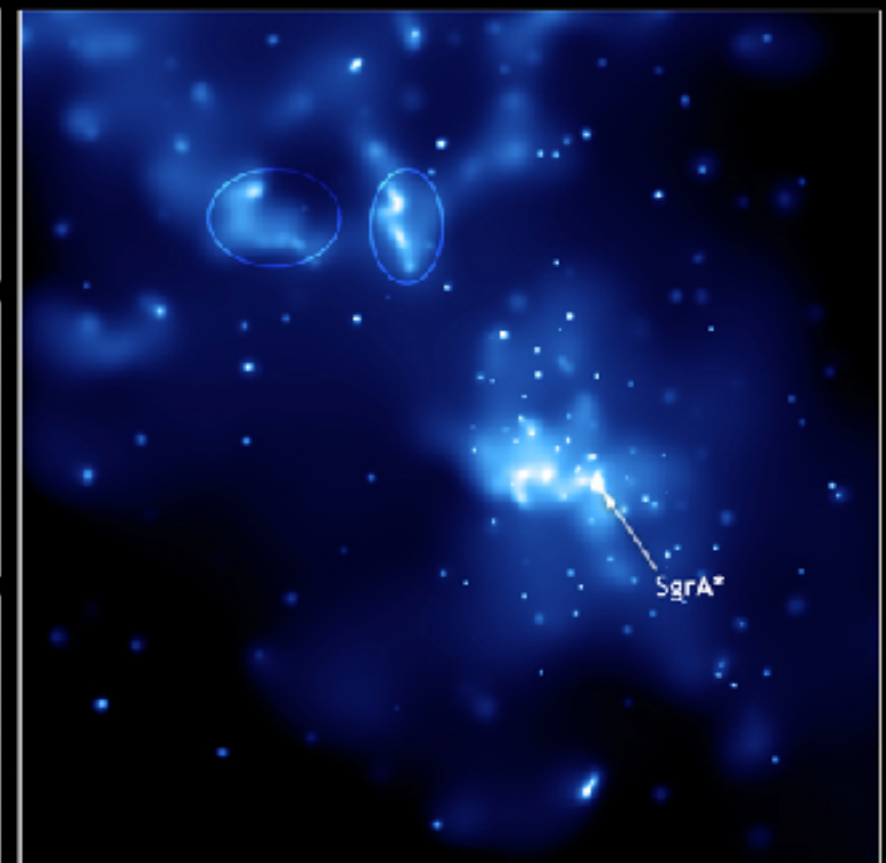
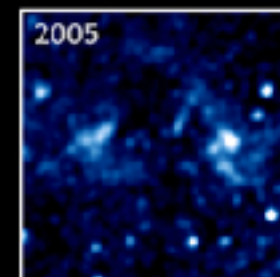
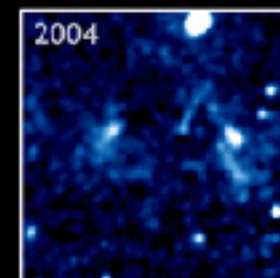
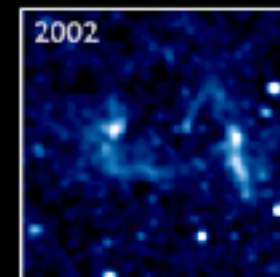


Proving an Outburst Interpretation



The origin of the WMAP haze was determined due to cross-correlation with the Fermi bubbles.

Is a similar cross-correlation (e.g. with X-Ray data) possible?

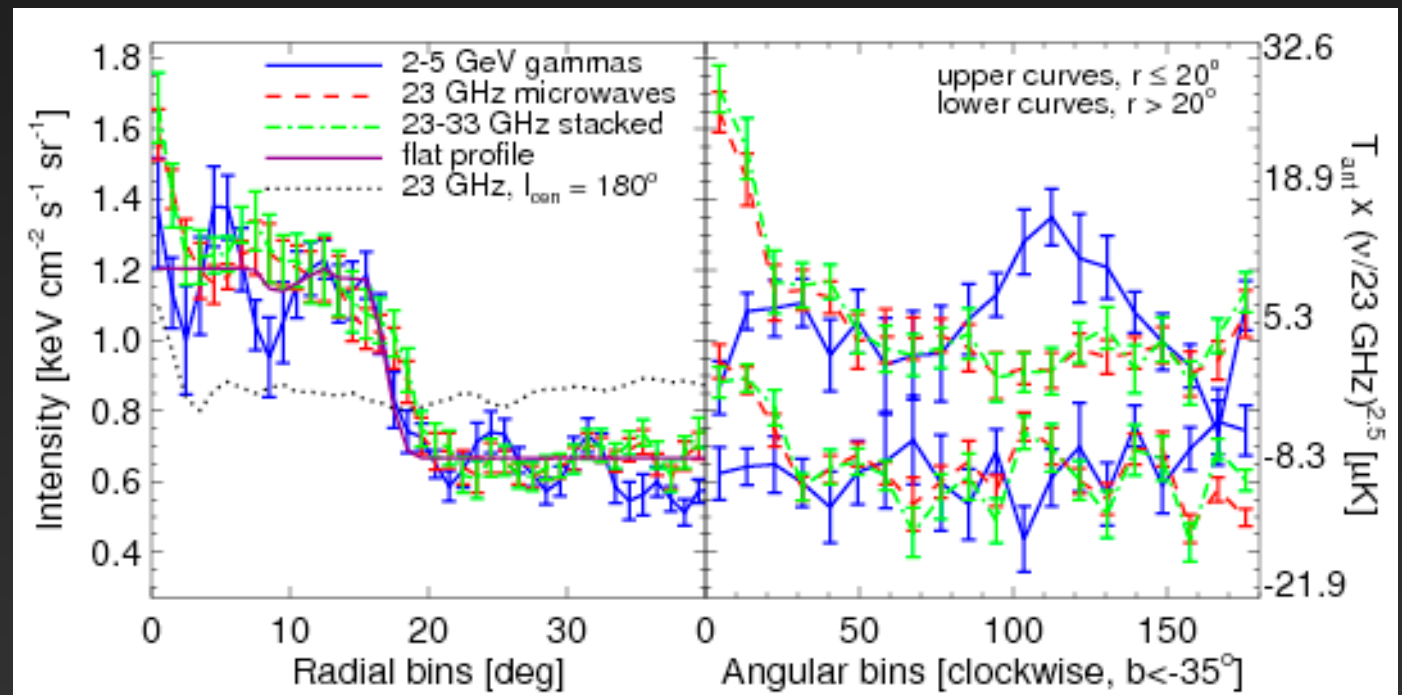


Can Outbursts be Ruled Out?

Leptonic Outbursts at high latitude produce an associated synchrotron flux given by the ratio of the magnetic field and ISRF energy densities.

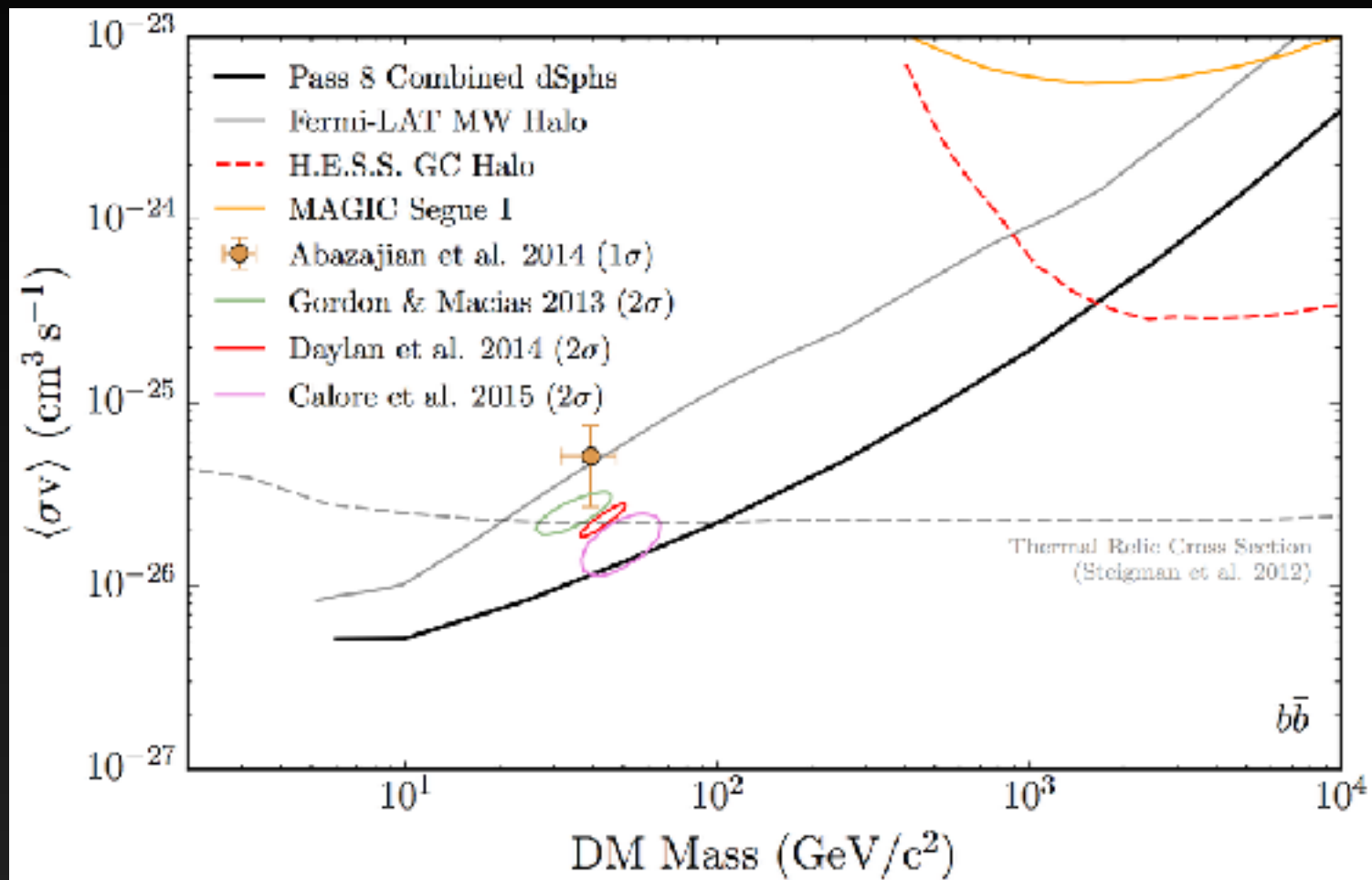
$$\left. \frac{F_{\text{radio}}}{F_{\gamma}} \right|_{\text{DM}} = \frac{B_e \left(\frac{\rho_B}{\rho_B + \rho_{\text{rad}}} \right)}{B_e \left(\frac{\rho_{\text{rad}}}{\rho_B + \rho_B} \right) + B_{\gamma}}$$

Enhanced measurements of the low-energy synchrotron signal at the Galactic center may rule out any associated synchrotron flux.



Comparison to Dwarf Constraints

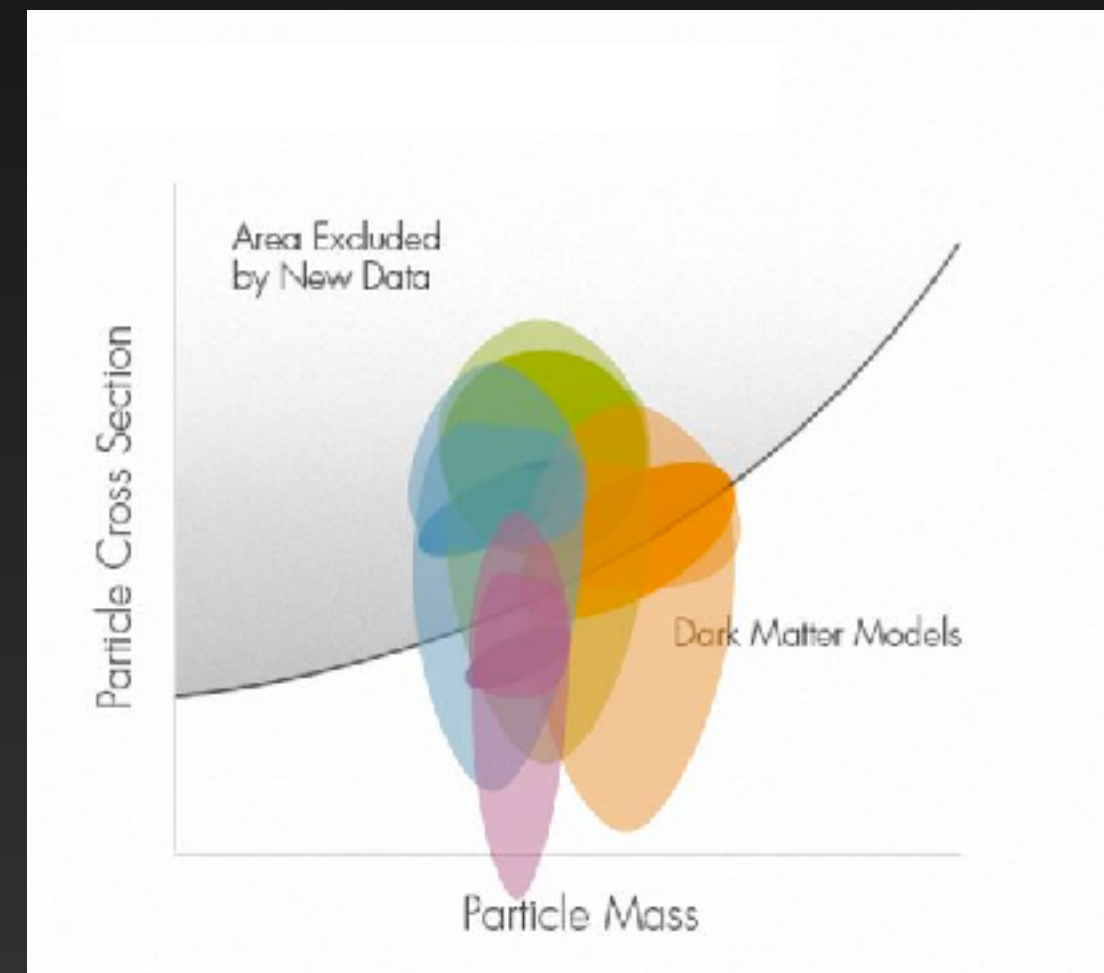
Ackermann et al. (2015)



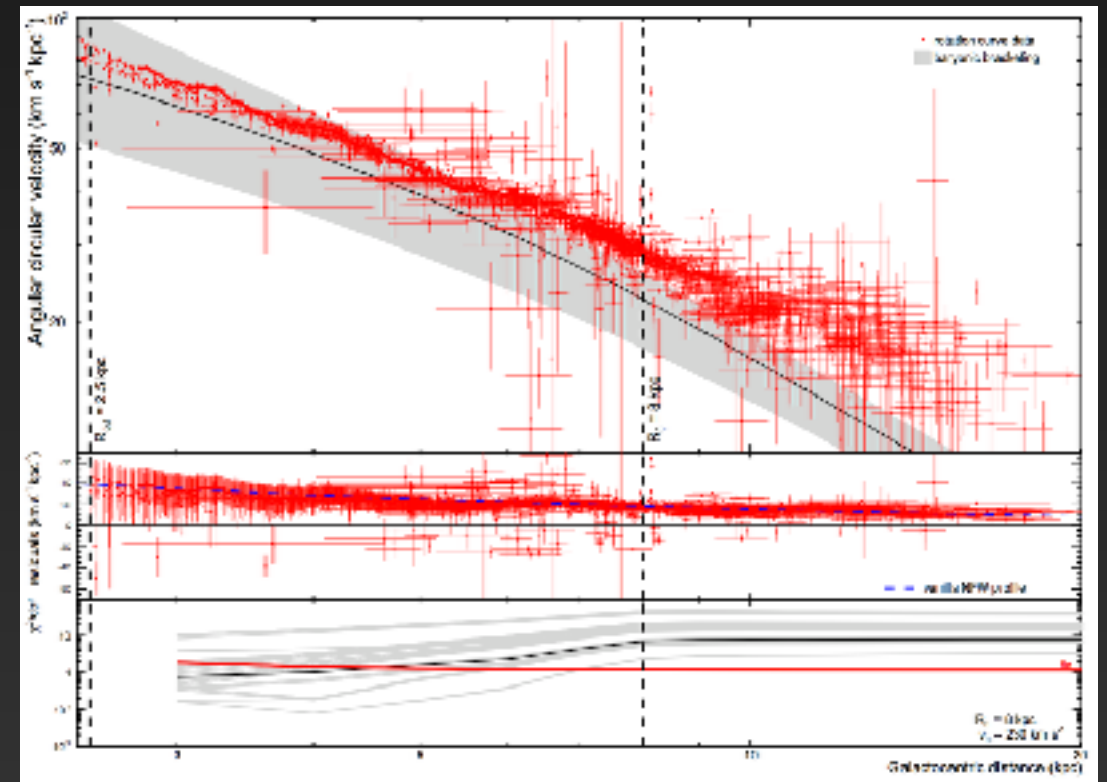
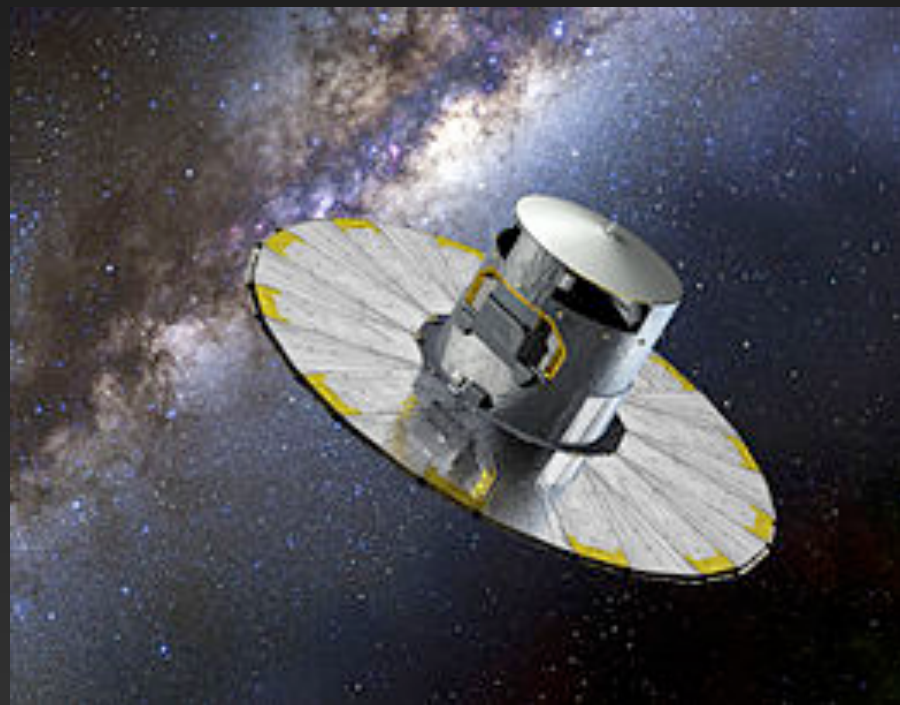
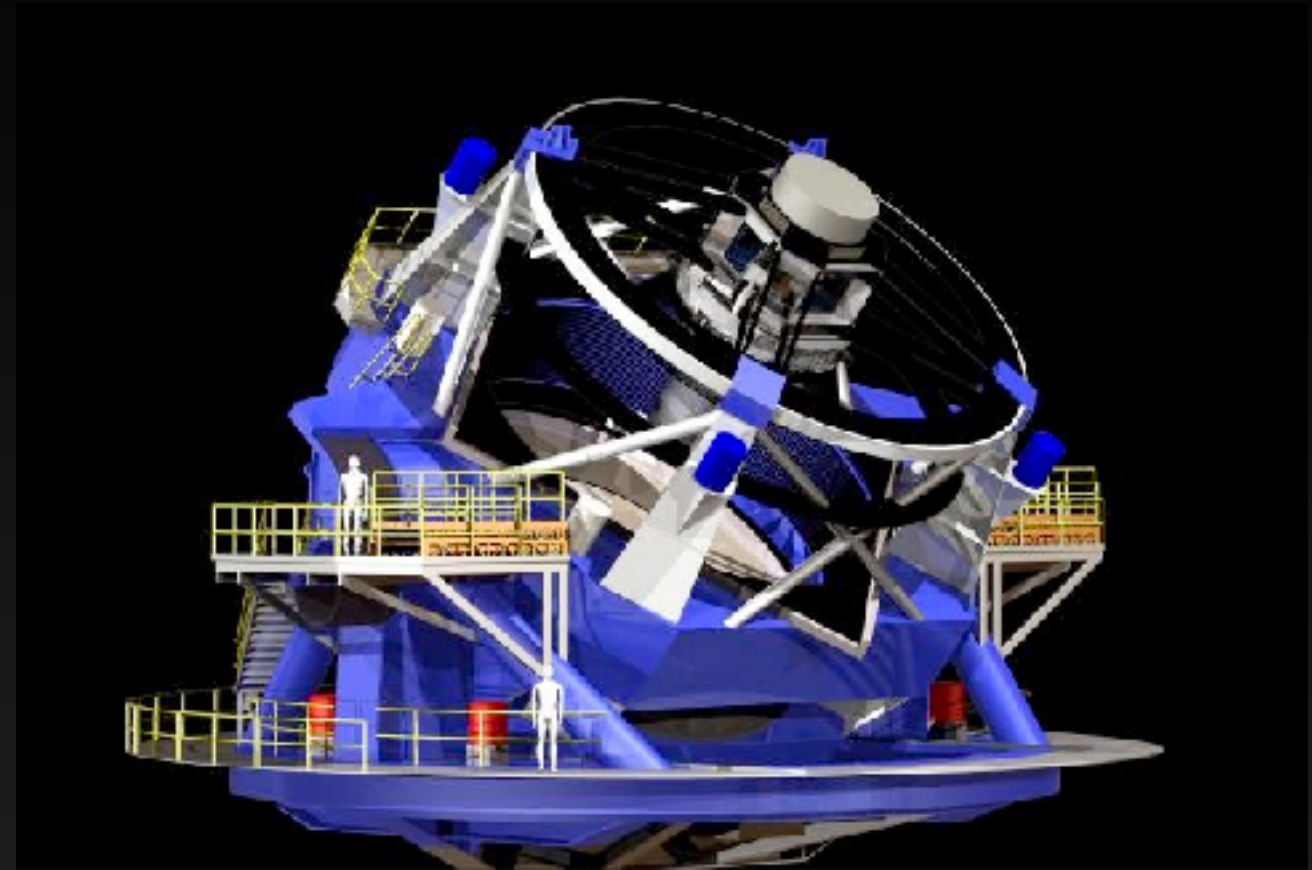
Constraints from dSphs are statistically in 1-2 σ tension with the GC excess.

However, uncertainties in the dark matter density profile can easily resolve this tension.

credit: Kev Abazajian (2015)



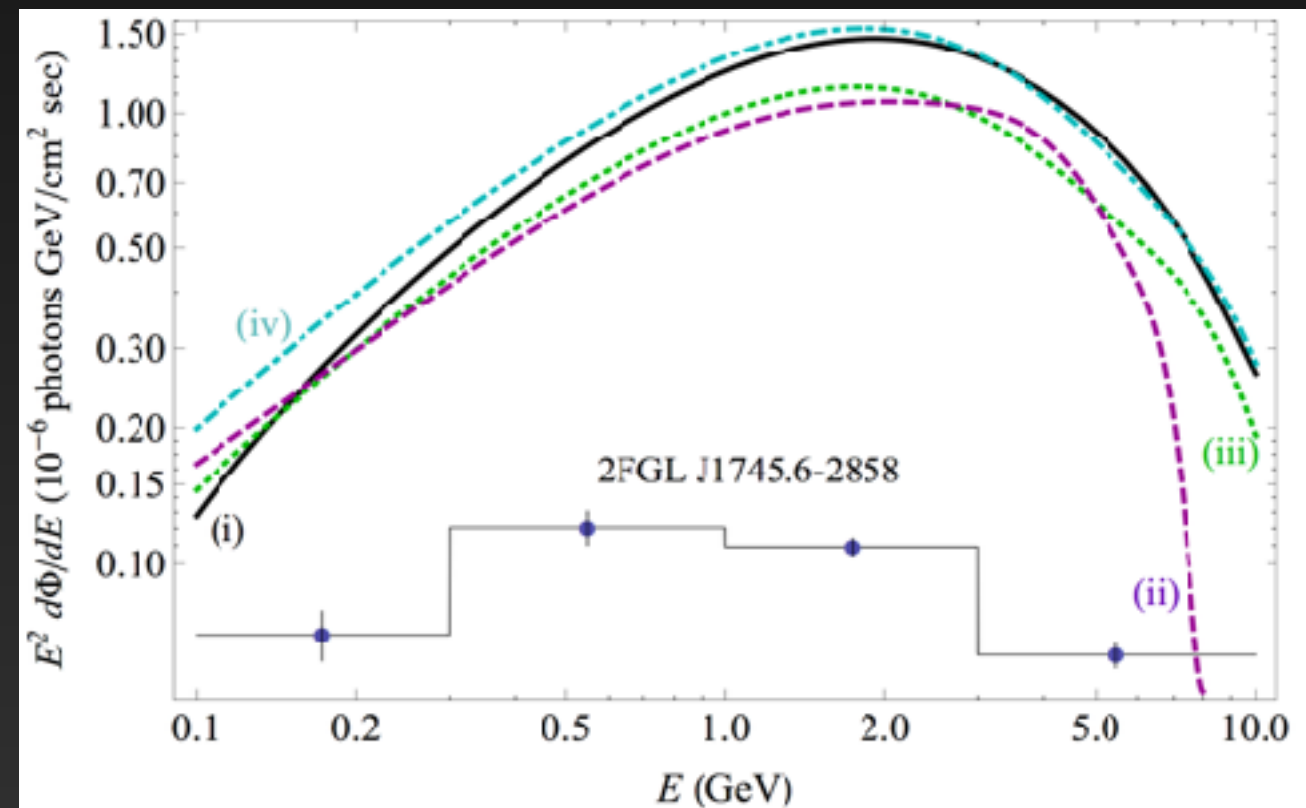
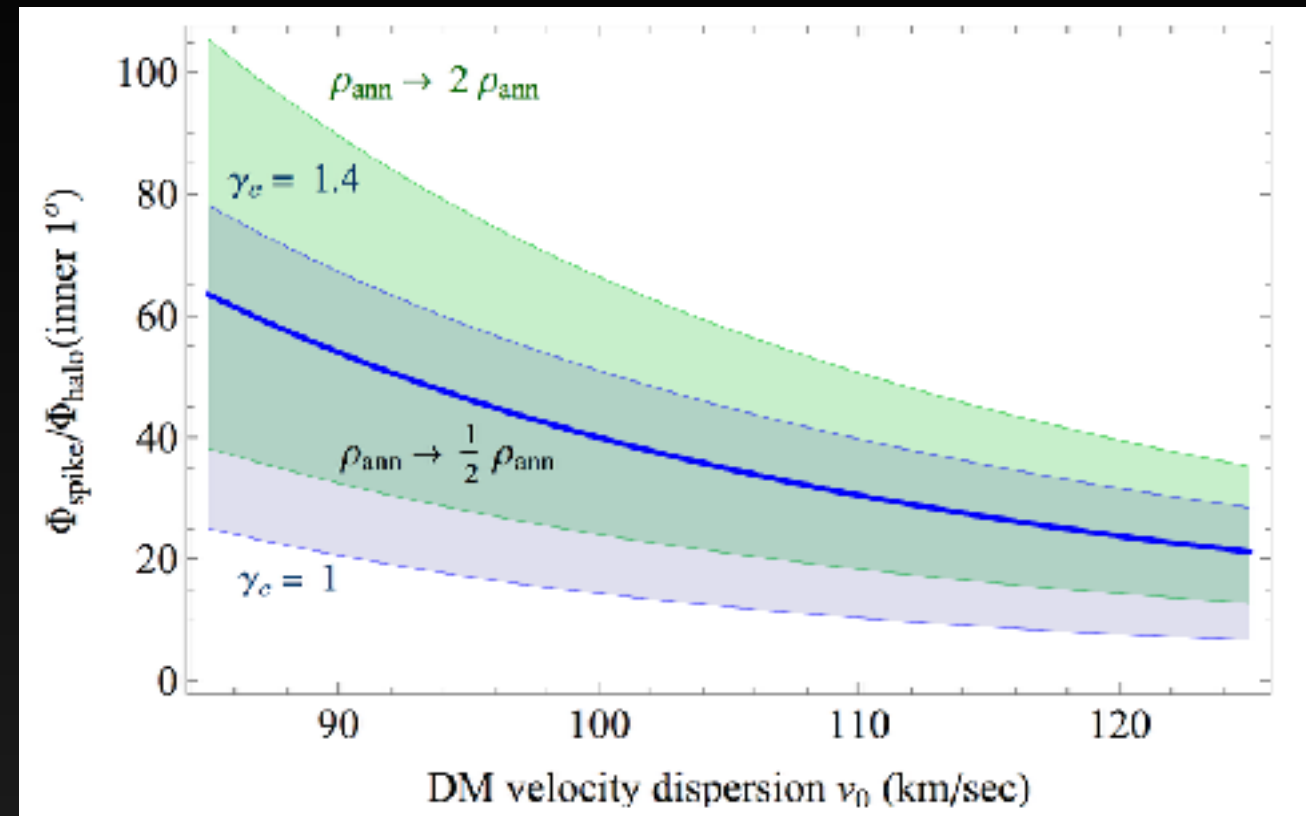
Comparison to Dwarf Constraints



Can DM be Ruled out by GC Observations?

In models with adiabatic BH growth, a significant DM spike is expected near the position of Sgr A*.

This would dominate the total gamma-ray emission, and is currently ruled out by observations of the gamma-ray point source.



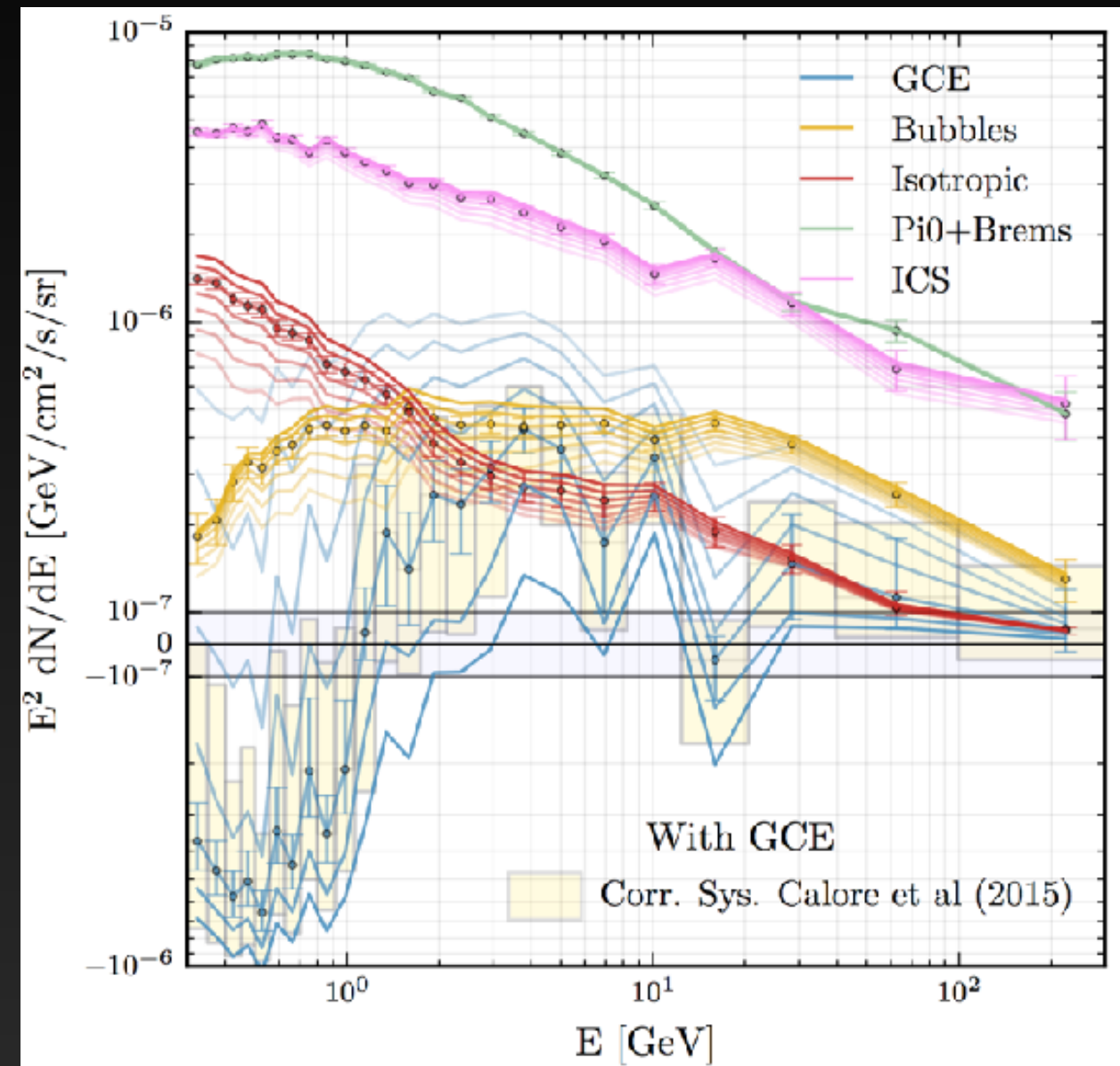
Extra Slides

Effect on the Excess Spectrum

IG

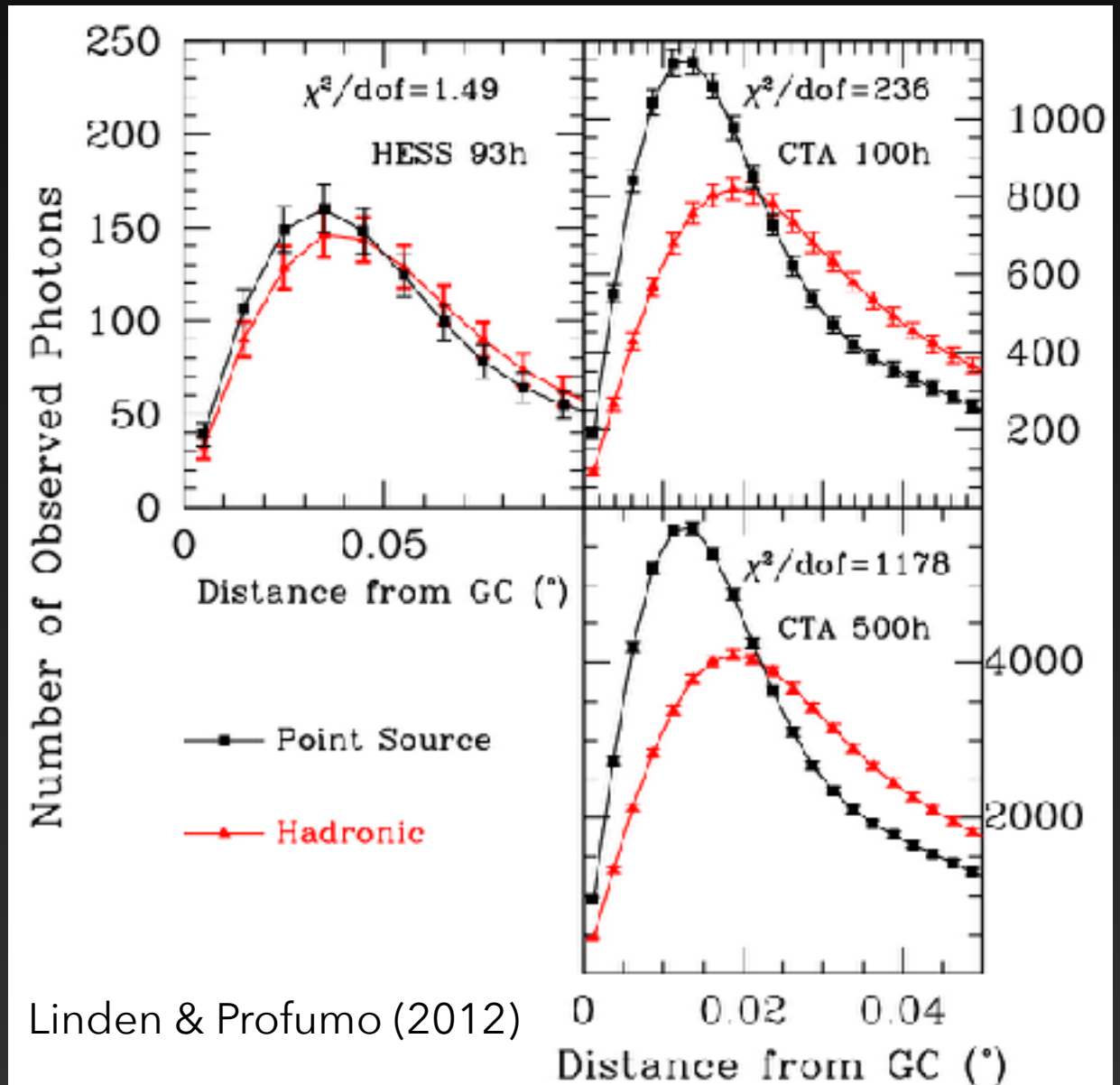
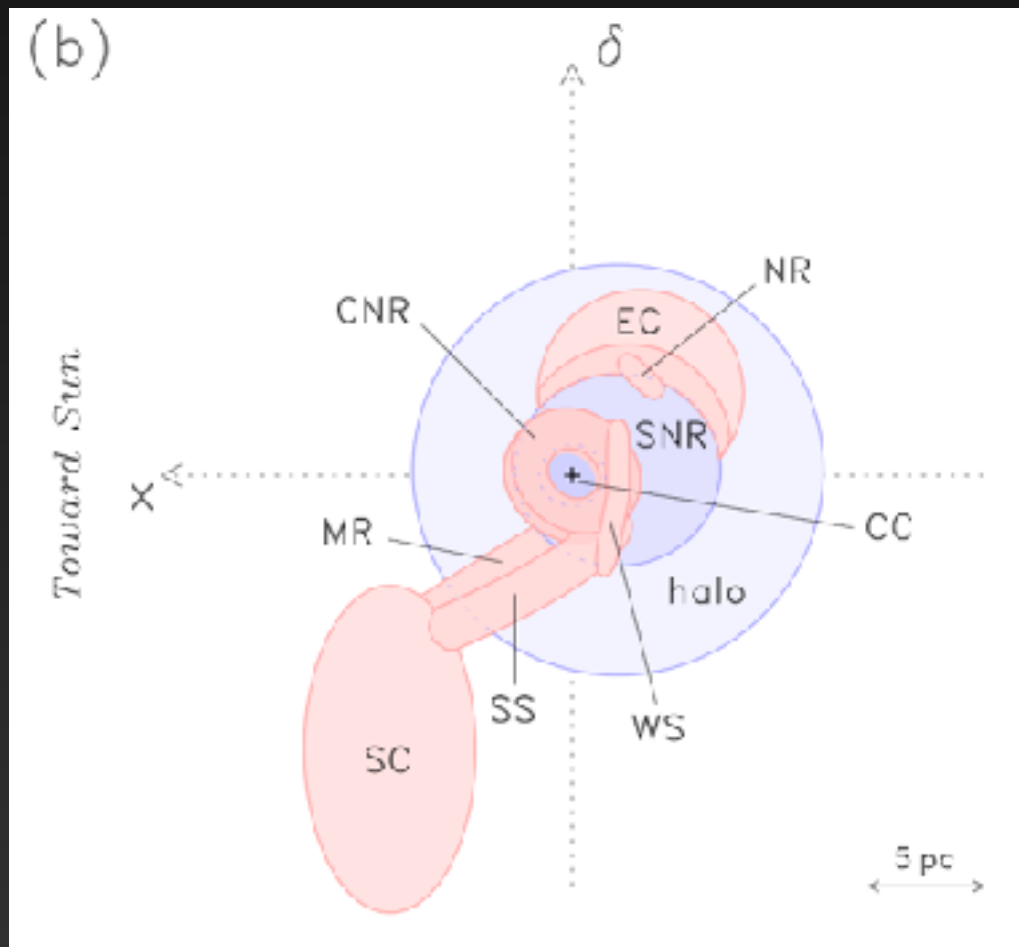
Changing the morphology of the excess has a significant effect on the spectrum of the gamma-ray excess.

The spectrum becomes extremely hard as f_{H2} is increased, most likely indicating that the GCE template is picking up mismodeling of some residual.

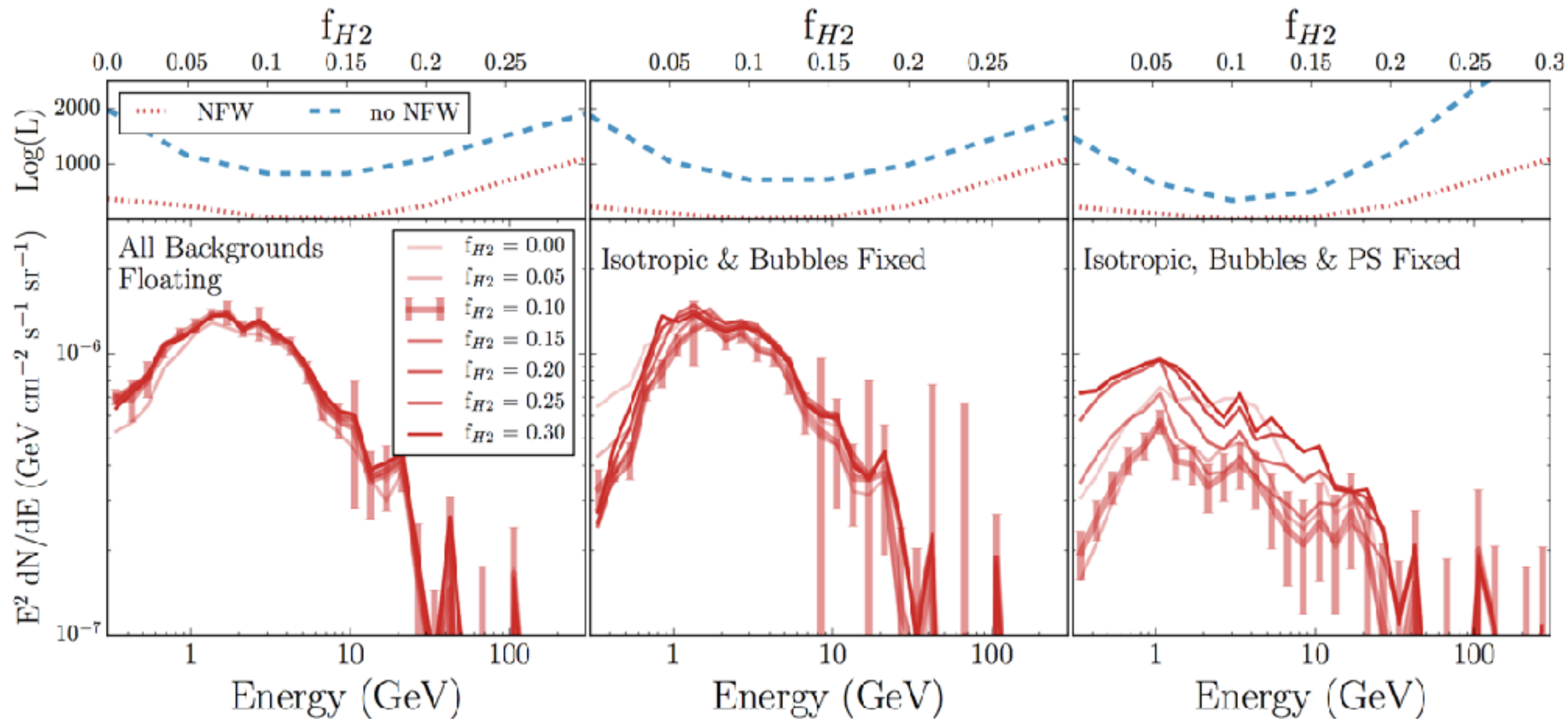


The Sgr A* Source

Region	$L_\gamma (1 \text{ TeV} \leq E_\gamma) [\times 10^{34} \text{ erg s}^{-1}]$	Mass [$\times 10^6 M_\odot$]		
		CS	CO	HCN
R1	$1.54 \pm 0.06_{\text{stat}} \pm 0.23_{\text{sys}}$	1.35	0.88	0.88
R2	$1.21 \pm 0.05_{\text{stat}} \pm 0.18_{\text{sys}}$	1.11	0.98	0.86
R3	$2.05 \pm 0.08_{\text{stat}} \pm 0.30_{\text{sys}}$	2.65	2.01	1.65
C1	$0.73 \pm 0.03_{\text{stat}} \pm 0.11_{\text{sys}}$	1.51	1.00	1.02
C1b	$0.63 \pm 0.03_{\text{stat}} \pm 0.09_{\text{sys}}$	1.49	1.03	0.82
C2	$0.84 \pm 0.03_{\text{stat}} \pm 0.12_{\text{sys}}$	1.84	1.40	1.34
C2b	$0.51 \pm 0.02_{\text{stat}} \pm 0.07_{\text{sys}}$	1.01	0.86	nc
C3	$0.87 \pm 0.03_{\text{stat}} \pm 0.13_{\text{sys}}$	2.69	1.55	1.73
C4	$0.42 \pm 0.02_{\text{stat}} \pm 0.06_{\text{sys}}$	1.54	0.98	1.33
C5	$0.49 \pm 0.02_{\text{stat}} \pm 0.07_{\text{sys}}$	1.60	1.02	1.15

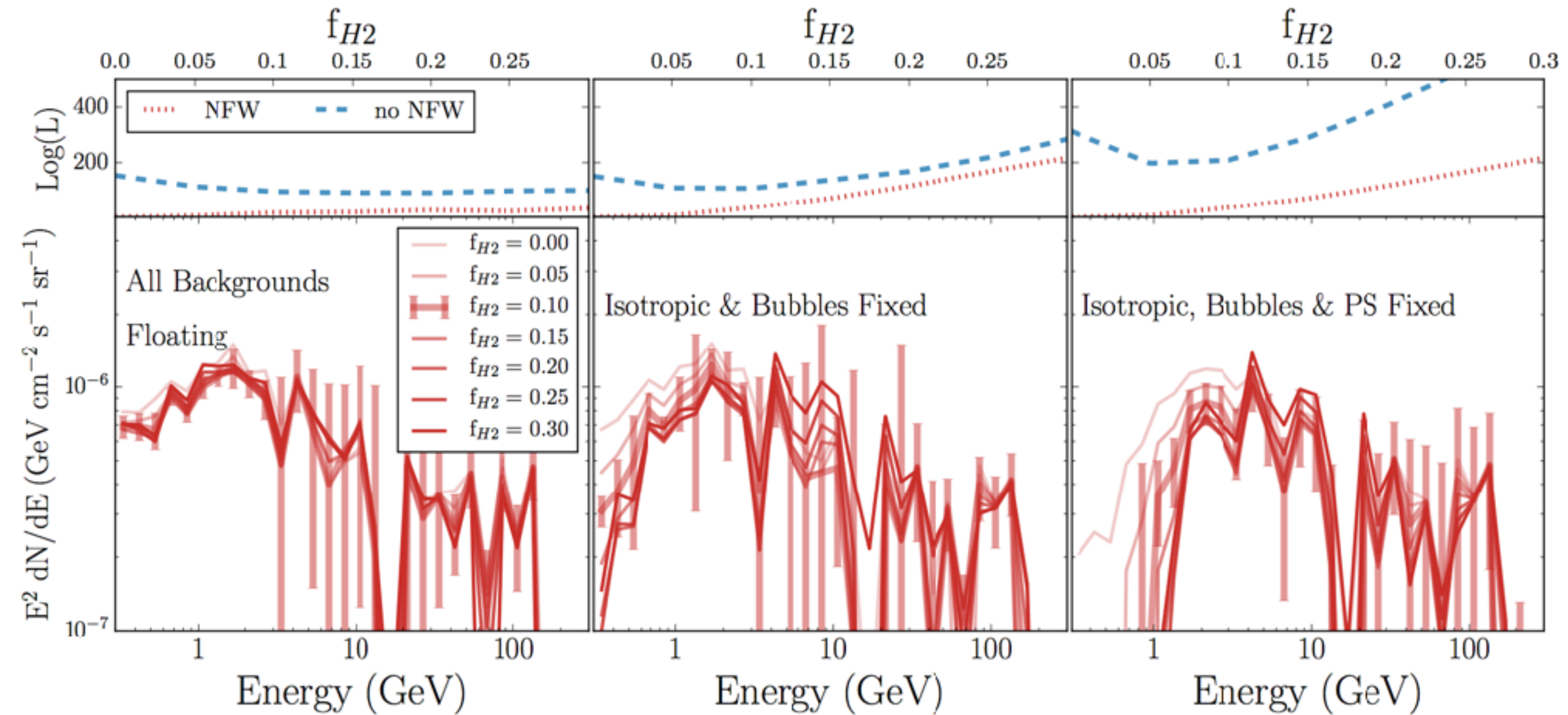


Masking 1FIG Sources in the GC



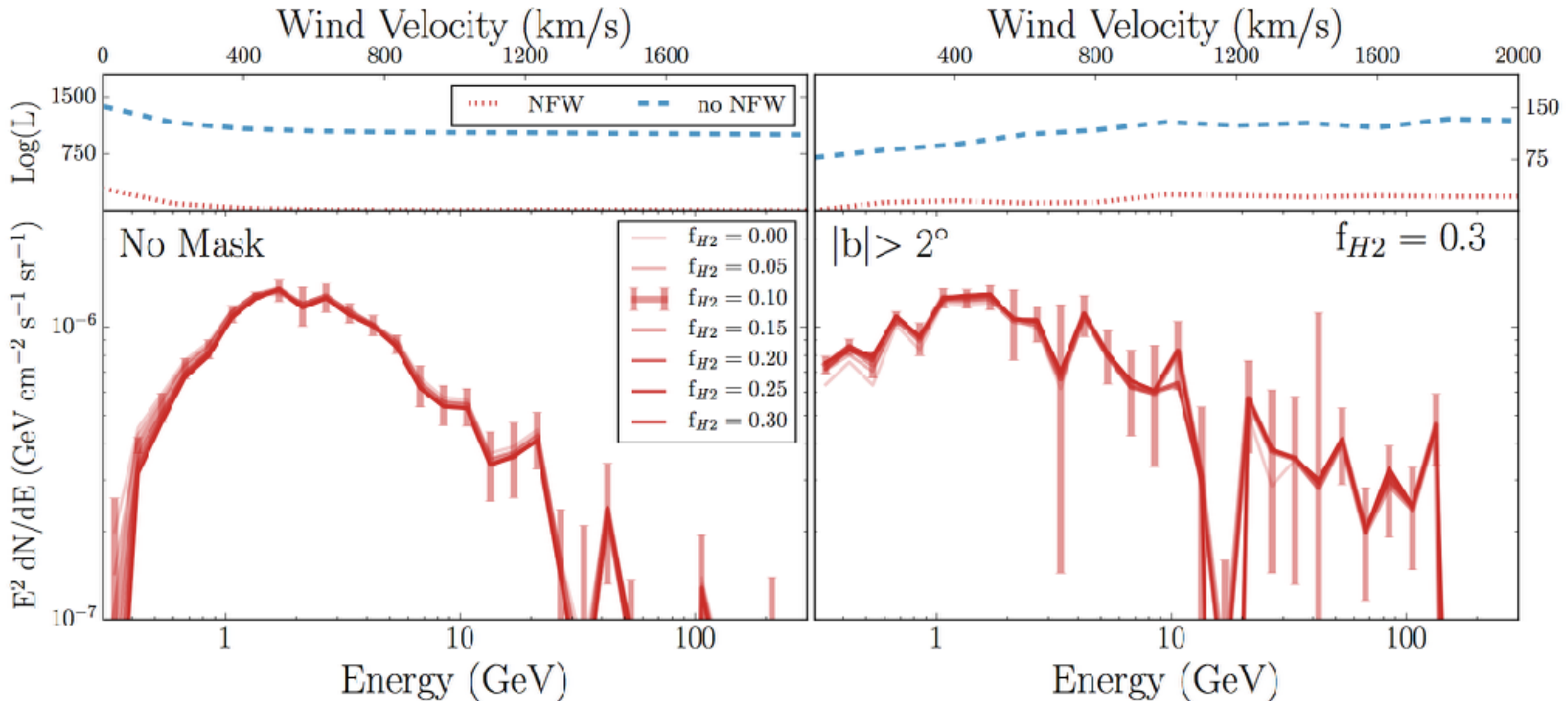
Changing the point source catalog from the 3FGL to the 1FIG has only a negligible effect on the gamma-ray excess.

The Effect on the Galactic center Excess (masking $|b| < 2^\circ$)



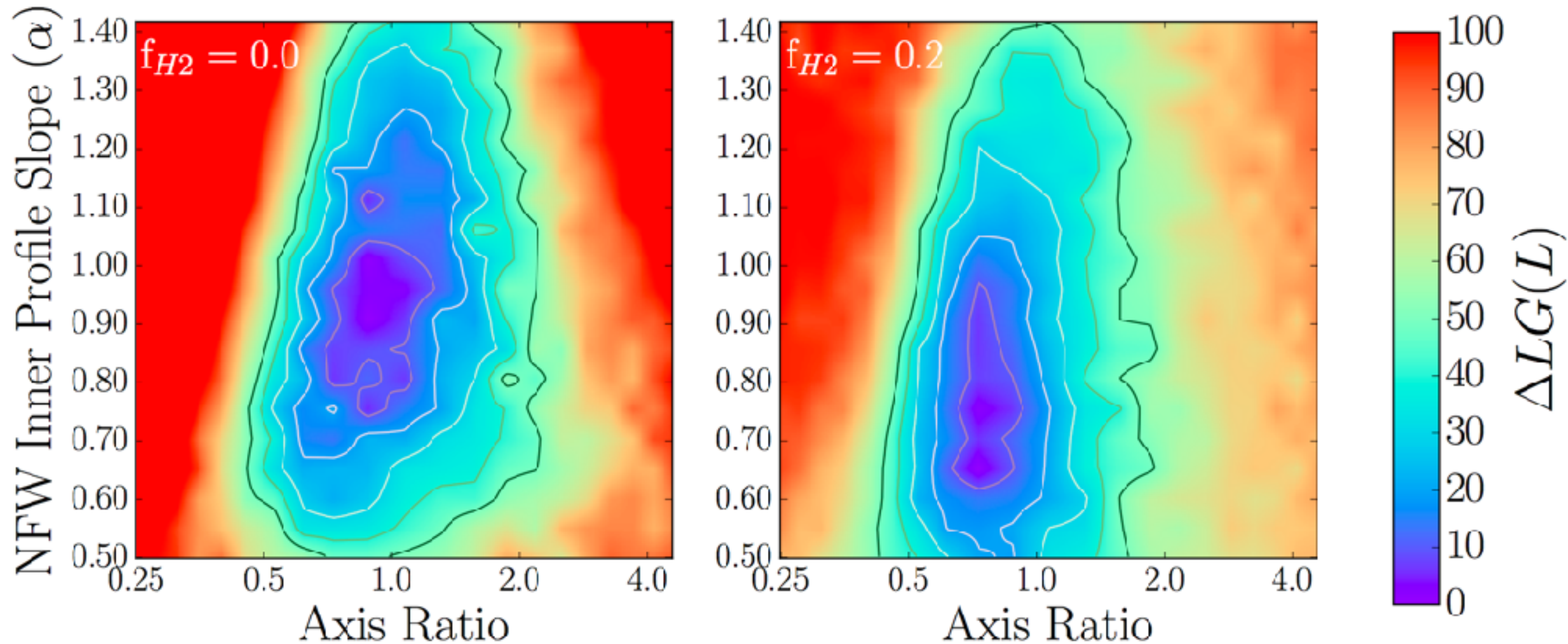
Intriguingly, this persists even when the inner 2° are masked - implying that analyses of small ROIs favors the excess.

The Low Energy Spectrum



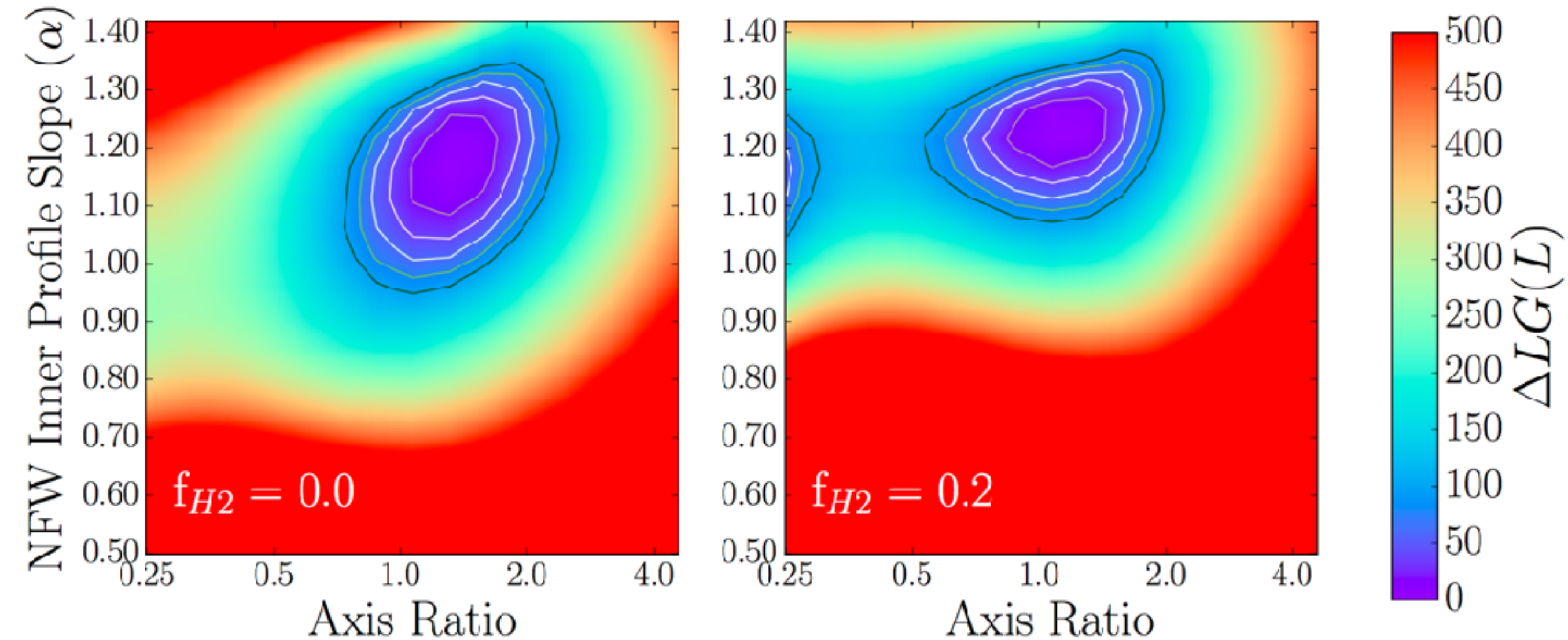
The Galactic Center models contain only a small preference for the convective winds, and the spectrum and intensity of the Galactic center excess component remains resilient.

The Galactic Center Excess Morphology (masking $|b| < 2^\circ$)



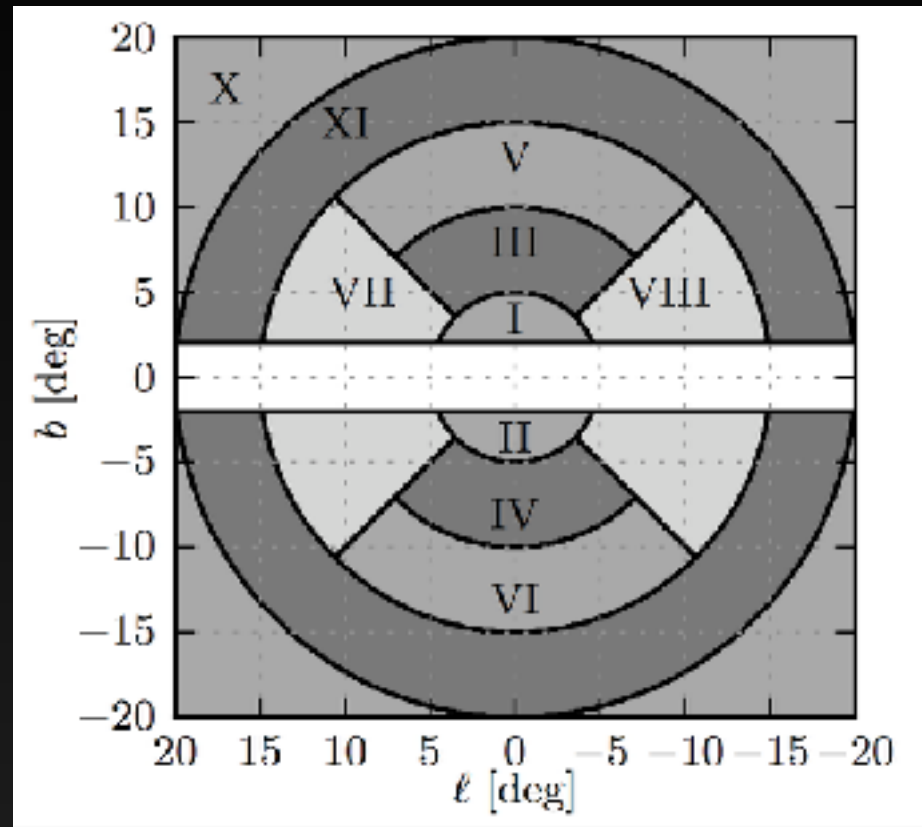
The deviations from typical NFW profiles are more extreme when the $|b| < 2^\circ$ is masked from the analysis, with a shallower emission profile preferred by the data.

Morphology in the Galactic Center



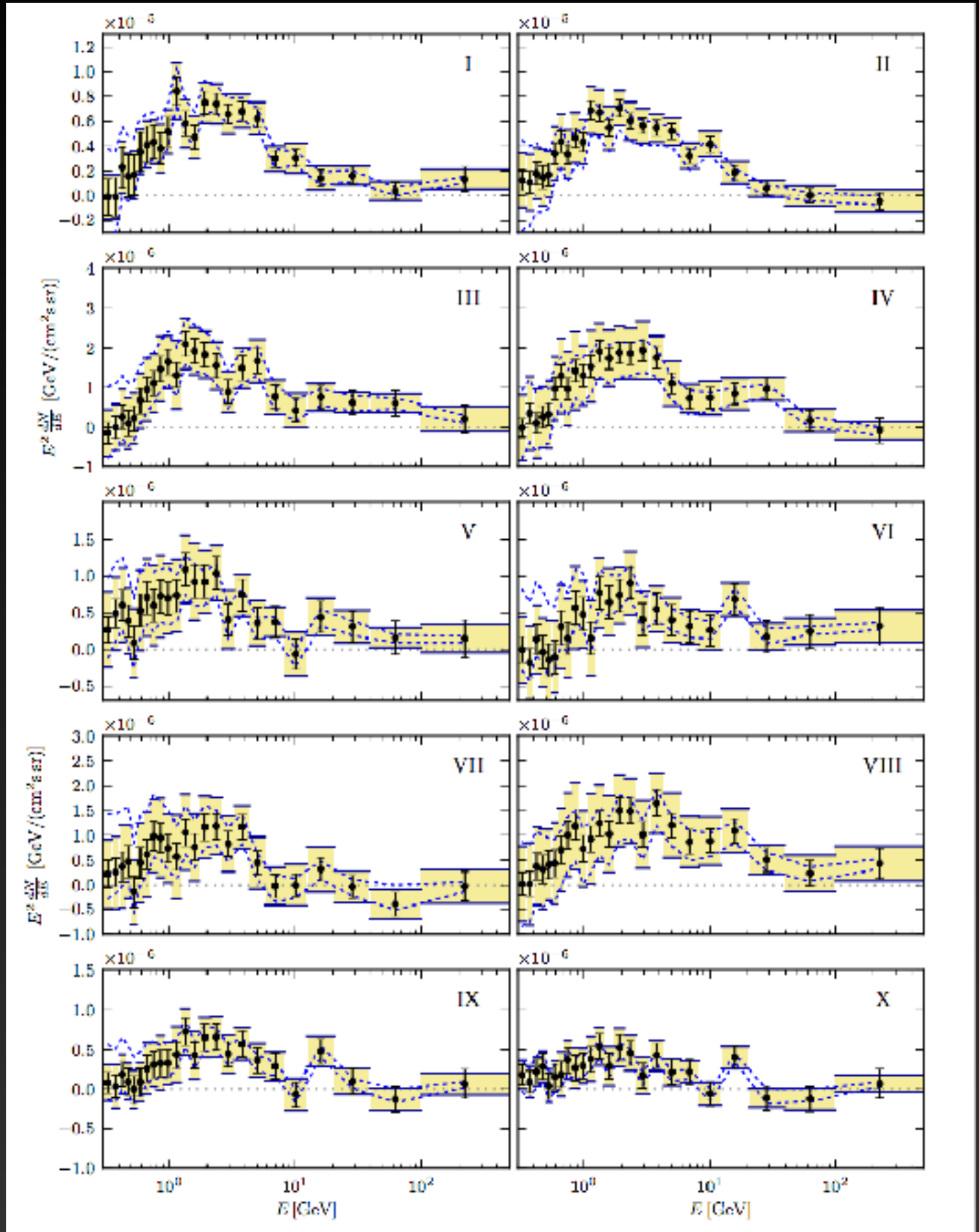
For the Galactic Center analysis, the morphology of the excess component remains relatively robust

Analysis Far from the GC

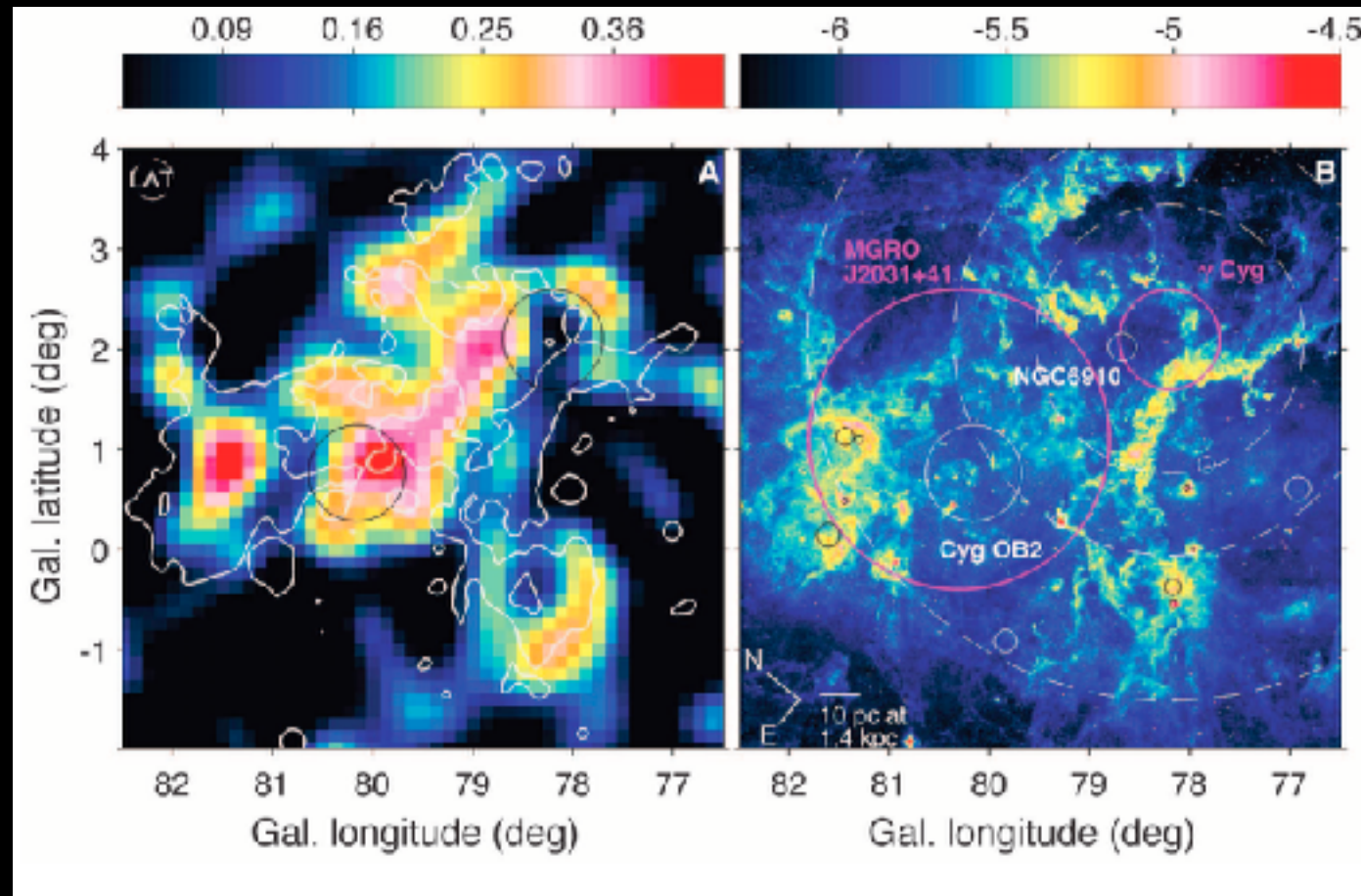


Analysis regions far from the GC also show an excess – not much star formation occurs a few degrees above the Galactic plane.

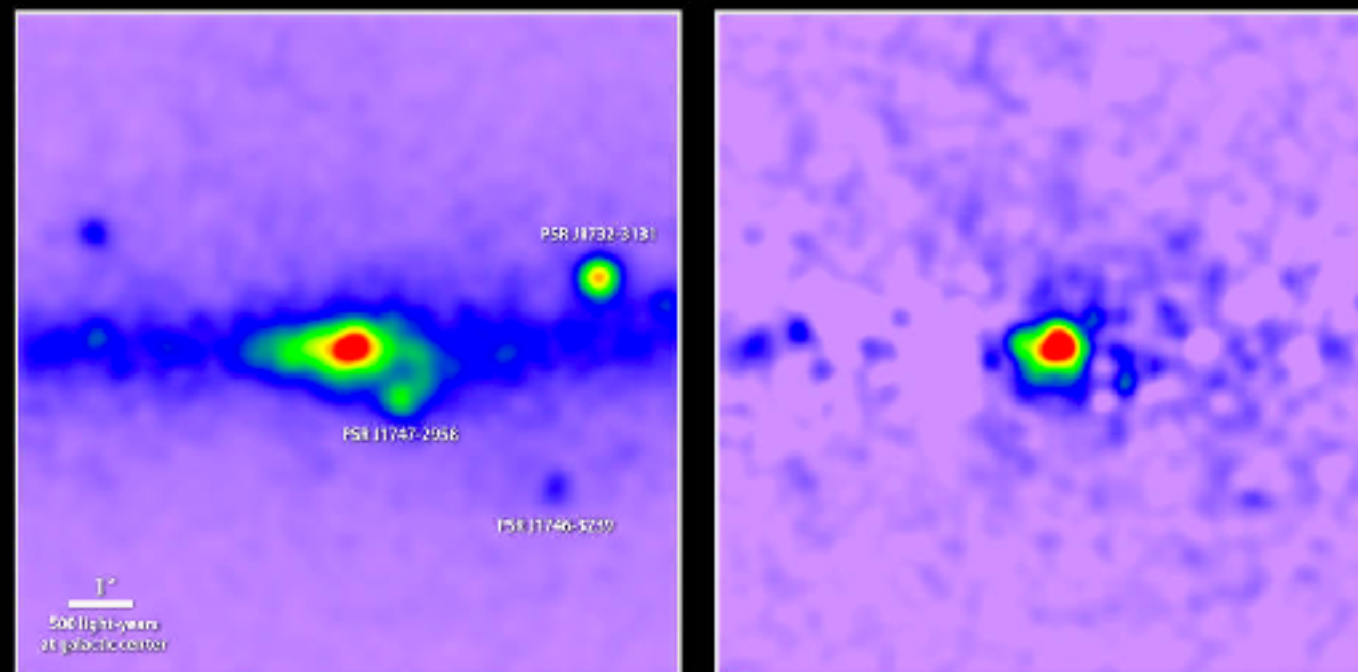
Calore et al. (2014, 1409.0042)



Comparison to Cygnus-X



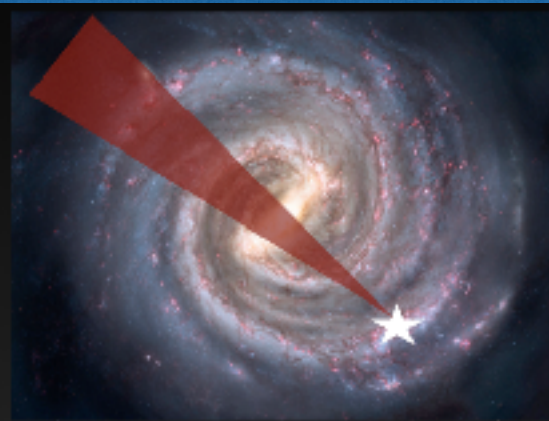
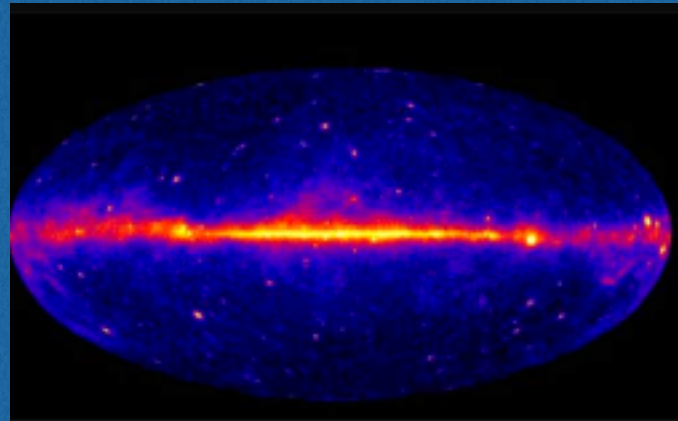
Uncovering a gamma-ray excess at the galactic center



Unprocessed map of 1.0 to 3.16 GeV gamma rays

Known sources removed

A Fermi-LAT Based Example



Total Gamma-Ray Flux (>1 GeV) in inner 1° is $1.1 \times 10^{-9} \text{ erg cm}^2 \text{ s}^{-1}$

Approximately half of this emission is produced along the line of sight towards the GC, and thus we approximate the total gamma-ray luminosity of the central one degree to be $5 \times 10^{36} \text{ erg s}^{-1}$

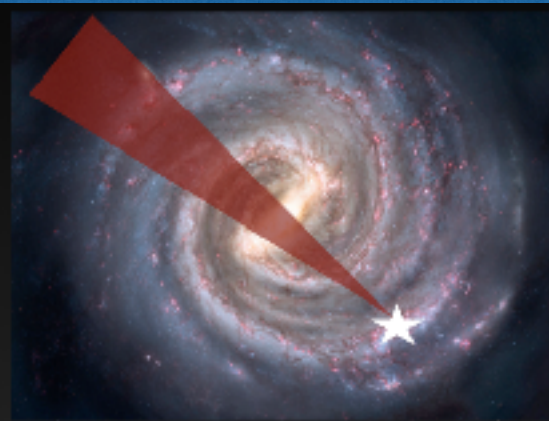
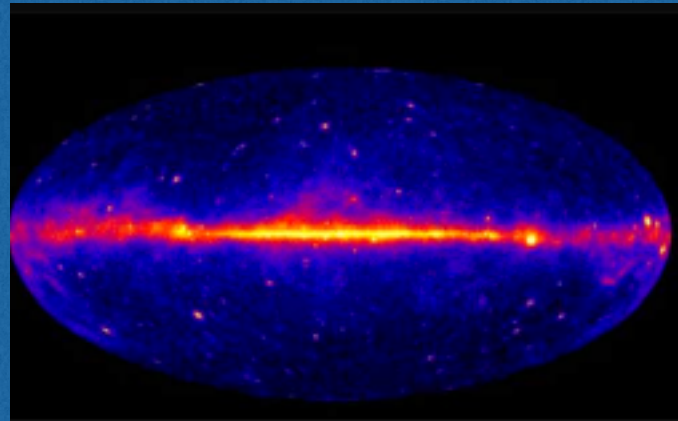
Reacceleration

A $100 M_\odot$ molecular cloud with a gas density of 200 cm^{-3} in a $10 \mu\text{G}$ B-field supports a Kinetic Energy transfer (via magnetic turbulence) of $5.0 \times 10^{32} \text{ erg s}^{-1}$.

Given a total molecular cloud mass of $10^7 M_\odot$, the total reacceleration of cosmic-ray electrons is $5.0 \times 10^{37} \text{ erg s}^{-1}$.

If these electrons are trapped until losing their energy to bremsstrahlung and synchrotron emission with a standard spectrum):

A Fermi-LAT Based Example



Total Gamma-Ray Flux (>1 GeV) in inner 1° is $1.1 \times 10^{-9} \text{ erg cm}^2 \text{ s}^{-1}$

Approximately half of this emission is produced along the line of sight towards the GC, and thus we approximate the total gamma-ray luminosity of the central one degree to be $5 \times 10^{36} \text{ erg s}^{-1}$

Reacceleration

A $100 M_\odot$ molecular cloud with a gas density of 200 cm^{-3} in a $10 \mu\text{G}$ B-field supports a Kinetic Energy transfer (via magnetic turbulence) of $5.0 \times 10^{32} \text{ erg s}^{-1}$.

Given a total molecular cloud mass of $10^7 M_\odot$, the total reacceleration of cosmic-ray electrons is $5.0 \times 10^{37} \text{ erg s}^{-1}$.

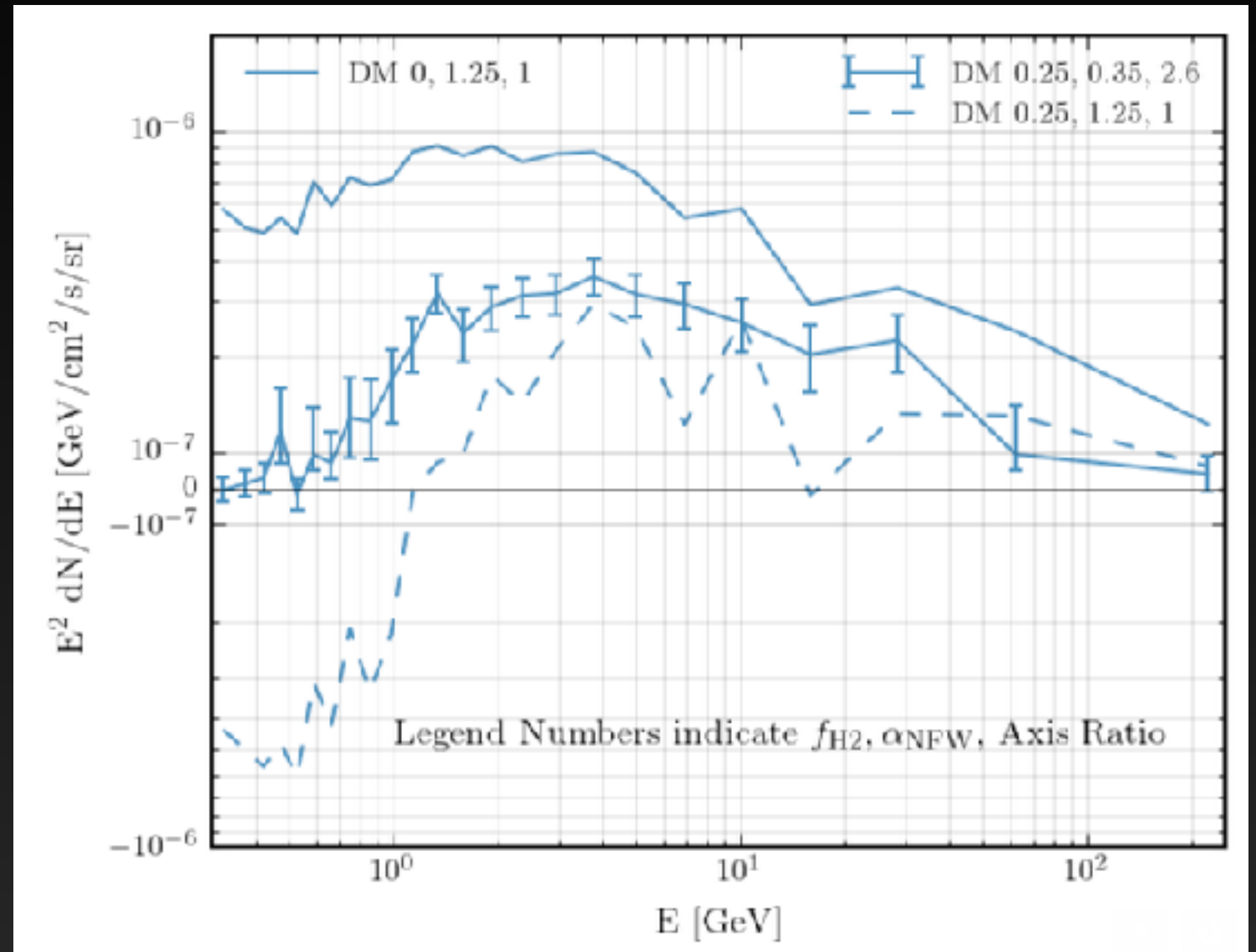
If these electrons are trapped until losing their energy to bremsstrahlung and synchrotron emission with a standard spectrum):

$$6.1 \times 10^{36} \text{ erg s}^{-1} \quad \checkmark$$

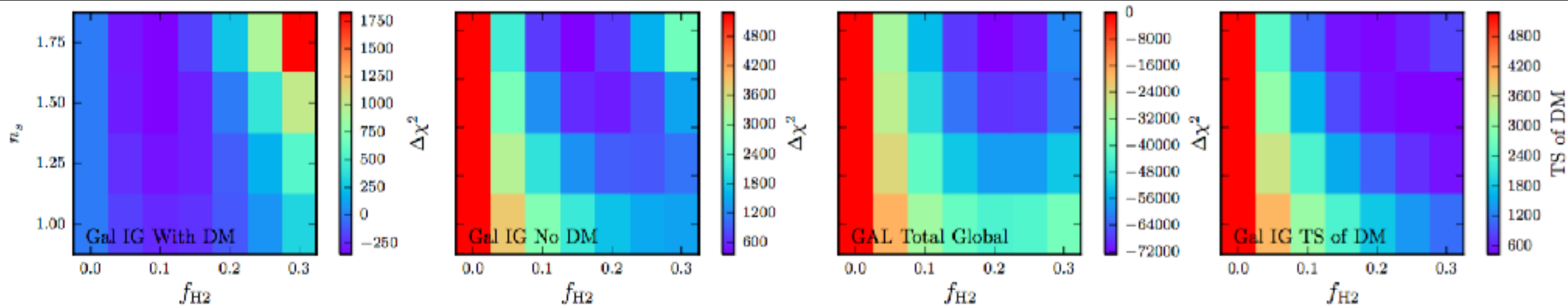
A Fermi Bubbles Component?

When the excess floats to the best fit morphological configuration, much of the excess intensity returns.

Most importantly, the over subtraction issue at low energies is fixed.



The Excess is Degenerate with $f_{\text{H}2}$

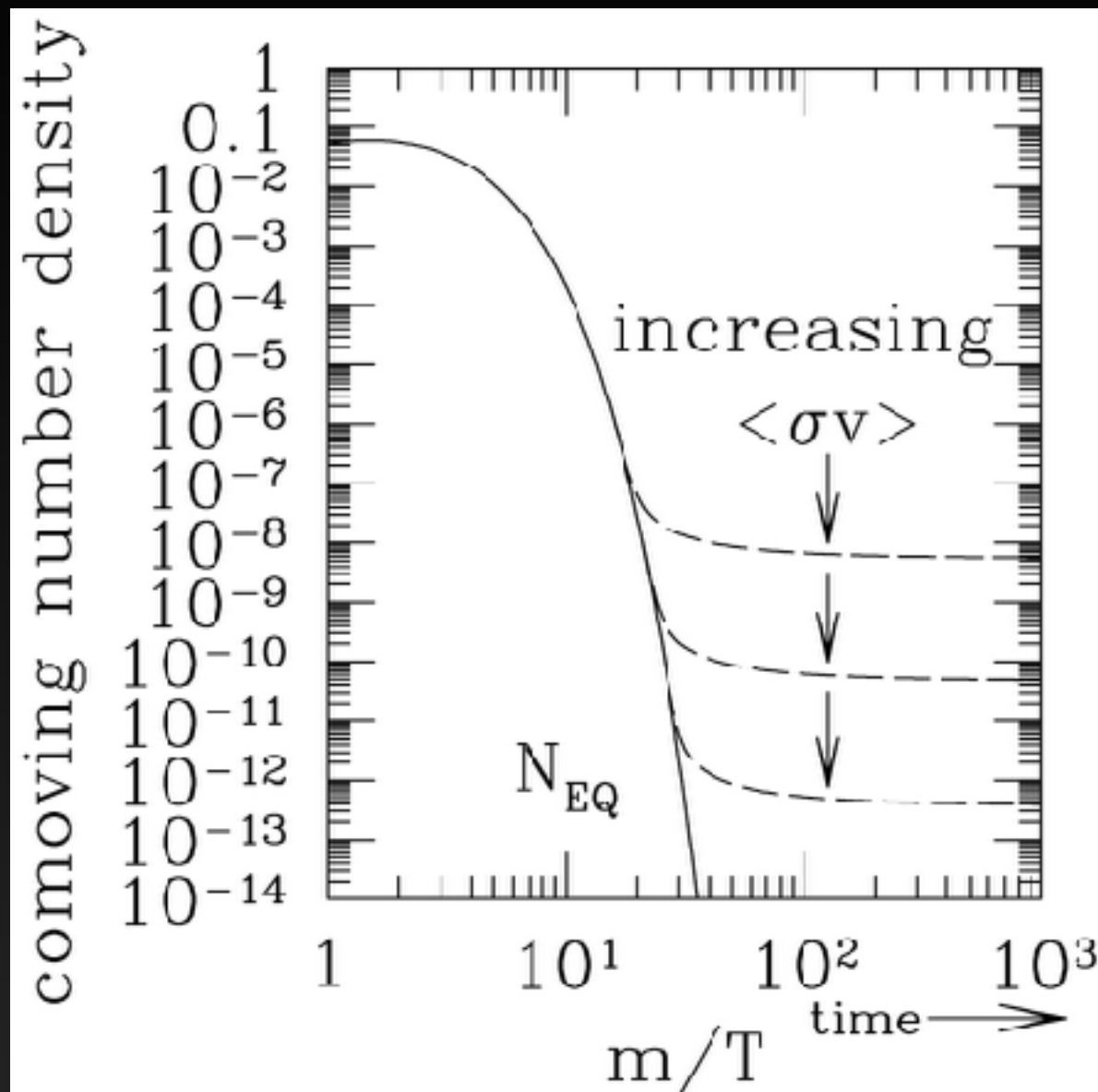


Models with no dark matter universally prefer $f_{\text{H}2} \sim 0.2$ for the $40^\circ \times 40^\circ$ region surrounding the GC.

Models with an NFW emission template prefer $f_{\text{H}2} \sim 0.1$.

The reduction in the normalization of the NFW template is ~ 1.5 for $f_{\text{H}2} \sim 0.1$, instead of a factor of 3 at $f_{\text{H}2} \sim 0.2$.

Dark Matter Annihilation?



$$\left(\frac{\Omega_\chi}{0.2} \right) \simeq \frac{x_{\text{f.o.}}}{20} \left(\frac{10^{-8} \text{ GeV}^{-2}}{\sigma} \right)$$

$$\langle \sigma v \rangle \sim 10^{-8} \text{ GeV}^{-2} (3 \times 10^{-28} \text{ GeV}^2 \text{ cm}^2) 10^{10} \frac{\text{cm}}{\text{s}} = 3 \times 10^{-26} \frac{\text{cm}^3}{\text{s}}$$

$$P(A|B) = \frac{P(B|A)P(A)}{P(B)}$$

A particle with a weak interaction cross-section and a mass on the weak scale is expected to naturally obtain the correct relic abundance through thermal freeze-out in the Early Universe.